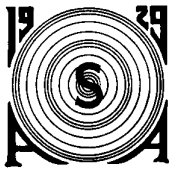

ELECTROACOUSTICS

The Analysis of Transduction, and Its Historical Background

rederick V. Hunt Late Rumford Professor of Physics
and Gordon McKay Professor
of Applied Physics,
Harvard University

**Published by the American Institute of Physics
for the Acoustical Society of America**

Printed in the United States of America

Library of Congress Catalog Card No. 82-72570
ISBN 0-88318-401-X

PREFACE TO THE PAPERBACK VERSION

Electroacoustics was published in 1954, the year the Acoustical Society of America celebrated its 25th anniversary. Now, more than another quarter-century celebration later, the Society is happy to be able to republish F. V. Hunt's monograph. The Society is grateful to Thomas K. Hunt, son of F. V. Hunt, and to Harvard University Press for granting permission to republish the book.

The only change in the book made with this reprinting is the addition of a list of Errata (p. iii), which had been compiled by the author himself.

Hunt's lucid and flowing style of writing, which old readers will enjoy and new readers discover, was a trademark. I am told that the easy reading of the finished product is due in part to Hunt's practice of running the drafts by his wife Kay and, in some cases, their son Tom. Besides being able to write well himself, Hunt had a knack for teaching good writing to his students. The student's pain and embarrassment on seeing how badly he had done with his first draft later turned to appreciation as, under Hunt's tutelage, his critical eye developed.

Another of Hunt's hallmarks was his attention to detail. Chapter 1, the historical introduction, is practically a book in itself. Hunt's dogged determination to record not just the players in the drama but their birth and death dates as well (see the Index of Names, pp. 247–253) produced more than one anecdote recalled by family, students, and colleagues. For example, it is related that Hunt elected to drive to an Acoustical Society Meeting in Washington (probably the one in 1951) rather than fly so that he and his wife Kay might visit a cemetery or cemeteries along the way. He had discovered that in some cases the only available source of an inventor's birth and/or death date was the person's headstone.

Of course, cemeteries were good primary sources only for those who had died. For those still living, Hunt turned to the telephone directory. In Chapter 1 we learn that the idea of using high-frequency sound to detect submarines was first proposed by a Russian engineer, Constantin Chilowsky, in Switzerland in 1914. The story of how Chilowsky satisfied a unique test in order to get a hearing for his proposal is recounted by Hunt in a footnote on p. 46. Almost as bizarre as the story itself is the tale of how Hunt dug up the material for the footnote. While in New York to attend a

meeting, he decided to see whether the New York telephone directory listed any Chilowsky's. It did, in fact a "C. Chilowsky," and when Hunt called the number, he found the man he was looking for. Hunt then visited Chilowsky and obtained from him the story related in the footnote.

F. V. Hunt died in 1972. It is a tribute to him that 28 years after it was first published, his book is still in demand.

David T. Blackstock

June 1982
The University of Texas at Austin

PREFACE

This monograph is concerned with three topics selected from the wide range of subject matter embraced by the general field of electroacoustics. The first of these is a long introduction devoted to the placement of electroacoustical transduction in its proper historical setting relative to the allied arts and to the basic sciences from which it derives. This is followed by three chapters that include the description of a new scheme for the analysis of both electrostatic and electromagnetic systems of electromechanical coupling in a single homogeneous frame of reference. This method of analysis is then illustrated in the succeeding chapters by examples of its application to three representative transducer systems.

Electric-circuit analogs have been widely exploited as a tool for the study of acoustical and mechanical systems. They have been less widely used, however, for the representation of electromechanical transducers owing to the disparity in the symmetry conditions pertaining to electromagnetic and electrostatic coupling. It has been standard practice to say that one type of analog recommends itself for use with one type of coupling, and that the "other" type must be used with the other — but never the twain could be connected back to back!

I had been experimenting pedagogically since about 1937 with a method for resolving this dilemma by using a *space operator* to import analytical symmetry into the electromechanical-coupling equations for the antireciprocal cases involving magnetic fields. After the war, when there was an opportunity to reëxamine the question, it became possible to resolve the basic issues more clearly and to establish, on sound physical grounds, the validity of using such a space operator to restore symmetry in the analysis of electromagnetic coupling. As a consequence, it now becomes possible to give a unified discussion of all types of electromechanical coupling, including magnetic, electric, and mixed transduction fields. I hope that the novelty of this unified approach will justify in part the publication of this material in advance of the completion of the textbook in whose context it was first drafted.

The ability to represent all transducer types with a single form of equivalent circuit makes it relatively more useful to invoke the methods of electric-impedance analysis for the study of transducer performance.

These methods, like the use of equivalent circuits, had already been widely exploited but they were still further developed during the war period. The account of this subject appearing in Chapter 4 leans heavily on the work carried out under NDRC auspices at the Harvard Underwater Sound Laboratory during the period 1941–1945. Although the relevant results of these studies are no longer classified, in the military sense, the research reports have not been generally available and their only summary was incorporated in another document that could receive only limited distribution. Most of the novel features of this work originated with Malcolm H. Hebb and Harvey Brooks, but Francis P. Bundy and many other members of the HUSL staff contributed significantly, and the cogency of the summary report owed much to Paul E. Sabine. In marshaling this material, I have attempted to act as spokesman for this group of wartime colleagues. None of them can be held responsible, however, for the form of presentation I have adopted, since substantial changes from the original have been introduced in order to adapt the procedures to the broadened frame of reference.

The primary generic types of electromechanical coupling include two that make use of a magnetic field and one that uses an electric field. These are exemplified by movable conductors in a fixed magnetic field, by fixed conductors linking a variable magnetic field, and by movable conductors bearing fixed or variable electric charges. The last two categories embrace both lumped-constant systems, such as the moving-armature earphone and the electrostatic loudspeaker, and distributed-constant systems, such as magnetostriction and piezoelectric transducers. Although the methods of analysis presented here are equally applicable to all these transducer types, the gamut of analytical procedures can be illustrated adequately, and a good bit more succinctly, in terms of the lumped-constant systems. This is fortunate, since an adequate discussion of magnetostriction and piezoelectric transducers could not have been included in any case without far exceeding the dimensional limitations of the monograph format. As a consequence, the consideration of these distributed systems, in which electromechanical coupling is effected through body forces, is perforce relegated to a later monograph or other publication.

In the original form of these notes, a few "firsts" had been mentioned casually as an introduction to the various sections devoted to specific mechanisms of transduction. The process of recasting the material in the form of a monograph provided an opportunity to broaden the scope of

these historical allusions and to draw them together into a coherent introduction designed to exhibit electroacoustical transduction in its relevant historical context. There is a close parallelism between electroacoustics and the science of electrical communication, and the mushroom expansion of the latter industry has provided incentive for the publication of many accounts dealing with the history of its growth. Some of these accounts contain useful material bearing on electroacoustics, but I had been well coached about not relying on such secondary sources except as an auxiliary guide in prospecting for original source material. For better or worse, these historical notes are based on the cited primary sources, and while it may not be fluent history, I can at least guarantee that every bibliographical reference has been verified at first hand.

Fortunately, most of the needed source material was available in the rich collections of the Harvard College Library, but a few items (identified by LC) had to be run to ground in the Library of Congress, a few in the Engineering Societies Library (New York) NNE, and a few in the Vail Library of the Massachusetts Institute of Technology MCM. I am also indebted to Mr. David P. Wheatland for graciously making available from his private collection the choice items listed in notes 10, 20, 21, and 68 to Chapter 1. The almost complete files of United States, British, and German patents maintained by the Boston Public Library were also invaluable.

Some readers may be surprised by the prominent role played by patent references in the documentation of a history of transduction. However one may feel about the probity of scientists applying for letters patent, if one wishes to be realistic it is necessary to recognize that electroacoustical transduction is an applied science that presents both electricity and acoustics in their working clothes. It follows that many of the most significant gains in know-how, as well as in basic understanding, have made their earliest public appearance — and some, their only appearance — as publications of the Patent Office. On the basis of my experience in assembling the material for Chapter 1, I am persuaded that a good many scientists and most of the science historians have paid too little attention to this class of source material.

I feel overwhelmed by the inadequacy of any acknowledgment I can record here of my indebtedness to others. Since this material has been accumulating throughout most of my adult life, the list needs to start with Professors G. W. Pierce and E. L. Chaffee, who initiated me into these mysteries a good many years ago. The history chapter presented

many problems that were novel, at least to me, but generous help came from many quarters. Professor I Bernard Cohen was always ready with wise guidance, kindly criticism, and warm encouragement. Mr. David Rines, patent expert extraordinary, deepened my long-standing obligation to him by making available documents, briefs, his collection of patents, and much good advice. I am also indebted to several makers of this history who were kind enough to read and criticize relevant portions of the manuscript. Among these were Robert W. Boyle, Willoughby G. Cady, Edward W. Kellogg, Edward C. Wente, Raymond L. Wegel, Hugh S. Knowles, and Harry F. Olson. I owe special thanks to Mr. Fred J. Harbaugh for comments and many helpful leads to the patent literature on dynamic loudspeakers.

To the students of many classes, and to my colleagues in our Acoustics Research Laboratory, I am deeply grateful for their patient forebearance through many long discussions of points and viewpoints. Professor Philippe Le Corbeiller has been a gracious tutor and a stout foil, and his careful reading and criticism of this manuscript now puts me further in his debt.

I am in no position to deny that completing a first book has its painful moments, alike for the author and for his wife and son. Without their unfailing devotion and indulgence this book probably never would have been finished.

F. V. HUNT

Belmont, Massachusetts
December 1953

ERRATA

Page	Line	
viii	8	W.G. Cady's first name is "Walter," not "Willoughby."
30	3rd from last	Add the final "t" on "contact."
93	6th of Note 2	Add caret over the "o" in "Bocher" so that it reads "Bôcher."
94	Eq. (2.3)	The determinant of capacitances and compliances should be in terms of their reciprocals, viz. $1/C_e, 1/C_T, 1/c_T, 1/c_m$. And add $R_e>0$, $L_e>0$, $1/C_e>0$.
98	Fig. 2.2(b)	Add minus sign to ordinate "b_m."
	Eq. (2.9)	Add parentheses and a bracket with subscript to the first term, making it $\left[d\theta \Big/ \left(\frac{d\omega}{\omega_0}\right)\right]_{\omega_0}$.
99	Eq. (2.10)	Add subscript "m" to the "x's" in the denominator of the fourth term, and add the missing exponent "2" on the second "x" in the fourth term.
	2nd before (2.12)	Insert "s" to make "contant" become "constant."
	Eq. (2.12)	The last factor in the first line should be $(1-\omega_0^2/\omega'^2)$, and in the last line, $(1-\omega_0^2/\omega''^2)$.
104	Eq. (3.3)	The algebraic sign between the two terms on the right-hand side should be a minus sign.
	Eq. (3.5)	Replace the equal sign with a plus sign and at the right add " $=0$."
115	Fig. 3.6	Add arrow to "i" in right-hand diagram.
	3rd of Fig. 3.6 caption	Put a dot over "B" to make it "$\dot{B}$."
120	2	Insert "resonance" before "diameter."
126	4	Subscript on "X_M" should be lower case, "X_m."
	Eq. (4.23)	Add missing subscript "L" to second "Q".
128	Column headings of Table 1	There should be lower case subscripts on "R_M" such as "R_m."
130	1	After "efficiency" insert "must always be real, and"
131	10th below Eq. (4.30)	Insert "resistance part of the" before "*total*"

ERRATA

132	Eq. (4.31*b*)	Replace $\left(1+\frac{R_L}{R_m}\right)$ by $\left(1+\frac{R_L}{R_m}\right)_E$ in numerator and replace $\left(1+\frac{R_L}{R_m}\right)^2$ by $\left(1+\frac{R_L}{R_m}\right)_E^2$ in denominator.
133	Eq. (4.34)	Make the last "$R^{1/2}$" read "$R_m^{\prime 1/2}$."
136	2	Replace the word "circle" with "loop."
137	5th below Eq. (4.38)	Insert after word "that"—"(Z_{em}^2, which appears in."
138	2nd below Eq. (4.43)	Replace "impedance" with "reactance."
139	1st below Eq. (4.44)	Remove the "bl" from "blelectric" and add it to "ocked."
140	1st above Eq. (4.47)	Last number should be "(4.46)."
141	8th of 2nd paragraph	Add parentheses to make fraction "$R_L/(R_m' + R_L)$."
146	2nd above Eq. (5.1)	Change "Equations (3.11)" to "Equations (3.10)."
150	Fig. 5.5	In the branch c–c, "C_m" should be "C_M."
152	2nd after Eq. (5.5)	Replace "reactance" with "parallel."
155	5th above "An Illustrative Example."	First word should be "by."
186	3rd above Fig. 6.6	Replace "without" by "with."
	Fig. 6.6	In the abscissa label, make "C_{00}" read "C_0."
191	Eq. (6.28*a*)	Omit term "$q_1 q_2^*$" in first line.
192	Eq. (6.30*a*)	In first line, delete "n" from "q_{a0n}^2."
192	Eq. (6.30*c*)	At end of first line $a2$ should be subscript.
199	Fig. 6.10(*a*)	Add "I_{b1}" for current in lower-left mesh.
	Fig. 6.10(*b*)	Add minus signs before $(d_a + x_0)^2/C_{a0}E_0^2$ and $(d_b + x_0)^2/C_{b0}E_0^2$. In the latter replace the plus sign with the minus sign to read $(d_b - x_0)^2/C_{b0}E_0^2$.
206	1st of labels in Fig. 6.13	Add a prime to the "c_m" on the right-hand side of the equation identifying $c_m'\varphi^2$.
	Eq. (6.42)	Note that r_m/ϕ^2 and Z_L/ϕ^2 were neglected in getting (6.42)

CONTENTS

1. Introduction — Historical Context 1
2. Electromechanical Coupling — General 92
3. Reciprocity and Symmetry Considerations in Electromechanical Coupling 103
4. Electrical-Impedance Analysis of Transducer Performance 117
5. Moving-Conductor (Dynamic) Transducer Systems 143
6. Electrostatic Transducer Systems 168
7. Moving-Armature (Magnetic) Transducer Systems 213

Appendix A. Dimensions and Units 236

Appendix B. Conversion Charts 238

Index of Names 247

Index of Subjects 255

CHAPTER 2

Electromechanical Coupling — General

The science of electroacoustics is based on the experimental observation that an electrical system *can* be associated with a mechanical system in such a way that a unique functional relation exists between the variables that characterize the electrical system and the variables that characterize the mechanical system. The existence of such a relation lies at the core of elementary electrodynamics, as exemplified by the role of mechanical quantities (such as force and work) in the definition of the basic electrical units. The analysis of electromechanical systems can begin then with the consideration of a simple but quite general case in which an electric circuit comprising a single mesh is coupled, through some sort of "black box" called a transducer, to a mechanical circuit having a single degree of freedom. Two equations will be required to describe the behavior of the system: one will need to be written in terms of the electrical variables and must include the electrical effects arising from motion in the mechanical system; and one will be written in terms of the mechanical variables and must include all the mechanical effects arising from currents or voltages in the electrical system. The symbols T_{em} and T_{me} appearing in Fig. 2.1 represent

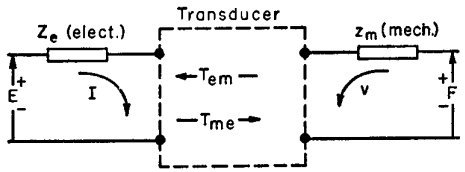

FIG. 2.1. Schematic representation of an electromechanical transducer.

transduction coefficients that describe the electromechanical coupling, the direction of transfer being indicated by the subscripts. (As a useful mnemonic, read *per*, or *due to*, between the two subscript symbols.) Thus, T_{em} is defined as the electromotive force appearing in the electrical

mesh per unit velocity in the mechanical mesh. Similarly, T_{me} is defined as the force acting in the mechanical mesh per unit current in the electrical mesh. Assuming the steady state, in which variation with time enters always as $e^{j\omega t}$, these defining relations allow the equations for the system to be written at once in the canonical form,[1]

$$\begin{aligned} E &= Z_e I + T_{em} v, \\ F &= T_{me} I + z_m v. \end{aligned} \tag{2.1}$$

Physical Realizability

If equations of this sort are to be written down arbitrarily, it is pertinent to inquire what restrictions must be imposed in order that the equations may describe a physically realizable system. It can be taken as axiomatic that a physical system can neither have negative kinetic energy nor store negative potential energy, so the positive-definiteness of the kinetic- and potential-energy functions is at least a *necessary* condition for physical realizability. It is equally axiomatic that the energy dissipation function for a passive system must also be positive-definite. In order to interpret these criteria in terms of the realizability of any particular network configuration, one must proceed to set up the most general type of network and to write down a total-energy function representing all the energy supplied from external sources or stored in the network. It is then straightforward [2] to show that this total-energy

[1] Poincaré seems to have pioneered in pairing two linear equations, to describe the coupling between an electrical and a mechanical system, in his "Etude du récepteur téléphonique," *L'Eclairage Electrique* **50**, 221–372 (16 February *et seq.* 1907). R. L. Wegel, in his "Theory of Magneto-Mechanical Systems as Applied to Telephone Receivers and Similar Structures," *J. Am. Inst. Elec. Engrs.* **40**, 791–802 (October 1921), was the first to make use of mechanical as well as electric impedances in this connection, so that the equations for the coupled system could be displayed in the symmetric form shown here.

[2] Most of the literature on this electric-network problem represents a paraphrase of the corresponding problem of small oscillations in dynamics. See, for example, A. G. Webster, *The Dynamics of Particles and of Rigid, Elastic, and Fluid Bodies*, 2nd ed., Chapter V (New York, G. E. Stechert, 1922; 3rd ed., Leipzig, B. G. Teubner, 1925); or E. T. Whittaker, *Analytical Dynamics*, 4th ed., §§ 76–78 (reprinted, New York, Dover Publications, 1944); also M. Bocher, *Introduction to Higher Algebra* (New York, Macmillan, 1927). The mathematical essence of the problem has been redistilled more recently by R. A. Frazer, W. J. Duncan, and A. R. Collar, *Elementary Matrices*, pp. 30–32 (New York, Macmillan, 1946) and by E. A. Guillemin, *Mathematics of Circuit Analysis*, Chapter IV (New York, Technology Press [MIT] and Wiley, 1949). A comprehensive and self-sufficient discussion of physical realizability in electric networks is given by H. W. Bode, *Network Analysis and Feedback Amplifier Design*, Chapter VII (New York, Van Nostrand, 1945).

function can always be separated into three quadratic forms, one in each of the three types of impedance coefficients. It can then be shown that the necessary and sufficient conditions for the positive-definiteness of each of these quadratic forms is that the determinants of the impedance coefficients of like type, and each of their principal minors, shall also be positive-definite. To illustrate this criterion by a simple example, assume that the several impedance coefficients of Eqs. (2.1) are of the general complex type:

$$Z_e = R_e + j\omega L_e + \frac{1}{j\omega C_e}; \quad z_m = r_m + j\omega l_m + \frac{1}{j\omega c_m};$$
$$T_{em} = R_T + j\omega L_T + \frac{1}{j\omega C_T}; \quad T_{me} = r_T + j\omega l_T + \frac{1}{j\omega c_T}. \tag{2.2}$$

Then it follows that the given impedances will represent a physically realizable system if, and only if,

$$\begin{vmatrix} R_e & R_T \\ r_T & r_m \end{vmatrix} \geq 0, \quad \begin{vmatrix} L_e & L_T \\ l_T & l_m \end{vmatrix} \geq 0, \quad \begin{vmatrix} C_e & C_T \\ c_T & c_m \end{vmatrix} \geq 0;$$
and
$$r_m \geq 0, \quad l_m \geq 0, \quad c_m \geq 0. \tag{2.3}$$

The *sufficiency* of this criterion of realizability can be demonstrated if a systematic procedure can be set up for finding physical configurations [3] that conform to any set of equations like (2.1) for which the impedance coefficients also satisfy Eqs. (2.3). In practice, interest often centers on the converse problem in which equations like (2.1) are written explicitly to describe a known physical system and are then used to study the behavior of the system for various allowable choices of the parameters. In this case, the criterion (2.3) can serve to determine what is "allowable" and thus to guard against setting up unrealizable design objectives.

Motional Impedance

The most distinctive feature of an electromechanical transducer, of course, is its ability to convert electrical energy into mechanical energy

[3] Although this procedure has not yet been reduced systematically to practice in electroacoustic-transducer design, it has been elegantly demonstrated for electric networks by H. W. Bode, "A General Theory of Electric Wave Filters," *Journal of Mathematics and Physics* **13**, 275–362 (1934).

and vice versa. Important properties of the electromechanical interaction can be revealed, however, by studying the driving-point impedance of the system at either its electrical or its mechanical terminals. The electric driving-point impedance at a terminal pair is always defined as the complex ratio of the voltage across the terminal pair to the current entering and leaving the pair terminals, when all other electromotive forces and current sources are suppressed. For the generalized system of Fig. 2.1, the driving-point impedance can be found by setting $F = 0$ in Eqs. (2.1) and then solving for the current I in terms of the terminal voltage E. This leads to

$$Z_{ee} = \left(\frac{E}{I}\right)_{F=0} = \frac{\Delta}{\Delta_{11}} = \frac{Z_e z_m - T_{em}T_{me}}{z_m} = Z_e + \frac{-T_{em}T_{me}}{z_m}, \tag{2.4}$$

where Δ_{11} is the signed minor, or cofactor, [4] of the first row and first column of the impedance determinant Δ.

In a similar way the mechanical driving-point impedance z_{mm} can be written at once as

$$z_{mm} = \left(\frac{F}{v}\right)_{E=0} = \frac{\Delta}{\Delta_{22}} = z_m + \frac{-T_{em}T_{me}}{Z_e}. \tag{2.5}$$

Inspection of Eqs. (2.4) and (2.5) reveals that the usual electric and mechanical impedances would appear without modification at their respective terminals if either of the transduction coefficients were to vanish. Additive terms appear in each equation, however, that represent the modification of the impedance caused by the presence of bilateral electromechanical coupling. For example, in Eq. (2.5) the additive term represents a change in the mechanical impedance arising as a result of current in the coupled electric circuit. Note that the magnitude of this term (which would account for "dynamic braking" if the transducer were a conventional electric motor) varies inversely with the total electric impedance in the external electric mesh.

The corresponding modification of the electric impedance is especially important because of its usefulness in connection with the design of electroacoustic transducers, and the additive term has been suggestively

[4] See any standard mathematics textbook for a review of the use of determinants in solving simultaneous linear equations: for example, L. A. Pipes, *Mathematics for Engineers and Physicists*, pp. 69–76 (New York, McGraw-Hill, 1946); I. S. and E. S. Sokolnikoff, *Higher Mathematics for Engineers and Physicists*, 2nd ed., pp. 102–113 (New York, McGraw-Hill, 1941); L. E. Dickson, *First Course in the Theory of Equations*, pp. 101–127 (New York, Wiley, 1922).

designated as the *motional impedance*. This term can be incorporated in Eq. (2.4) by rewriting it as the sum of the motional impedance Z_{mot} and the "clamped" or "blocked" impedance Z_e, the latter designating the impedance that is observed at the electrical terminals when the mechanical system is prevented from moving by some external constraint; thus

$$Z_{ee} = Z_e + Z_{mot}.$$

The motional impedance is defined explicitly by

$$Z_{mot} \equiv (-T_{em}T_{me})y_m, \tag{2.6}$$

in which the mechanical admittance y_m has been written for the reciprocal of the mechanical impedance, $1/z_m$. The term *motional impedance* was first introduced by A. E. Kennelly and G. W. Pierce in 1912, when they were studying the variation of impedance with frequency for a telephone receiver and discovered that the electric impedance could be influenced by the motion of the coupled mechanical system.[5]

The circumstances of this discovery are not without interest. In making their measurements, one of the experimenters would balance the impedance bridge while the other tended the signal source, a not-always-reliable Vreeland oscillator that was located in a nearby room. Quite by chance, one of them would habitually lay the receiver *on its side* on the laboratory bench while adjusting the bridge. The other always turned it *face down*, thereby altering the acoustic loading on the diaphragm, its motion, and the electric impedance! It is easy to understand how alarmed they were when their measurements showed a complete lack of agreement at all frequencies in the neighborhood of resonance. In the course of pursuing the source of this discrepancy, they finally decided to abandon the careful nursing of the oscillator and *watch* each other balance the bridge, whereupon the difference in their procedures became apparent at once. Kennelly and Pierce both appreciated the physical significance of the effect immediately, and each succeeded in working out a substantially complete theoretical analysis of the phenomenon within a few hours.[6]

[5] A. E. Kennelly and G. W. Pierce, "The Impedance of Telephone Receivers as affected by the Motion of their Diaphragms," *Proceedings of the American Academy of Arts and Sciences* **48**, 113–151 (September 1912); also, *Electrical World (New York)* **60**, 560–565 (14 September 1912).

[6] Recalled for the author and privately narrated by G. W. Pierce.

The motional modifications of the mechanical and electric impedances are seen to be proportional to the negative product of the two transduction coefficients. It follows that the magnitude and nature of the motional impedances will depend on the size of these coefficients and on whether they are real or complex. In order to study in detail the performance of any specific kind of electroacoustic transducer, it is obvious that the corresponding transduction coefficents must be evaluated explicitly. Even in advance of such explicit evaluations, however, a good bit of information of general applicability can be extracted from a preliminary study of Eq. (2.6). The general behavior of the motional impedance, and in particular its variation with frequency, can be studied by considering the behavior of the mechanical admittance y_m. Subsequently the transduction coefficients can be introduced as a scaling operator $(-T_{em}T_{me})$. The usefulness of this procedure stems, of course, from the fact that the same general form of admittance function y_m can be used to characterize a wide class of mechanical systems without regard to the type of motor mechanism employed for electromechanical transduction.

The Vector Impedance Locus

Consider first, then, the mechanical impedance z_m whose generalized expression was given by Eqs. (2.2) in the form

$$z_m = r_m + j\omega l_m + \frac{1}{j\omega c_m} = r_m + jx_m. \tag{2.7}$$

The variation of this impedance with frequency can be exhibited most usefully by representing the impedance as a vector drawn from the origin in the real-imaginary plane. As frequency changes, both the magnitude and the phase angle of the vector will also change and the tip of the vector will trace out a curve which can be called an *impedance locus*. If the mechanical resistance r_m does not vary with frequency, the impedance locus for z_m will be simply a straight vertical line passing through a point on the real axis at a distance r_m from the origin, as shown in Fig. 2.2(*a*). At very low frequencies the phase angle of z_m is very nearly $-\pi/2$, corresponding to "stiffness control" of the mechanical system, while at very high frequencies the phase angle approaches $+\pi/2$, as is characteristic for "mass control." The phase angle is zero, as usual, at the angular frequency of mechanical resonance $\omega_0^2 = (1/l_m c_m)$. For any specific values of the mechanical constants, a scale of angular frequency

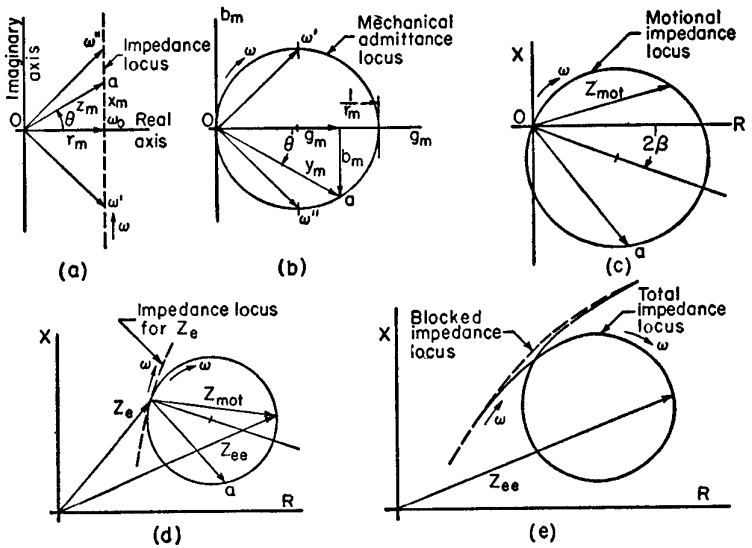

FIG. 2.2. Stages in the evolution of the vector-impedance locus.

could be laid out along the impedance locus, but this would not be a uniform scale since the rate at which the phase angle changes with ω depends on the relative values of the coefficients r_m, l_m, and c_m. More specifically, the rate of change of phase with angular frequency, at resonance, varies inversely with the damping constant; thus,

$$\left(\frac{d\theta}{d\omega}\right)_{\omega_0} = \frac{2l_m}{r_m}. \tag{2.8}$$

The rate at which phase angle changes with an incremental change of the ratio of the operating angular frequncy to the resonance frequency is found by multiplying both sides of Eq. (2.8) by ω_0, giving

$$\frac{d\theta}{\frac{d\omega}{\omega_0}} = \frac{2\omega_0 l_m}{r_m} \equiv 2Q_m. \tag{2.9}$$

The rapidity of phase shift near the frequency of resonance can be interpreted as one measure of the "sharpness of resonance" of a tuned system, and for such systems having a single degree of freedom this feature is characterized by introducing the "quality factor" Q_m as defined in Eq. (2.9). This mechanical "Q" can be interpreted in terms of the same concepts ordinarily used in discussing the corresponding electrical quantity. It can be defined explicitly in a variety of different ways, as will be seen later, but it is most fundamentally significant as an expression of the ratio of the peak value of the energy stored during a cycle to the total energy dissipated in a radian period, that is, in a time interval $t = 1/\omega$.

The locus of the tip of the mechanical admittance vector $y_m = 1/z_m$ can be exhibited in a similar way on the real-imaginary plane [Fig. 2.2(*b*)], where it represents simply an inversion of the straight-line impedance locus and is thus a circle of diameter $1/r_m$ with its center at $1/2r_m$ on the real axis. Proof of this geometrical relation can be given very simply by the following sequence of steps, which are largely self-explanatory:

$$y_m \equiv g_m - jb_m = \frac{1}{z_m} = \frac{r_m}{r_m^2 + x^2} - j\frac{x_m}{r_m^2 + x_m} = r_m \mid y_m \mid^2 - jx_m \mid y_m \mid^2; \tag{2.10}$$

$$\cos\theta = \frac{g_m}{\mid y_m \mid} = r_m \mid y_m \mid; \quad \text{whence} \quad \mid y_m \mid = \frac{1}{r_m}\cos\theta.$$

The proof is completed by recognizing that the last expression is simply the equation of a circle of diameter $1/r_m$ in polar coördinates.

The tip of the admittance vector traverses its circular locus in a clockwise direction as ω increases. Since the mechanical impedance is real at the resonance frequency, the mechanical admittance is likewise real when

$$\omega_0^2 = \frac{1}{l_m c_m}. \tag{2.11}$$

Special interest attaches to the critical frequencies ω' and ω'' indicated in Fig. 2.2(*b*). These were designated as "quadrantal frequencies" by Kennelly.[5,6] They are the frequencies for which the real and imaginary parts of the mechanical admittance (or impedance) are equal, and for which the phase angle of the mechanical admittance (or impedance) is 45°; and they would be the "half-power" frequencies if the voltage across the motional impedance were maintained contant. At these frequencies one can write

$$\begin{aligned} r_m &= -\omega' l_m + \frac{1}{\omega' c_m} = -\omega' l_m \left(\frac{1 - \omega_0^2}{\omega'^2}\right), \\ r_m &= +\omega'' l_m - \frac{1}{\omega'' c_m} = \omega'' l_m \left(\frac{1 - \omega_0^2}{\omega''^2}\right). \end{aligned} \tag{2.12}$$

By subtracting one of these equations from the other, it can be shown with a little manipulation that $\omega'\omega'' = \omega_0^2$. It can also be shown with a little further manipulation that the damping constant of the mechanical system, $r_m/2l_m$, is just half the difference between the quadrantal frequencies, and that the mechanical Q can be expressed as the ratio of the resonance frequency to the difference between the quadrantal frequencies. Thus

$$\frac{r_m}{2l_m} = \frac{(\omega'' - \omega')}{2} \tag{2.13}$$

and

$$\frac{\omega_0 l_m}{r_m} = Q_m = \frac{\omega_0}{(\omega'' - \omega')}.$$

It is interesting to note that measurement of the resonance frequency and the two quadrantal frequencies furnishes enough data to determine uniquely the *relative* values of r_m, l_m, and c_m. However, observing these critical frequencies alone does not provide enough information to fix the magnitudes of any of these constants. Of course, since these constants are characteristic of the mechanical system, they might be determined by direct measurement; but what is available for observation at the electrical terminals is the admittance locus of Fig. 2.2(b) multiplied by the scaling factor $-(T_{em}T_{me})$. This transduction factor must be considered as a vector operator which not only may alter the scale of Fig. 2.2(b), but also may rotate the diameter of the admittance circle about the origin by an angle identified as 2β; but more importantly, the transduction factor is a "units" operator having such dimensions as to convert the locus of mechanical admittance [Fig. 2.2(b)] into a locus of electric impedance, as shown schematically in Fig. 2.2(c).

Before assembling the final vector representation of the driving-point impedance it may be observed that the electric impedance vector Z_e can be represented in a similar way on the real-imaginary plane. It thus becomes necessary to take into account the fact that the tip of the Z_e vector will traverse its own impedance locus as the frequency changes, as shown schematically by the dashed line passing through the tip of the Z_e vector in Fig. 2.2(d). The origin of the circular locus of the motional impedance is located, as shown in Fig. 2.2(d), at the tip of the Z_e vector. Thus, as the angular frequency ω varies from low values to high values, the tip of the Z_e vector moves along its dashed locus while the Z_{mot}

vector, drawn from a moving origin at the tip of the Z_e vector, simultaneously traverses its circular locus. As a result, the vector resultant of $Z_e + Z_{mot}$, that is, the total driving-point impedance, traverses a locus exhibiting a typical "motional loop," as illustrated schematically in Fig. 2.2(e). The phase shift 2β and the impedance locus for Z_e as shown in Fig. 2.2 are typical for a magnetic earphone of the type studied by Kennelly and Pierce in their original research on motional impedance [cf. Fig. 7.7 of Chapter 7], or for magnetostriction transducers in general. For different types of transducer mechanisms, the dip-angle 2β may take on different values (including zero), and the electric blocked-impedance locus may lie in either the first or the fourth quadrant; but a motional loop superimposed on the total impedance locus, as shown in Fig. 2.2(e), is typical in a qualitative sense for all types of transducer mechanisms.

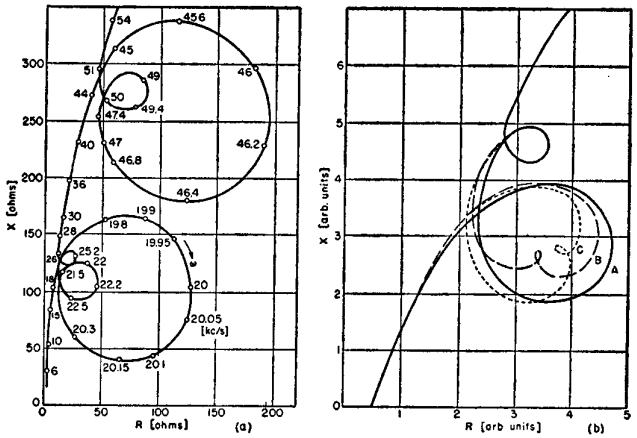

FIG. 2.3 (a) Vector-impedance locus for a multi-resonant magnetostriction transducer operating in air; (b) typical impedance loci for a magnetostriction transducer operating in water, [A] without nearby reflections, and [B,C] for two positions relative to a reflecting surface. [From reference 1 of Chapter 4.]

A mechanical system having a single degree of freedom was premised in the foregoing discussion. When the mechanical system, or the mechanoacoustical system, has more than a single degree of freedom, each mode of vibration that is coupled to the electrical system will display its presence in the appropriate frequency interval by an additional loop in the impedance locus. A particularly good (or bad!) example of this kind is shown in Fig. 2.3(a), where both parasitic and harmonic modes

make their appearance. The fact that one of these spurious loops persists in the harmonic mode of vibration while the other does not might be regarded as a useful clue by the designer, who would usually be (and was) concerned with the elimination of these departures from normal behavior.

It can be emphasized in passing that acoustical end-use has not yet intruded in this discussion, and the foregoing analysis is equally applicable to any other electromechanical transducer systems, such as vibration or string oscillographs,[7] light valves, vibration test equipment, and phonograph recorders and reproducers. When the vibration is coupled to a sound radiation field, acoustic reaction on the source will reveal the effect of sound reflections if they exist, whether such reflections are introduced deliberately, as in some methods for measuring the velocity of sound, or accidentally in the course of making acoustic transmission measurements. The latter situation is illustrated by curves B and C of Fig. 2.3(b), which show how the impedance locus can reveal the presence of troublesome reflections by exhibiting a pronounced alteration of shape when the transducer is moved with respect to its acoustical environment.

Before proceeding further with the analysis of impedance diagrams, it will be useful to consider in detail some of the general properties of the transduction coefficients.

[7] A. E. Kennelly, *Electrical Vibration Instruments*, pp. 56 and 99ff (New York, Macmillan, 1923).

CHAPTER 3

Reciprocity and Symmetry Considerations in Electromechanical Coupling

The principle of reciprocity occupies a prominent place in both theoretical and practical electroacoustics. It will reward careful study, both because this will promote understanding of the fundamental nature of electromechanical coupling and because the principle underlies an important technique for the absolute calibration of transducers. Rayleigh enunciated a reciprocity theorem for mechanical systems and ascribed to Helmholtz a similar theorem for acoustical systems.[1] Reciprocity relations for *coupled* electromechanical systems [2] appear to have been stated first by Ballantine in substantially the form that follows. The canonical equations (2.1), repeated here for convenience, are written in terms of the currents and velocities that are established in the electromechanical system of Fig. 2.1 by the impressed electromotive force E and the impressed mechanical force F;

$$\begin{aligned} E &= Z_e I + T_{em} v, \\ F &= T_{me} I + z_m v. \end{aligned} \tag{3.1}$$

Consider now another pair of electromotive and mechanical forces E'' and F'', applied to the same system. These will give rise to new currents and velocities as follows:

$$\begin{aligned} E'' &= Z_e I'' + T_{em} v'', \\ F'' &= T_{me} I'' + z_m v''. \end{aligned} \tag{3.2}$$

The reciprocity relation can be exhibited by adding Eqs. (3.1) to Eqs. (3.2) if, before adding, the first of Eqs. (3.1) is multiplied by I'', the

[1] Rayleigh, . . . *Sound;* I, § 108 and II, § 294 (see note 225, Chapter 1).

[2] Stuart Ballantine, "Reciprocity in Electromagnetic, Mechanical, Acoustical, and Interconnected Systems," *Proc. Inst. Radio Engrs.* **17,** 929 (June 1929). See also Walter Schottky, "Das Gesetz des Tiefempfangs in der Akustik und Elektroakustik," *Zeitschrift für Physik* **36,** 689–736 (April 1926).

second by v'', the first of Eqs. (3.2) by $(-I)$, and the second by $(-v)$. This manipulation allows the terms in Z_e and z_m to cancel, leaving

$$I''E + v''F - IE'' - vF'' = I''v(T_{em} - T_{me}) + Iv''(T_{em} - T_{me}). \quad (3.3)$$

The right-hand member of Eq. (3.3) then vanishes *if* the transduction coefficients are bilateral or "reversible," that is, if $T_{em} = T_{me}$. Subject to this condition, a statement of the reciprocity theorem emerges in the following form:

$$I''E + v''F = IE'' + vF''. \quad (3.4)$$

Note that the unprimed and double-primed quantities appearing in Eq. (3.4) do not coexist in the coupled network at the same time; thus, $I''E$ is not to be interpreted as electric power.

A more conventional statement of the reciprocity theorem can be derived from Eq. (3.4) by considering the simplified case in which $F = 0$ in the first, or unprimed, set of variables, and $E'' = 0$ in the second set of impressed quantities. It then follows from Eq. (3.4) that

$$\frac{I''}{F''} = \frac{v}{E}. \quad (3.4a)$$

If the two coupled meshes were both electric, the latter form would be equivalent to the familiar statement of the electrical reciprocity theorem, which is usually expressed by saying that in any network composed of linear bilateral elements excited by a single zero-impedance generator, the reading of a zero-impedance ammeter is unchanged when the positions of ammeter and generator are interchanged.

If the electromechanical system has more degrees of freedom than are shown in Fig. 2.1, Eqs. (3.1) and (3.2) can be generalized to include n electric meshes coupled to each other and to m mechanical meshes. Then if all the transduction coefficients are reversible, and all the mutual impedances (both electric and mechanical) are similarly bilateral, the same algebraic procedure used above leads to the following general statement of the electromechanical reciprocity theorem:

$$\sum (I''E - IE'') = \sum (v''F - vF''). \quad (3.5)$$

An alternative method of exhibiting the physical nature of the reciprocity relation is afforded by solving Eqs. (3.1) directly for the electromechanical transfer impedance Z_{e-m}. This can be defined as the complex ratio of an emf E impressed in the electric mesh to the velocity

v observed in the mechanical mesh, all other impressed emf's or forces being suppressed. Setting $F = 0$ and solving Eqs. (3.1) for v allows Z_{e-m} to be written as

$$Z_{e-m} = \left(\frac{E}{v}\right)_{F=0} = \frac{\Delta}{\Delta_{12}} = \frac{Z_e z_m - T_{me}T_{em}}{-T_{me}} = T_{em} - \frac{Z_e z_m}{T_{me}}, \quad (3.6)$$

where Δ_{12} is the signed minor, or cofactor, of the first row and second column of the impedance determinant Δ. In a similar way the mechano-electrical transfer impedance Z_{m-e} can be defined as the complex ratio of the force acting in the mechanical mesh to the current in the electric mesh, all other impressed forces or emf's being suppressed. Thus, setting $E = 0$ and solving Eqs. (3.1) for I gives Z_{m-e} as

$$Z_{m-e} = \left(\frac{F}{I}\right)_{E=0} = \frac{\Delta}{\Delta_{21}} = T_{me} - \frac{Z_e z_m}{T_{em}}. \quad (3.7)$$

It follows at once that the electromechanical transfer impedance is the same for either direction of transmission, that is, it is reversible or bilateral, provided only that $\Delta_{12} = \Delta_{21}$. This condition will always be satisfied if the impedance determinant of the interconnected system is symmetric about its principal diagonal.

Symmetry and Equivalent Circuits

The preceding discussion makes it clear that symmetry of the impedance determinant, or reversibility of the transduction coefficients, is a central feature of the reciprocity principle. It will be shown explicitly in the following sections that electromechanical systems of the electrostatic or piezoelectric type do indeed have transduction coefficients that are reversible, from which it follows that transducers incorporating this type of coupling can be expected to obey the reciprocity principle.

There is another type of electromechanical coupling for which it has been customary in the literature to say that the identity of T_{me} and T_{em} holds with respect to magnitude, but not with respect to algebraic sign. In these cases, introduction of the relation $T'_{me} = -T'_{em}$ in Eqs. (3.6) and (3.7) yields the result that the electromechanical transfer impedances are also identical in magnitude but reversed in algebraic sign. Moving-conductor, moving-armature, and magnetostriction systems are of this type, and are said, therefore, to be *antireciprocal*. In what follows it will be shown that this sign reversal, or antisymmetry, stems from a shortcoming of the symbolic method by which the sign conventions have

been customarily introduced in the analysis. When the basic physical relations that underlie the sign conventions for electromagnetic transduction are properly included in the analytical symbolism, the formal symmetry of the impedance determinant is found to be preserved even for these "antireciprocal" systems.[3] This is not to deny that there is a fundamental distinction to be made between electrostatic and electromagnetic transducer mechanisms, but rather to say that it is not necessary to sacrifice the inherent symmetry of the transduction process in order to give a proper analytical account of the physical phenomena.

Before discussing these sign conventions in detail it will be useful first to examine what consequences the symmetry of the impedance determinant may have with respect to the ability to represent the coupling Eqs. (3.1) by an equivalent electric network.

When the impedance determinant is symmetric it is always possible to find an electric-network representation that "conforms" to the set of Eqs. (3.1). This statement can be supported inductively by describing a successful procedure for drawing such network representations, and by observing that the same or any other procedure based on a permutation of algebraic signs fails if the determinant is antisymmetric. Such a network can be said to conform to the equations, or to be "equivalent" to the actual electromechanical system, if these same Eqs. (3.1) can be obtained by applying Kirchhoff's laws in the way they are usually employed in dealing with electric networks. The equivalence is, of course, symbolic; it does not follow that such an electric network could actually be constructed with coils and condensers, for one reason because in all cases the equivalent circuit will need to contain some kind of transforming element to represent symbolically the conversion from electrical to mechanical units of measurement. There will be more to say about the special properties of such units transformers when they actually turn up in the equivalent circuits now to be described.

The procedure for setting up the appropriate network configuration can be illustrated by exhibiting Fig. 3.1 and showing how it is obtained from Eqs. (3.1), which are again rewritten for convenient reference, this time with the subscripts on T dropped:

$$\begin{aligned} E &= Z_e I + Tv, \\ F &= TI + z_m v. \end{aligned} \qquad (3.1a)$$

[3] F. V. Hunt, "Symmetry in the Equations for Electromechanical Coupling," *J. Acoust. Soc. Am.* **22**, 672 (A) (September 1950).

Figure 3.1 represents a simple two-mesh network in which the impedance element $+T$ has been made common to the two meshes, since it appears as the common coefficient of v in the electrical equation and of I in the mechanical equation. However, since $+T$ does *not* appear in the

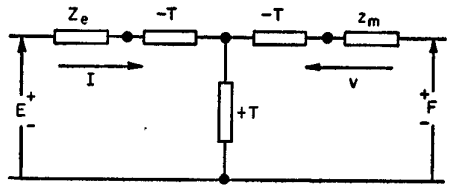

FIG. 3.1. The canonical form of the equivalent circuit symbolizing one electric mesh coupled to one mechanical mesh by a symmetric transduction coefficient.

coefficient of I in the first of Eqs. (3.1a), *or* in the coefficient of v in the second, the effect of its presence in the common branch must be compensated by introducing it again, with reversed sign, in each individual mesh. Thus the T-configuration of impedances $-T$, $+T$, $-T$, as shown in the central part of Fig. 3.1, constitutes a network representation of the coupling impedance common to the two Eqs. (3.1). This procedure can be recognized as exactly that followed in drawing an equivalent circuit for two magnetically coupled inductances. For example, as shown in Fig. 3.2, the common mutual inductance is placed in the staff of the

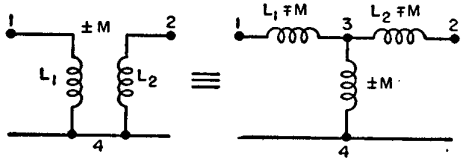

FIG. 3.2. The T-network equivalent for two inductances coupled magnetically.

T and then added, with reversed sign, in each series arm of the T. Note that the branch point numbered 3 is an "inaccessible" terminal, as is the corresponding branch point in Fig. 3.1.

Once the network of Fig. 3.1 is obtained, it may be redrawn in a variety of forms by means of the conventional network transformations [4] shown in Fig. 3.3. The equivalence between the network of Fig. 3.3(a) and the other three configurations, each including an ideal transformer of the indicated impedance ratio, can be established readily by direct comparison of the open- and short-circuit impedances.

[4] A. T. Starr, *Electric Circuits and Wave Filters*, 2nd ed., p. 133 (New York, Pitman, 1938); also T. E. Shea, *Transmission Networks and Wave Filters*, p. 325–328 (New York, Van Nostrand, 1929).

It follows that the symbolic networks of Fig. 3.3 are "equivalent" to the electromechanical system because the *application of conventional electric-network analysis to any of the circuits of Fig. 3.3 produces the same set of Eqs. (3.1) that are obtained by solving the differential equations for the original system.* This feature is not only a necessary criterion of equivalence but is also the principal — and adequate — justification for the effort devoted to finding equivalent circuits for mechanical and acoustical systems.

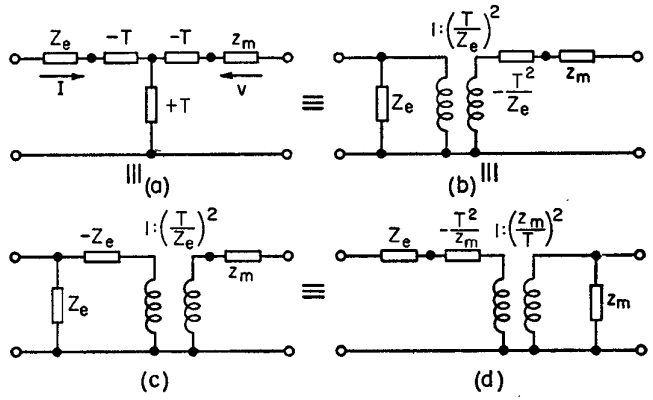

FIG. 3.3. Typical transformations of the canonical two-mesh equivalent circuit with electromechanical coupling.

Note that careful distinction is being made here between the terms "equivalent" and "analogous." In many cases the motivation for deriving network configurations that bear a topological resemblance to mechanical systems is to make it possible to construct electric models whose electrical behavior can be regarded as analogous to the behavior of the mechanical system. In using such models, the electric quantities that are analogous to the mechanical variables are, of course, to be measured in electrical units and then interpreted in terms of mechanical units by applying a scaling factor. It is obvious that for such an analogous network to be "physically realizable" it is necessary to insist that the circuit elements, transformers, etc., that are called for should also be "practically realizable"; and if the required network elements cannot be realized in this sense, the network analog is said to "fail." On the other hand, the term "equivalent," as applied to such networks as those

shown in Fig. 3.3, is not similarly restricted by any requirements on realizability except those based on energy considerations as expressed by Eqs. (2.3). The variables appearing on the right-hand side of Fig. 3.1, for example, are symbolic representations of the real mechanical variables, *not* representations of electrical quantities that are proportional or analogous to the mechanical variables. This distinction can be emphasized by considering the interpretation of Fig. 3.3 in which transformers appear. With the meaning here attached to such equivalent circuits, these transformers are not conventional electric transformers in which electrical quantities appear at either pair of terminals; *they are electromechanical transformers* whose turns ratio is not a simple numeric but has such dimensions that the quantities appearing on either side are "transformed" with the required conversion between electrical units on one side and mechanical units on the other. In this sense, the "equivalence" of these network representations is complete and explicit, and the electromechanical transducers themselves stand as the physical realization of such novel circuit elements as transformers that convert units as well as impedances.

The Burdens of Antisymmetry

Two methods have been advanced previously in the literature for drawing equivalent circuits to represent a set of linear equations having an antisymmetric determinant. In the first of these, proposed originally by Norton [5] and used extensively by W. P. Mason, the canonical equations are transposed so that the voltage and the velocity appear on the left as "impressed" quantities expressed in terms of current and force as independent variables. Rearranging Eqs. (3.1) in this way leads to

$$\begin{aligned} E &= \left(Z_e - \frac{T_{em}T_{me}}{z_m}\right) I + \frac{T_{em}}{z_m} F, \\ v &= -\frac{T_{me}}{z_m} I + \frac{1}{z_m} F. \end{aligned} \tag{3.8}$$

Then, if $T_{em} = -T_{me}$, Eqs. (3.8) have a symmetric determinant and lead at once to the equivalent circuit shown on the left in Fig. 3.4, in which the force represents the "through" quantity, or "current," in the mechanical mesh. The transformation $(a) \rightarrow (d)$ of Fig. 3.3 allows this

[5] Edward L. Norton (B.T.L.), U. S. Pat. No. 1,642,506 (filed 23 September 1926) issued 13 September 1927; see also W. P. Mason, *Electromechanical Transducers and Wave Filters*, Chapter VI (New York, Van Nostrand, 1st ed., 1942; 2nd ed., 1948).

circuit to be redrawn in the simplified form shown on the right in Fig. 3.4. Note that the mechanical impedance appears in Fig. 3.4 as a reciprocal impedance, or admittance, for which Firestone [6] has proposed the designation *mechanical mobility*. The ability of either circuit of Fig. 3.4 to yield Eqs. (3.8) qualifies these symbolic representations under the same criterion of equivalence applied previously.

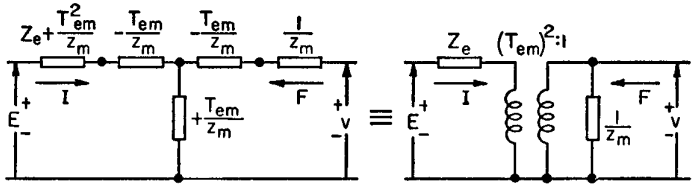

Fig. 3.4. Alternative equivalent forms of an electric-network analog for electromagnetic coupling making use of the mobility analog for the mechanical mesh.

In general, the E–v, I–F (mobility) pairing is related to the more conventional E–F, I–v (impedance) association by the duality principle that relates nodal and mesh analyses of electric networks. P. Le Corbeiller [7] has discussed in a very illuminating way the relation of this general principle to the analogies between electric networks and all-mechanical systems. The analog problem for electromagnetic coupling, however, presents the anomalous situation in which one half only of the physical system — and it may be either the electrical or the mechanical half — must be represented by its dual in order to obtain a self-consistent network representation. Such an introduction of mixed duality has been discussed by H. Jefferson [8] and by A. Bloch,[9] the latter pointing out again the close kinship previously noted by Le Corbeiller [10]

[6] F. A. Firestone, "New Analogy Between Mechanical and Electrical Systems," *J. Acoust. Soc. Am.* **4,** 249–267 (January 1933); see also W. Hähnle, "Die Darstellung Elektromechanischer Gebilde durch rein elektrische Schaltbilder," *Wissenschaftliche Veröffentlichungen aus dem Siemens-Konzern* **11,** part 1, 1–23 (1932).

[7] P. Le Corbeiller and Ying-Wa Yeung, "Duality in Mechanics," *J. Acoust. Soc. Am.* **24,** 643–648 (November 1952).

[8] H. Jefferson, "Notes on Electromechanical Equivalence," *Wireless Engineer* **21,** 563–570 (1944); also "Gyroscopic Coupling Terms," *Phil. Mag.* [7] **36,** 223–224 (March 1945).

[9] A. Bloch, "Electromechanical Analogies and their Use for the Analysis of Mechanical and Electromechanical Systems," *J. Inst. Elec. Engrs. (London)* **92,** Part I, 157–169 (April 1945); also "A new Approach to the Dynamics of Systems with Gyroscopic Coupling Terms," *Phil. Mag.* [7] **35,** 315–334 (May 1944).

[10] P. Le Corbeiller, "Origine des termes gyroscopiques," *Annales des Postes, Télégraphes et Téléphones* **18,** 1–22 (1929).

between electromagnetic coupling and the mechanical coupling between two orthogonal axes of a gyrostat. In dealing with duality transformation within the interior of the network, Jefferson introduced and discussed some of the properties of an "inverting transformer" or "reciprocating ideal transformer of ratio $1:j$". The suggestive term *gyrator* was proposed later by Tellegen [11] for any network element that exhibits a similar inverting property. These authors pointed out that an all-electric gyrator can be realized with a combination of passive network elements and a unilateral amplifier, and more recent work [12] indicates that the transistor, under certain conditions, can serve this function in an especially simple way.

Bloch called attention to some inconsistencies that can arise in dealing with antisymmetrical coupling by just introducing an ideal transformer with an imaginary turns ratio. These difficulties had already been overcome, in part at least, by still another method of handling this problem that was proposed by M. H. Hebb [13] and which amounts to a simple substitution of variables. If the mechanical force and velocity appearing in Eqs. (3.1) are effectively shifted 90° in phase, by setting $F = jF'$ and $v = jv'$, these equations become, in terms of the primed variables,

$$\begin{aligned} E &= Z_e I + jT_{em}v', \\ F' &= -jT_{me}I + z_m v'. \end{aligned} \tag{3.9}$$

It follows that if $T_{em} = -T_{me}$, the formal symmetry is restored and an equivalent circuit like that of Fig. 3.1 can be drawn, with jT_{em} replacing T and with the phase-shifted variables F' and v' appearing in the mechanical mesh. The ideal transformers that appear when the circuit of Fig. 3.1 is transformed as in Fig. 3.3 will, as in Jefferson's proposal, exhibit an imaginary turns ratio; but this scheme does deal successfully with the antisymmetry dilemma and leads to terminal meshes involving conventional electric and mechanical impedances. This is especially advantageous when the mechanical system is to be coupled to an acoustic

[11] B. D. H. Tellegen, "The gyrator, a new electric network element," *Philips Research Reports* **3,** 81–101 (April 1948).

[12] See, for example, Fig. 11 and related discussion in R. M. Ryder and R. J. Kircher, "Some Circuit Aspects of the Transistor," *Bell System Tech. J.* **28,** 367–400 (July 1949); also, R. L. Wallace, Jr. and G. Raisbeck, "Duality as a Guide in Transistor Circuit Design," *ibid.* **30,** 381–417 (April 1951).

[13] Hebb's method was used in transducer design work at the Harvard Underwater Sound Laboratory during 1943–1945 and is reported in Chapter 3 of the *Summary Technical Report* . . . (see note 1, Chapter 4).

medium, as in the present instance, since the dimensions of mechanical impedance permit easy transformation or coupling to the acoustic impedances that characterize the sound-transmission medium.[14] In this case, however, the method used to achieve this advantage is quite arbitrary, and it has the serious disadvantage that it exhibits an apparent time-phase difference between the electrical and mechanical variables that does not exist in the physical system.

Sign Conventions and Symmetry: A New Approach

Any proper analytical formulation of the principles of mechanical interaction between currents and magnetic fields must always include rules for determining the direction as well as the magnitude of the mechanical forces and emf's arising from the interaction. The simple case of a straight conductor lying in a steady transverse magnetic field will serve to illustrate the logical process of formulation. According to Ampère's law, the wire carrying a current I will experience a force F of magnitude BlI, where B is the magnetic induction and l is the length of wire in the field (mks units). In addition to stating the magnitude relation $F = BlI$, a supplementary statement must be made about the *direction* of the force in relation to the directions of B and I. This directional information may be given in any one of three forms:

(*a*) Apply Fleming's *left-hand rule* (point the forefinger along $+B$ and the middle finger along $+I$; then the thumb will point in the direction of $+F$);

(*b*) Write $\mathbf{F} = l(\mathbf{I} \times \mathbf{B})$, and *define* the vector cross product as another *vector*, called an axial vector, directed normal to the plane containing **B** and **I** and positive in the direction that a right-hand screw would advance when turned in the direction to carry **I** into coincidence with **B**;

(*c*) Write $F = Blk I$, and define k as a space operator that rotates the positive direction of the vector that follows it, $+I$, by 90° counterclockwise around the direction of the vector, $+B$, that precedes it, in order to determine the positive direction of F. [See Fig. 3.5(*a*).]

Before comparing these different forms of expressing the physical laws governing motor action, consider the corresponding expressions relating to generator action. According to Faraday's law, the conductor moving with velocity v will have induced in it an emf E of magnitude

[14] P. W. Smith, Jr., "Analogies and Schematic Networks," *J. Acoust. Soc. Am.* **25**, 828 (A) (July 1953).

Blv. The additional statements required to establish the direction of the induced emf are obliged also to satisfy Lenz's law, which expresses for electromagnetism Nature's uniform habit of opposing departures from equilibrium with a contrary reaction. As before, these supplementary statements may take three forms:

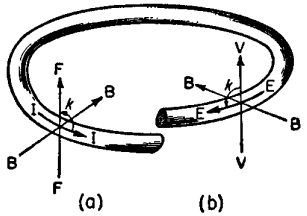

FIG. 3.5. Schematic illustration of the role of the space operator k in determining the directions of F and E for the case of a movable conductor in a fixed magnetic field. Note that k rotates the direction of I or V counterclockwise around the positive direction of B.

(*a*) Apply Fleming's right-hand rule (point the forefinger along $+B$ and the thumb in the direction of motion; then the middle finger will point in the direction of the induced emf);

(*b*) Write the emf as $\mathbf{E} = l(\mathbf{v} \times \mathbf{B})$, and, as before, *define* the vector cross product as an axial vector whose positive direction corresponds to the advance of a right-hand screw turning to bring **v** into coincidence with **B**;

(*c*) Write $E = Blkv$, and, as before, *define* k as a space operator rotating the positive direction of the following vector, v, by 90° counterclockwise around the preceding vector, $+B$, in order to determine the positive direction of the induced emf E. [See Fig. 3.5(*b*).]

No choice can be made among these expressions on the basis of correctness, since each is written in such a way as to give results that agree with experiment. The right- and left-hand rules give the comfortable assurance of a direct appeal to experiment, but they are obviously not well adapted for mathematical manipulation. The arbitrary symbolism of each of the other forms is adapted to such manipulation. That the vector language used in the expressions (*b*) provides a powerful mathematical tool is beyond question, but its power and generality are not ordinarily invoked in the present application. In practical electromechanical systems the construction usually constrains each of the quantities E, I, B, F, and v to a fixed line of action, so that the equations in (*b*) can be (and usually are) written as scalar relations. Then if the positive directions of E and I, and of F and v, coincide, these scalar relations become $F = BlI$, and $E = -Blv$, and put boldly into evidence the antisymmetry discussed above. On the other hand, *symmetry is*

preserved in these relations when choice (c) is exercised and the sign convention is embodied symmetrically in the space operator **k**, as exemplified by writing

$$F = BlkI,$$
$$E = Blkv. \tag{3.10}$$

The operator **k** is neither more nor less arbitrary than the vector symbolism of (*b*). Since it only turns, or rotates, the direction in space of the quantity it "multiplies," without altering the magnitude of the quantity, it can be assigned the absolute magnitude unity. When applied twice to the same quantity, the total rotation of 180° corresponds to a change of sign, so that $k^2 = -1$. There is a vital inherent difference between **k** and the imaginary j, however, since **k** signifies a 90° rotation in physical space, rather than a 90° rotation in the complex plane where rotating "vectors" (or *phasors*, according to revised terminology) represent, by their projection on a fixed axis, harmonic variation with time.

Readers who are or who may become familiar with Hamilton's quaternions will recognize **k** as a *versor*. Only a little of the theory of quaternions needs to be invoked in order to deal with the problem in hand, which is probably fortunate in view of the extent to which vector analysis has displaced quaternions in science teaching. For example, the one additional property of the new space operator **k** that needs to be introduced at this time is the fact that it does not commute with the conventional "time" imaginary j; instead, one has the relation $jk = -kj$. This is "standard behavior" for quaternion space operators, and it turns out to be just what is needed to deal systematically and successfully with interconnected and coupled systems involving both electrostatic and electromagnetic (or gyroscopic) coupling. E. M. McMillan [15] pointed out first, and a good many others have discussed since, the fact that a linear passive system of bilateral elements can violate the reciprocity theorem with respect to magnitude as well as sign if it contains both symmetrical and "antisymmetrical" coupling devices. This conclusion is in no sense contradicted by the restoration of symmetry gained for electromagnetic coupling by the introduction of the **k** operator. Instead, the full power of electric-circuit analysis is now made available for the analysis of such mixed systems by virtue of the fact that a homogeneous network representation can be used for the entire system.

[15] Edwin M. McMillan, "Violation of the Reciprocity Theorem in Linear Passive Electromechanical Systems," *J. Acoust. Soc. Am.* **18**, 344–347 (October 1946).

The example of a moving conductor in a steady magnetic field has been discussed in some detail. There is another electromagnetic situation providing electromechanical coupling that can be discussed in substantially the same way. This is the case in which mechanical action occurs along the direction lines of the magnetic-induction vector. Two examples of this type are of practical importance: the tractive force across an air gap in a ferromagnetic circuit and the strain induced by magnetization in a magnetostrictive material. Coupling to the external electric circuit is provided in these cases by a fixed coil of wire linking

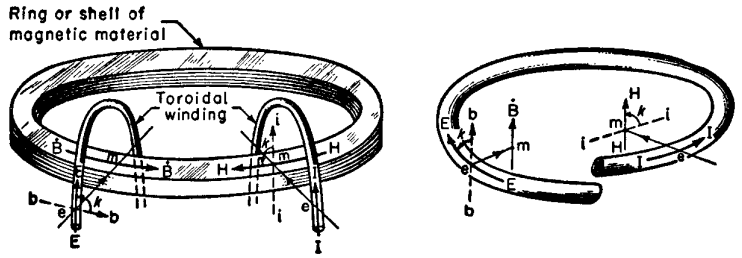

FIG. 3.6. Schematic illustrations of the role of the space operator **k** in determining the directions of H and E for the case of a fixed winding on a magnetic core. Note that **k** rotates the (translated) direction of I or B counterclockwise around a line ($e \rightarrow m$) directed from the electric to the magnetic site.

the magnetic circuit. In vector notation, the required expressions are obtained by manipulation of the fundamental relations curl $\mathbf{H} = \mathbf{I}$ and curl $\mathbf{E} = -\mathbf{B}$, where $\mathbf{H}$ is the magnetic-field vector and $\mathbf{E}$ stands in this case for the electric-field vector whose line integral around a complete circuit gives the electromotive force. These curl vectors, like the vector products that appeared before, are represented as axial vectors whose direction and sense are defined arbitrarily, and they are used here with the sign conventions adjusted to give results that accord with experiment — but again the antisymmetry dilemma rears its head. As before, a parallel formulation using the rotational operator **k** preserves the symmetry and delivers the necessary relations in the form

$$H = \frac{N}{l} kI,$$
$$E = NAk\dot{B}, \tag{3.11}$$

where l is the length and A the cross-sectional area of the magnetic path, and N is the number of turns in the coil linking the magnetic circuit. The space operator k acts again to rotate the direction of $+I$, or the direction of increasing B, by 90° counterclockwise, this time around a line directed from the site at which the current or the induced electromotive force is observed toward the point where H or the change in B is observed. (See Fig. 3.6.)

In the following chapters the transduction coefficients will be considered in detail for representative exemplars of each of the principal types of electromechanical coupling. The introduction of the rotational operator in the analysis of the electromagnetic systems will permit the common properties of all these coupling systems to be displayed. For example, in electrostatic systems, the mechanical forces arise from direct interaction between electric charges, as typified in Coulomb's classical experiments. But since the transduction coefficient is defined as a force-to-*current* ratio in the steady state, the differentiation of charge with respect to time (to yield current) always leads to the appearance of the time-imaginary j in the transduction coefficient for electrostatic or piezoelectric systems. The preceding discussion of electromagnetic coupling has indicated that the space-imaginary k appears with corresponding uniformity in those cases. The appearance of an imaginary factor, representing either time phase or space quadrature, thereby emerges as a universal feature of the transduction coefficients that characterize electromechanical coupling. As a result, the theory of electromechanical systems becomes substantially identical with the theory of electric networks. No attempt will be made here to point out all the relevant aspects of electric-network theory (such as the background for filter and equalizer design, the use of Thévenin's theorem, the compensation theorem, and so on), but the reader is warned that professional competence in electroacoustics demands either thorough understanding of electric-network theory or an equally extensive study of what might be called "high-frequency" mechanics.

CHAPTER 4

Electric-Impedance Analysis of Transducer Performance

It was suggested in Chapter 2 that a substantial amount of information concerning the electromechanical behavior of a transducer can be deduced from the analysis of impedance measurements made at the electric terminals of the transducer. The fruitfulness of this procedure can now be examined in detail.[1] The behavior that is to be regarded as typical for the various impedances that appear in the equations will vary from one transducer type to another, and these differences will sometimes suggest that different experimental techniques would be advantageous for their measurement. Nevertheless, it will be useful to set forth some of the general relations that are relevant for all transducer types in order that these may provide a common basis of reference for discussing later the specialized interpretations that are appropriate for particular transducers.

Consider first the two terms that appear [cf. Eq. (2.6)] in the expression for Z_{ee}, the total driving-point impedance,

$$Z_{ee} = Z_e + Z_{mot} = Z_e + \frac{(-T_{em}T_{me})}{z_m}. \tag{4.1}$$

When the mechanical system is "blocked," or clamped so that it cannot move, the electric impedance Z_e, and its variation with frequency, can be measured directly. The motional impedance can then be found, after making similar measurements when the mechanical system is allowed

[1] Much of the material of this chapter is based on research conducted at the Harvard Underwater Sound Laboratory and reported in unpublished Internal Memoranda and in the *Summary Technical Report of Division 6, NDRC*, Vol. 13. Microfilm or photostatic copies of the unclassified portions of this report, which includes all the material drawn on here, are available [identified as PB 77,669] from the U. S. Department of Commerce, Office of Technical Services.

to vibrate without external restraint, by subtracting Z_e from Z_{ee} at each frequency of measurement. The required vectorial subtraction can be carried out graphically and the vectors can then be translated to a common origin. However, it is sometimes difficult, if not impossible, to "block" adequately the motion of the mechanical system, especially for transducers designed to operate in water. In such cases it is necessary to infer the shape of the blocked-impedance locus by drawing a curve that joins smoothly the measured values of Z_e made at frequencies far below and far above resonance. Such an interpolation can usually be made with greater accuracy if the measurements of Z_{ee} are plotted in rectangular coördinates as shown in Fig. 4.1(a). When the observed

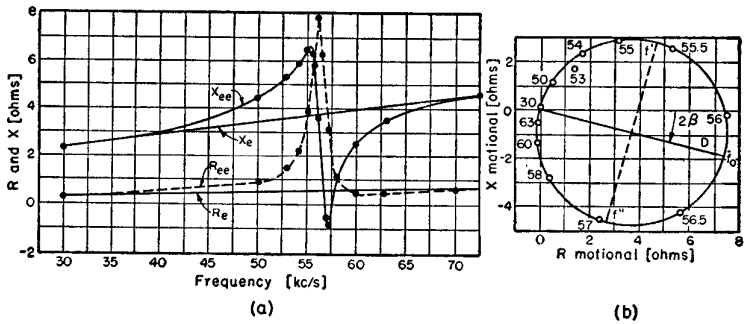

FIG. 4.1. (a) Typical resistance and reactance data for a magnetostriction transducer operating in air ("free") and the interpolated curves corresponding to the blocked condition; (b) the vector locus of motional impedance derived from the data of (a). [From reference 1 of Chapter 4.]

data are available in this form, direct subtraction yields at once the R- and X-coördinates of each point on the motional-impedance locus:

$$\begin{aligned} R_{mot} &= R_{ee} - R_e, \\ X_{mot} &= X_{ee} - X_e, \end{aligned} \tag{4.2}$$

where corresponding subscripts are used to identify the real and imaginary parts of complex impedances according to the uniform convention $Z_a = R_a + jX_a$. By proceeding in this way the motional-impedance circle can be plotted as shown in Fig. 4.1(b), and its diameter and the resonance and quadrantal frequencies can be scaled off directly or deduced by interpolation.

Evaluation of Mechanical Constants

The diameter of the motional-impedance circle is simply related to one of the constants of the mechanical system since the mechanical impedance reduces to r_m at resonance. Thus Eq. (4.1) can be specialized in this case to read

$$D = |Z_{mot}|_{max} = \left|\frac{-T_{em}T_{me}}{r_m}\right| = \frac{A^2}{r_m}, \tag{4.3}$$

where A^2 has been introduced as an abbreviation for the absolute value of the product of the transduction coefficients.

Two other relations among the mechanical constants are available in Eqs. (2.11) and (2.13), which are repeated here for reference:

$$\omega_0 = \frac{1}{\sqrt{l_m c_m}}, \tag{4.4}$$

$$\omega'' - \omega' = \frac{r_m}{l_m}. \tag{4.5}$$

The three relations represented by Eqs. (4.3), (4.4), and (4.5) need to be fortified by a fourth relation in order to permit the magnitude of the force factor A and all three mechanical constants r_m, l_m, and c_m to be fixed uniquely. Such a relation can usually be obtained most easily by producing some known change in one of the mechanical constants and redetermining the resonance frequency. The *added-mass method*, for example, requires only the attachment of an auxiliary mass δl_m to the moving system and the redetermination of the new resonance frequency ω_{0M}. This new resonance frequency can be expressed by an equation similar to Eq. (4.4); thus

$$\omega_{0M}^2 = \frac{1}{c_m(l_m + \delta l_m)}. \tag{4.6}$$

Elimination of the mechanical compliance c_m between Eqs. (4.4) and (4.6) leads to the following expression for the effective mass of the mechanical system:

$$l_m = \frac{\delta l_m \omega_{0M}^2}{(\omega_0^2 - \omega_{0M}^2)}. \tag{4.7}$$

This value of l_m can then be used in Eq. (4.5) to find the resistance r_m, and this can in turn be used in Eq. (4.3) to determine the magnitude of the force factor. This round-up of system constants is completed by

observing that the lagging phase angle β to be associated with the force factor A is just half the dip angle of the diameter of the motional impedance circle, and that this angle can be deduced directly from the measurements made to determine the motional-impedance circle.

An alternative method of evaluating the magnitude of the force factor involves a measurement of the amplitude of mechanical vibration at the resonance frequency for a measured value of the exciting current. This procedure is often more troublesome experimentally than is the added-mass method, but its examination will introduce some useful relations. An equation involving the force factor, the displacement, and the current can be obtained by evaluating the "current transformation ratio" v/I, and by introducing the vibratory displacement ξ through the familiar steady-state relation, $v = j\omega\xi$. The ratio of velocity to current can be found by solving the basic coupling equations [cf. Eqs. (3.1)] for v and for I with the external force set equal to zero. This leads to

$$\frac{j\omega\xi}{I} = \frac{v}{I} = \frac{\Delta_{12}}{\Delta_{11}} = \frac{-T_{me}}{z_m}. \tag{4.8}$$

The last term in Eq. (4.8) can be recognized as the ratio of Z_{mot} to T_{em} so that Eq. (4.8) can also be written

$$\frac{j\omega\xi}{I} = \frac{Z_{mot}}{T_{em}}. \tag{4.9}$$

Finally, since it is only the magnitude of the displacements and currents that will be observed experimentally, and since the motional impedance at resonance is just the diameter of the impedance circle, the resonance values can be identified by zero subscripts and Eq. (4.9) rewritten as

$$| T_{em} | = \frac{DI_0}{\omega_0\xi_0} = A. \tag{4.10}$$

The mechanical constants determined by the foregoing procedures are "effective constants" that include all effects of the vibratory motion without differentiating between mechanical power dissipated internally and that delivered to an associated load. As a result these procedures are chiefly useful in dealing with vibration instruments such as galvanometers, or telephone receivers having a single effective degree of mechanical freedom. However, since the transfer of power to a load constitutes a primary function of most of the transducers to be considered, it will be useful to particularize the mechanical impedance z_m so that the effects of acoustic loading can be separated from those associated with

the inherent properties of the mechanical system. This can be done by replacing the external force appearing in Eqs. (3.1) by $F = -vZ_L$ and transposing, or more simply by redefining the mechanical impedance z_m through

$$z_m \equiv Z_m + Z_L = (R_m + R_L) + j(X_m + X_L), \tag{4.11}$$

where the subscript L identifies the resistance and reactance associated with the external load, and the subscript m identifies the resistance and reactance that describe the mechanical system exclusive of load. If the effective mass and stiffness of the loaded mechanical system are identified by M and K respectively, Eq. (4.11) can be rewritten in the form

$$Z_m + Z_L = (R_m + R_L) + j\left(\omega M - \frac{K}{\omega}\right). \tag{4.12a}$$

This equation can also be cast in a variety of other forms that will introduce some abbreviations which will prove useful later:

$$(Z_m + Z_L) = (R_m + R_L)(1 + j2Qp) = | Z_m + Z_L | e^{j\theta}; \tag{4.12b}$$

$$2Qp = \frac{X_m + X_L}{R_m + R_L} = \tan\theta; \tag{4.12c}$$

$$\omega_0^2 = \frac{K}{M}; \quad Q = \frac{\omega_0 M}{R_m + R_L} = \frac{K}{\omega_0(R_m + R_L)} = \frac{\sqrt{MK}}{R_m + R_L}; \tag{4.12d}$$

$$p \equiv \frac{1}{2}\left(\frac{\omega}{\omega_0} - \frac{\omega_0}{\omega}\right); \quad p \doteq \frac{\omega}{\omega_0} - 1, \quad \text{when} \quad \omega \doteq \omega_0. \tag{4.12e}$$

Transduction Coefficients and the Vector Force Factor

It will be prudent to examine more closely the introduction of A as an abbreviation for the force factor. In the preceding chapter it was demonstrated that transducers obeying the reciprocity principle have identical transduction coefficients for either direction of energy transmission, and that each transduction coefficient always contains either a time- or a space-quadrature factor. As a consequence, the quadrature term can be factored out and the remainder of the transduction coefficient defined as the *vector force factor*, Z_{em}; thus,

$$T_{em} = T_{me} = (j \text{ or } k)Z_{em} = (j \text{ or } k)(R_{em} + jX_{em}). \tag{4.13}$$

Factoring the transduction coefficients in this way has a sound physical basis. The quadrature factor appears in the transduction coefficient either to express the time quadrature existing in the steady state be-

tween current and electric charge, or to express the intrinsic orthogonality of the force reactions in electromagnetism. The complex force factor represents by its magnitude the scalar ratio of transduction, and by its phase angle the influence of any dissipative effects that are inherently coupled to the transducing mechanism. For example, the imaginary part of Z_{em} will be found to derive either from dielectric absorption in electrostatic coupling or from the effect of eddy currents and hysteresis associated with the magnetic-induction field in electromagnetic coupling. Detailed accounting for these effects can be deferred until specific transducer mechanisms are considered, and for the present it will be sufficient to represent the force factor as a vector with magnitude A and a lagging phase angle measured by β. These defining relations can be written in a variety of forms that will provide useful algebraic tools for subsequent manipulations:

$$Z_{em} = R_{em} + jX_{em} = Ae^{-i\beta}; \qquad \tan\beta = \frac{-X_{em}}{R_{em}}; \tag{4.14a}$$

$$(-T_{em}T_{me}) = -(j \text{ or } k)^2(R_{em} + jX_{em})^2 = (R_{em}^2 - X_{em}^2) + j(2R_{em}X_{em}) \tag{4.14b}$$

$$= A^2e^{-i2\beta}; \qquad \tan 2\beta = \frac{-2R_{em}X_{em}}{R_{em}^2 - X_{em}^2};$$

$$|Z_{em}| = |R_{em} + jX_{em}| = |T_{em}| = |T_{me}| = A = (R_{em}^2 + X_{em}^2)^{\frac{1}{2}}; \tag{4.14c}$$

$$|-T_{em}T_{me}| = |T_{em}|^2 = |T_{me}|^2 = A^2 = R_{em}^2 + X_{em}^2; \tag{4.14d}$$

$$\frac{R_{em}^2 - X_{em}^2}{R_{em}^2 + X_{em}^2} = \cos 2\beta; \qquad \frac{-2R_{em}X_{em}}{R_{em}^2 + X_{em}^2} = \sin 2\beta. \tag{4.14e}$$

Efficiency Considerations

One purpose of marshaling this algebraic ammunition is to facilitate an examination of the over-all efficiency at which the transducer operates and the conditions required for best matching of the transducer and its load. The over-all efficiency can be defined in its most fundamental terms as the ratio of the power delivered to an external load connected at the output terminals of the transducer to the total power accepted at its input terminals. Since the load is represented in the output mesh of the transducer by Z_L, the efficiency can be written at once as

$$\text{Efficiency} \equiv \eta \equiv \frac{R_L|v|^2}{R_{ee}|I|^2} = \frac{R_L|T_{em}|^2}{R_{ee}|Z_m + Z_L|^2}, \tag{4.15}$$

wherein the ratio of the squares of the absolute values of velocity and current has been taken from Eq. (4.8). With the further help of Eqs. (4.3), (4.14), and (4.12), the efficiency can also be written in the alternative forms

$$\eta = \frac{R_L}{|Z_m + Z_L|}\frac{|Z_{mot}|}{R_{ee}} = \left[\frac{R_L}{R_m + R_L}\right]\left[\frac{R_{em}^2 + X_{em}^2}{(1 + 4Q^2p^2)(R_m + R_L)(R_e + R_{mot})}\right]$$

$$= \frac{R_L}{R_{ee}}\frac{|Z_{mot}|^2}{|T_{em}|^2} = \frac{R_L|Z_{mot}|^2}{R_{ee}A^2}. \tag{4.16}$$

In view of the definition of η as a gross over-all electromechanical efficiency, it would seem at first sight reasonable to interpret the factor $R_L/(R_M + R_L)$ in the second equality of Eq. (4.16) as a purely mechanical efficiency since it represents the fraction of the total mechanical power made available by transduction that is actually delivered to the external load R_L. Such a separation of the gross efficiency into mechanical and electromechanical factors is not always unambiguous, however, since the second factor can sometimes exceed unity (although the product, of course, never can). For any fixed condition of transducer operation, there is usually no simple way to evaluate the mechanical efficiency, or, as it might better be called, the mechanical power-utilization factor, $R_L/(R_m + R_L)$. This situation is similar, however, to the one considered above, where an additional relation needed to determine the mechanical constants was obtained by adding a mass to the vibrating system and redetermining the resonance frequency. Since a resistance ratio is involved in this case, the additional relations can be obtained by changing the external load resistance and observing the corresponding change in the diameter of the motional-impedance circle. Moreover, the known change in external load resistance that can be produced most easily is to remove the external load entirely. For transducers whose useful output is in the form of sound radiation, the external load can be removed by operating the transducer in a vacuum, and measurements pertaining to such an unloaded condition will be identified by the subscript V. This reference condition is especially easy to achieve for transducers designed to radiate sound in water or other liquid medium, since they can be "unloaded" to a satisfactory degree merely by operating them in air.

The mechanical power-utilization factor can be evaluated simply in terms of the loaded (D_L) and the unloaded (D_V) diameters of the motional-impedance circle, as may be seen by writing out the motional

impedance explicitly in the notation made available by Eqs. (4.12) and (4.14):

$$\begin{aligned} Z_{mot} &= \frac{(-T_{em}T_{me})}{Z_m + Z_L} = \frac{(R_{em}^2 - X_{em}^2) + j2R_{em}X_{em}}{(R_m + R_L)(1 + j2Qp)} = \frac{D_L(\cos 2\beta - j \sin 2\beta)}{1 + j2Qp} \\ &= \frac{(R_{em}^2 - X_{em}^2)(R_m + R_L) + 2R_{em}X_{em}(X_m + X_L)}{(R_m + R_L)^2 + (X_m + X_L)^2} \\ &\quad + j\frac{2R_{em}X_{em}(R_m + R_L) - (R_{em}^2 - X_{em}^2)(X_m + X_L)}{(R_m + R_L)^2 + (X_m + X_L)^2} \\ &= \frac{D_L}{(1 + 4Q^2p^2)^{\frac{1}{2}}}\left(\frac{\cos 2\beta - j \sin 2\beta}{\cos\theta + j \sin\theta}\right) = \frac{D_L}{(1 + 4Q^2p^2)^{\frac{1}{2}}} e^{-j(2\beta+\theta)}. \end{aligned} \tag{4.17}$$

The normalized frequency variable p vanishes conveniently at the frequency of mechanical resonance, and so does θ, the phase angle of the total mechanical impedance. Note that θ is shown explicitly by the last line of Eq. (4.17) to be the angle by which the motional-impedance vector deviates from 2β, the inclination of the resonance diameter. By further reference to Eqs. (4.12), the loaded and unloaded resonance diameters can be extracted from Eq. (4.17) by inspection, and the mechanical power-utilization factor can then be expressed readily, either in terms of these diameters or in terms of the loaded and unloaded values of Q:

$$\begin{gathered} D_L = \frac{R_{em}^2 + X_{em}^2}{R_m + R_L}; \quad D_V = \frac{R_{em}^2 + X_{em}^2}{R_m}; \\ \frac{R_L}{R_m + R_L} = \frac{D_V - D_L}{D_V} = \frac{Q_V - Q_L}{Q_V}. \end{gathered} \tag{4.18}$$

Return now to further consideration of the gross efficiency. With the help of Eq. (4.17), the efficiency equation (4.16) can be rewritten in either of the following two forms, the first of which is arranged to show the influence of the frequency variable p; the second is obtained by reverting to the primary variables and manipulating the expression so as to display the denominator factored in a useful way:

$$\eta = \frac{R_L}{(R_m + R_L)} \frac{R_{em}^2 + X_{em}^2}{R_e(R_m + R_L)(1 + 4Q^2p^2) + R_{em}^2 - X_{em}^2 + 4R_{em}X_{em}Qp}; \tag{4.19}$$

$$\eta = \frac{R_eR_L(R_{em}^2 + X_{em}^2)}{[R_e(R_m + R_L) + R_{em}^2][R_e(R_m + R_L) - X_{em}^2] + [R_e(X_m + X_L) + R_{em}X_{em}]^2}. \tag{4.20}$$

At the frequency of mechanical resonance, $p = 0 = X_m + X_L$, and the motional impedance reduces to the diameter of the impedance circle. As a result, either of Eqs. (4.16), (4.19), or (4.20) may be used as a basis for writing the efficiency at resonance as

$$\eta_{res} = \frac{(D_V - D_L)}{D_V}\frac{D_L}{R_{ee}} = \frac{D_V - D_L}{D_V}\frac{D_L}{(R_e + D_L \cos 2\beta)}. \tag{4.21}$$

The significance of these relations can be demonstrated with the help of Fig. 4.2 in which the impedance loci are plotted for both air and water

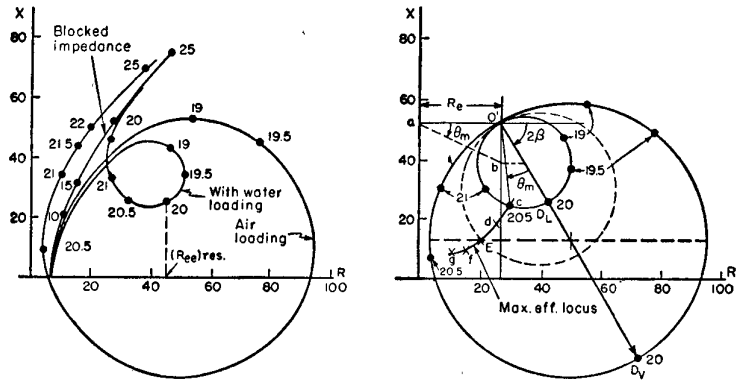

FIG. 4.2. Vector-impedance loci and the derived motional-impedance circles for an experimental magnetostriction transducer operating in air and in water.

loading of an experimental magnetostriction transducer. It is of some interest to note that, in spite of the fact that this particular transducer had a relatively high-resistance winding, relatively high internal mechanical damping, and a considerable amount of leakage reactance, its motional impedance in the unloaded condition is such as to make the total input impedance remain capacitive over a substantial frequency interval. The various quantities appearing in Eq. (4.21) can be scaled off directly from these impedance loci and, since the efficiency is a numeric, they can be measured in any convenient units without regard for the actual values of resistance and reactance appearing on the abscissa and ordinate scales. In this way the mechanical power-utilization factor for the loading used for the "water circle" of Fig. 4.2 can be evaluated as approximately 0.66, and the over-all efficiency at resonance as 0.45.

Conditions for Maximum Efficiency

While it is customary to assume that maximum efficiency always occurs at "resonance," a closer examination of Eqs. (4.19) and (4.20) reveals that a still higher efficiency can be obtained for some other value of frequency or reactance than the one for which $p = 0 = X_M + X_L$. Thus, if all variables remain constant except the frequency, the condition for maximum efficiency can be found by setting the derivative of the denominator of Eq. (4.19) equal to zero. Alternatively, if everything else remains fixed and only the total reactance can be varied, it is obvious that the reactance should be "tuned" in such a way as to make the squared term in the denominator of Eq. (4.20) vanish. Either approach leads to equivalent conditions for maximum efficiency, which are

$$2Qp = \frac{-R_{em}X_{em}}{R_e(R_m + R_L)} = \tan\theta_m = \frac{D_L \sin 2\beta}{2R_e}; \qquad (4.22a)$$

$$(X_m + X_L) = \frac{-R_{em}X_{em}}{R_e}. \qquad (4.22b)$$

When the dip angle is positive, as it is for electromagnetic transducers, R_{em} and X_{em} are always of opposite sign, and maximum efficiency occurs at a frequency somewhat higher than the resonance frequency, as may be seen by solving Eq. (4.22*a*) for the frequency parameter,

$$(p)_{\text{max eff}} = \frac{D_L \sin 2\beta}{4R_eQ_L} = \frac{(-X_{mot})_{\text{res}}}{4R_eQ} = \frac{-R_{em}X_{em}}{2R_e\sqrt{MK}}. \qquad (4.23)$$

It may be noted that the value of p required for maximum efficiency is independent of the load, since load changes affect D_L and Q_L proportionally, so it can be evaluated most easily in terms of the data for the unloaded impedance circle. The corresponding value of efficiency, when it is maximized by variation of either frequency or reactance, is to be found by putting conditions (4.22) or (4.23) into Eqs. (4.19) or (4.20). For the latter, this merely amounts to dropping the squared term from the denominator, with the result shown in Eq. (4.24*a*). A little algebraic manipulation then makes it possible to rewrite the maximum efficiency in terms of quantities that can be scaled off more easily from the impedance diagram, as shown in Eq. (4.24*b*):

$$\eta_{\max} = \frac{R_eR_L(R_{em}^2 + X_{em}^2)}{[R_e(R_m + R_L) + R_{em}^2][R_e(R_m + R_L) - X_{em}^2]} \qquad (4.24a)$$

$$= \left(\frac{D_V - D_L}{D_V}\right)\left[\frac{D_L \cos^2\theta_m}{R_e + D_L \cos\theta_m \cos(2\beta + \theta_m)}\right]. \qquad (4.24b)$$

The increase in efficiency made available by operating at the maximum-efficiency point, rather than at resonance, is by no means trivial, and may amount to as much as two-to-one when the transducer is lightly loaded. The relative increase in efficiency can be evaluated explicitly by dividing Eq. (4.24*b*) by Eq. (4.21), which gives

$$\frac{\eta_{\max}}{\eta_{\text{res}}} = \frac{(R_e + D_L \cos 2\beta)}{R_e + D_L \cos\theta_m \cos(2\beta + \theta_m)} \cos^2\theta_m = \frac{(\text{total resistance at resonance})\ \cos^2\theta_m}{\text{total resistance at maximum efficiency}}. \qquad (4.25)$$

The operating point for maximum efficiency can be located on the motional-impedance locus by a simple graphical construction illustrated in Fig. 4.2. If the center of the loaded circle is projected horizontally to the point b on the vertical through O', the vertical distance $O'b$ can be identified as half the motional reactance at resonance. When the point b is joined to a, which lies on the horizontal through O', the angle $O'ab$ is just the mechanical phase angle θ_m, as may be verified by reference to Eq. (4.22*a*). By drawing the line $O'c$ so that it makes the same angle θ_m with the resonance diameter, as shown, the intersection of $O'c$ with the motional-impedance circle at c establishes the operating point for maximum efficiency under this particular condition of loading. By repeating this operation for different assumed values of D_L, the graphical construction for each corresponding value of θ_m can be carried out and the intersections they determine with the various D_L circles can be identified as the sequence of points labeled c, d, E, f, g. A line drawn through these points then constitutes a *maximum-efficiency locus*, along which the frequency variable p has the constant value given by Eq. (4.23).

The graphical construction for each of these assumed conditions of loading yields the quantities needed in order to use Eqs. (4.21) and (4.24*b*) to calculate the maximum efficiency and the efficiency at resonance. As an alternative, the graphical construction can be avoided altogether by assuming arbitrary values of D_L, using Eq. (4.22*a*) to find θ_m, and putting these results into Eqs. (4.21) and (4.24*b*). The same results are obtained by either procedure and can be tabulated as in Table 1, or plotted as shown in Fig. 4.3. Examination of these results will show that the electromechanical factor in the efficiency equation can indeed exceed unity, as suggested in the discussion following Eq. (4.16). It is also revealed — and this might have been expected at the outset — that the maximum efficiency and the efficiency at resonance

TABLE 1. Computation of efficiency at resonance and maximum efficiency, under different assumed loading conditions, for the transducer of Fig. 4.2.

Point in Fig. 4.2	$\frac{D_L}{D_V}$	$\frac{R_L}{R_L+R_M}$ $=1-\frac{D_L}{D_V}$	$\frac{R_L}{R_M}$ $=\frac{D_V-D_L}{D_L}$	$\cos\theta_M$	$\frac{R_e}{D_L}$ $=\frac{R_e}{D_V}\frac{D_V}{D_L}$	η_{res}	η_{max}	$\frac{\eta_{max}}{\eta_{res}}$
	1.0	0	0		0.294	0	0	
	0.9	0.10	0.11	0.601	.33	0.12	0.40	3.29
g	.80	.20	.25	.646	.37	.23	.56	2.43
f	.68	.32	.47	.706	.43	.34	.64	1.87
E	.575	.425	.739	.7627	.510	.421	.662	1.57
d	.45	.55	1.22	.833	.65	.48	.64	1.33
c	.34	.66	1.94	.894	.86	.48	.57	1.19
	.20	.80	4.00	.959	1.47	.41	.43	1.07

Numerical data from vacuum circle: $(D_V/R_e) = 3.40$; $2\beta = 60°$.

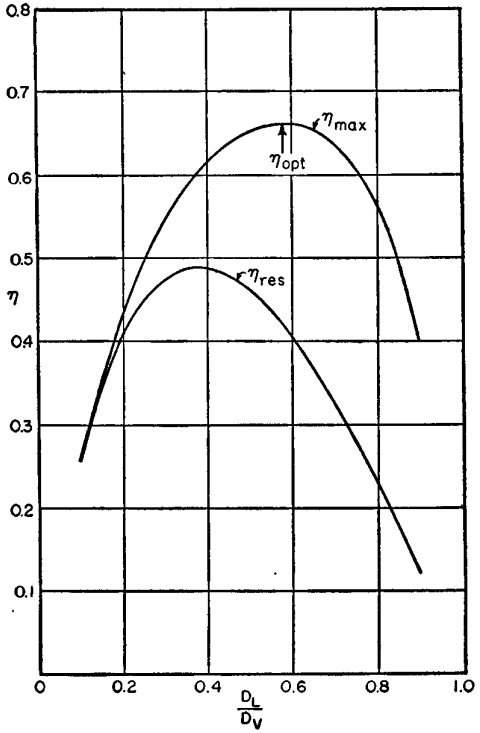

FIG. 4.3. Calculated values of maximum efficiency and the efficiency at resonance as a function of loading for the transducer of Fig. 4.2.

each has its own maximum with respect to variation of the relative loading as measured by D_L/D_V or by R_L/R_m. The relative gain in efficiency obtained by operating at a frequency above resonance is greater for light loading since the peak of the maximum-efficiency curve occurs at lighter loads than does the peak for efficiency at resonance.

The Potential Efficiency and Its Determinants

The optimum, or max-max, value of efficiency with respect to variations of *both* frequency and load resistance is called the *potential efficiency* and the condition for its occurrence can be found by setting the R_L-derivative of Eq. (4.24*a*) equal to zero: thus,

$$\left(\frac{R_L}{R_m}\right)_E = \left(1+\frac{R_{em}^2}{R_eR_m}\right)^{\frac{1}{2}}\left(1-\frac{X_{em}^2}{R_eR_m}\right)^{\frac{1}{2}} = \left(1+\frac{D_V}{R_e}\cos^2\beta\right)^{\frac{1}{2}}\left(1-\frac{D_V}{R_e}\sin^2\beta\right)^{\frac{1}{2}}, \tag{4.26}$$

where the subscript E identifies quantities associated with operation at the potential efficiency. By putting condition (4.26) back into Eq. (4.24*a*), the potential efficiency can, after some algebraic manipulation, be expressed in the forms

$$\text{Pot. Eff.} = \frac{\left(R_m+\frac{R_{em}^2}{R_e}\right)^{\frac{1}{2}}-\left(R_m-\frac{X_{em}^2}{R_e}\right)^{\frac{1}{2}}}{\left(R_m+\frac{R_{em}^2}{R_e}\right)^{\frac{1}{2}}+\left(R_m-\frac{X_{em}^2}{R_e}\right)^{\frac{1}{2}}} = \frac{\left(1+\frac{D_V}{R_e}\cos^2\beta\right)^{\frac{1}{2}}-\left(1-\frac{D_V}{R_e}\sin^2\beta\right)^{\frac{1}{2}}}{\left(1+\frac{D_V}{R_e}\cos^2\beta\right)^{\frac{1}{2}}+\left(1-\frac{D_V}{R_e}\sin^2\beta\right)^{\frac{1}{2}}}. \tag{4.27}$$

The potential efficiency is obviously an important performance criterion for any transducer, since it denotes the optimum efficiency of transduction that can be obtained under the most favorable conditions of external loading. It may be observed that all frequency and reactance variables have dropped out of the expression for potential efficiency, which is shown by Eq. (4.27) to depend only on the blocked electric resistance, the internal mechanical resistance, and the complex force factor. It may also be observed that Eq. (4.27) provides a simple neces-

sary criterion of physical realizability: since the efficiency can never exceed unity, it must always follow that

$$R_m \geq \frac{X_{em}^2}{R_e}. \tag{4.28}$$

A simpler expression for the potential efficiency than Eq. (4.27) can be obtained by considering the maximum and minimum values of the motional resistance for the unloaded circle. A little study of the geometry of the motional-impedance diagram, as suggested by the construction lines shown in the sketch of Fig. 4.4, will permit these extreme values

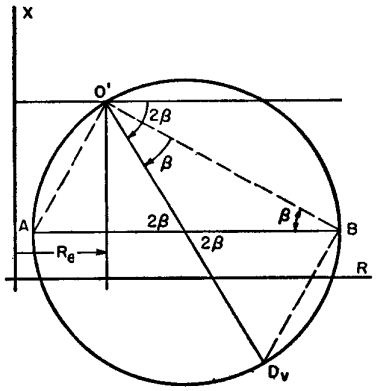

FIG. 4.4. Construction lines showing certain geometrical properties of the motional-impedance circle.

of the total electric resistance to be readily evaluated. For example, the chord $O'B$ bisects the dip angle 2β and has the length $D_V \cos\beta$. When this chord is projected on the horizontal diameter AB, the maximum resistance, which occurs at the point B, is seen to be

$$R_{max} = R_e + D_V \cos^2\beta = R_e + \frac{R_{em}^2}{R_m}. \tag{4.29a}$$

By proceeding in a similar way the minimum value of resistance, which occurs at the point A, is found to be

$$R_{min} = R_e - D_V \sin^2\beta = R_e - X_{em}^2/R_m. \tag{4.29b}$$

In these two equations, the alternative expressions given in terms of the components of the force factor were identified with the help of Eq. (4.14*a*), and they can be seen to have just the form appropriate for insertion in the radicals appearing in Eq. (4.27). Subject to one important

restriction, these equations can be substituted in Eq. (4.27) to give an expression for the potential efficiency in the simple form

$$\text{Pot. Eff.} = \frac{\sqrt{R_{max}} - \sqrt{R_{min}}}{\sqrt{R_{max}} + \sqrt{R_{min}}}. \tag{4.30}$$

The restriction on the validity of this simplified expression consists in the assumption that it is allowable to use the same value for the blocked electric resistance R_e in combining Eqs. (4.27), (4.29*a*), and (4.29*b*). This is equivalent to assuming that the transducer has a relatively sharp resonance, which is to say that its mechanical Q_V is high enough for there to be relatively little change in the blocked impedance Z_e within the frequency interval required for the total-impedance vector to trace out its motional-impedance circle. Study of the specific example used for Fig. 4.2 indicates that for Q's of 30 or higher, substantially no accuracy is sacrificed in using the maximum and minimum values of the *total* impedance for prediction of the potential efficiency. For example, within the precision allowed by graphical measurements, the same value of 66 percent is obtained for η_E by using Eq. (4.30) or Eq. (4.27), or by reading off the peak value of the η_{max} curve plotted in Fig. 4.3. Moreover, even though Eq. (4.30) becomes increasingly inaccurate for very low Q's, its convenient simplicity allows it to serve in these cases also as a useful predictive criterion of transducer performance.

In connection with the development of any new transducer, it is a great convenience for the designer to be able to separate the variables so that independent consideration can be given to the internal properties of the transducer and the external conditions that must be satisfied for its optimum loading. A significant advance in this direction has been made by casting up the preceding expressions for each transducer performance parameter in such terms that its evaluation does not require any experimental measurements except those that can be made when the transducer is operating in the unloaded or vacuum condition. In the procedures so far described, however, a series of graphical constructions is still required in order to locate the potential-efficiency point E; but even this graphical step can be avoided by solving analytically for the R- and X-coördinates of the potential-efficiency point and again putting these in terms of quantities that can be derived from the unloaded-impedance circle. By introducing conditions (4.26) and (4.22) into the expressions for motional resistance and reactance [cf. Eq. (4.17)], and with some more algebraic manipulation, it can be shown that the

components of the motional impedance at the potential-efficiency point E are given by

$$(X_{mot})_E = \frac{R_{em}X_{em}}{R_m} = -\frac{D_V \sin 2\beta}{2}; \tag{4.31a}$$

$$(R_{mot})_E = \frac{\left(1+\frac{R_L}{R_m}\right)D_V \cos 2\beta - 2R_e\left(\frac{D_V \sin 2\beta}{2R_e}\right)^2}{\left(1+\frac{R_L}{R_m}\right)^2 + \left(\frac{D_V \sin 2\beta}{2R_e}\right)^2}. \tag{4.31b}$$

The implications of Eq. (4.31a) were already anticipated in selecting point E on the maximum-efficiency locus shown in Fig. 4.2. Since the motional reactance at the potential-efficiency point is just half the unloaded motional reactance at resonance, the point E must lie on a horizontal line drawn through the center of the vacuum circle. The intersection of this horizontal with the maximum-efficiency locus thus determines the potential-efficiency point uniquely.

Before going on it will be worth while to pause and take stock of the physical situation revealed by the foregoing results. Any reader who is already familiar with the analysis of either electrical or mechanical systems is entitled to regard it as a remarkable circumstance that substantial increases in efficiency can be achieved by operating the transducer at a frequency that appears to be well removed from resonance. If this does indeed make good physical sense, a closer examination of the situation may yield further insight into the physical nature of electromechanical transduction.

Consider first the implications of the criterion of realizability expressed by Eq. (4.28). This inequality will be satisfied automatically if the mechanical resistance R_m is separated into two parts, one of which is just equal to the right-hand member of (4.28), while the other is required to be positive. Such a partition can be symbolized by writing

$$R_m = R'_m + R''_m; \quad R'_m = \frac{X_{em}^2}{R_e}; \quad R''_m \geq 0. \tag{4.32}$$

If Eq. (4.32) is now introduced into the expression for the potential efficiency, Eq. (4.27), the potential efficiency takes the form

$$\text{Pot. Eff.} = \frac{\left(R_m + \frac{R_{em}^2}{R_e}\right)^{\frac{1}{2}} - R_m''^{\frac{1}{2}}}{\left(R_m + \frac{R_{em}^2}{R_e}\right)^{\frac{1}{2}} + R_m''^{\frac{1}{2}}}. \tag{4.33}$$

This expression makes it obvious that it is not the total effective mechanical resistance R_m that limits the attainable potential efficiency, but only the part of the resistance that is of purely mechanical — not electromechanical — origin and that can be shown to be represented by the excess of R_m over X_{em}^2/R_e. Obviously if R''_m can be made to approach zero, the potential efficiency will approach 100 percent. However, the value of load resistance R_L for which the potential efficiency is attained is also influenced by such an assumed reduction in R''_m, as may be seen by introducing Eq. (4.32) in Eq. (4.26) to give

$$(R_L)_E = \left(R_m + \frac{R_{em}^2}{R_e}\right)^{\frac{1}{2}} R''^{\frac{1}{2}}_m. \tag{4.34}$$

This would seem to lead to a relatively sterile situation in which perfect efficiency could be achieved, but only if the useful load were made to vanish. Such a result also suggests that operation at maximum efficiency may not necessarily coincide with the condition for maximum power transfer between a specified generator and a specified external load.

A Generalized Equivalent Circuit

It was pointed out above that the imaginary part of the complex force factor is intimately associated with some dissipative process associated with the primary mechanism of transduction. Prime examples of this effect are offered by eddy currents and hysteresis losses that occur in magnetostriction and electromagnetic transducers (such as the telephone receiver). When comparable effects are of relatively small magnitude (as they are in electrostatic, piezoelectric, and some electrodynamic transducers), X_{em} is very small, the dip angle of the motional-impedance circle approaches zero, and the mechanical-resistance component R'_m is correspondingly small. And whether small or large, it will turn out that the mechanical-resistance component R'_m is just the reflected effect of these losses "transduced," as it were, into the mechanical circuit by electromechanical coupling. Such a transduction of losses is bilateral, however, and a similar resolution of the blocked electric impedance Z_e can be made into two components Z''_e and Z'_e. The double-primed quantity, as before, will represent the blocked electric self-impedance that is independent of electromechanical coupling (for example, the ohmic resistance of leads and electrodes or windings, and leakage reactance, if any); the single-primed quantity represents the electric reactance and

resistance that is inherently associated with the electric or magnetic fields that furnish the electromechanical coupling.

The over-all situation is completely symmetrical, therefore, and may be represented by the three-terminal equivalent network shown in Fig. 4.5(a). The intrinsic inseparability of the electric-impedance com-

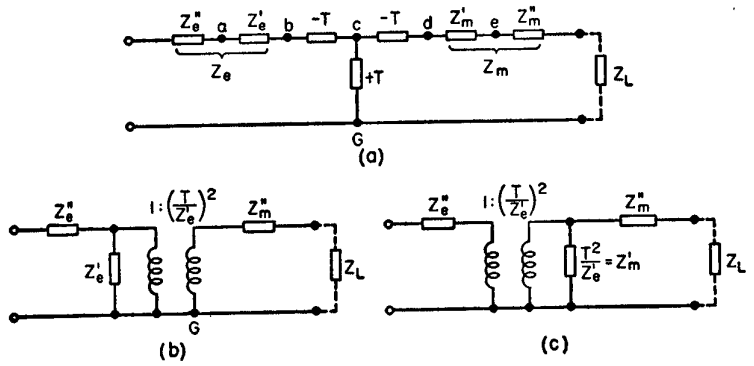

FIG. 4.5. Equivalent networks for a coupled electromechanical system in which there is a permanent electromechanical contribution to the self-impedance of each mesh.

ponent Z_e' and the mechanical-impedance component Z_m' from the elements of the T-network representing the transducing mechanism is expressed by requiring that a, b, c, d, and e be regarded as inaccessible terminals in the sense used in the discussion of Fig. 3.2 in the preceding chapter. With the help of the $(a) \rightarrow (b)$ transformation of Fig. 3.3, the network of Fig. 4.5(a) can be redrawn in the equivalent form shown in Fig. 4.5(b). In the process of carrying out this transformation, it can be recalled that when the series impedance Z_e' is moved to the shunt position, an impedance $(-T^2/Z_e')$ appears in series on the mechanical side. By virtue of the manner in which Z_e' and Z_m' have been defined, this negative impedance element automatically cancels Z_m'. This is not to say that the electromechanical component of mechanical impedance has been eliminated, but rather that it is now represented by the electric impedance Z_e' appearing on the other side of the ideal electromechanical transformer. It may be remarked, incidentally, that the transformation from Fig. 4.5(a) to Fig. 4.5(b) is one of a complementary pair; an equivalent form could be exhibited in which Z_m' would appear in shunt on the mechanical side while only Z_e'' would appear on the left. It may also

be noted for future reference that the single-primed impedances are defined in such a way that

$$Z_e'Z_m' = +T^2 = -Z_{em}^2. \tag{4.35}$$

A useful interpretation of the conditions for operation at resonance and at maximum efficiency can be made with the help of these circuit diagrams. Consider Fig. 4.5(c), which represents the circuit of Fig. 4.5(b) modified by transposing the electric impedance Z_e' to the right-hand side of the electromechanical transformer. In the preceding discussion of the conditions for resonance, it was assumed that the blocked impedance would not change significantly within a small frequency interval around resonance. When interpreted with reference to Fig. 4.5(c), this assumption is equivalent to saying that Z_e' can be regarded as substantially constant, and that Z_e'' is likewise either constant or very small, or else it can be merged with the generator impedance. It follows that when Z_e'' is small enough to be negligible, or wholly resistive, the condition of resonance will occur when the total series reactance of the three elements standing on the right of the electromechanical transformer vanishes — that is when $X_m' + X_m'' + X_L = 0$, in agreement with the discussion following Eqs. (4.17) and (4.20).

The conditions that must be satisfied to assure operation at maximum efficiency do not appear to be equally self-evident, except under restrictive conditions on Z_e'' and the generator impedance. The configuration of Fig. 4.5(c), in which Z_m' appears in parallel with the series combination of Z_m'' and Z_L, suggests, however, that it might be useful to examine the *admittance* of this combination. This procedure will, in due course, yield the expected information about maximum efficiency; but in the meantime, it will also afford an alternative frame of reference in which to reëxamine broadly several aspects of the electrical analysis of transducer performance.

Admittance and Impedance Diagrams

The same physical information that is embodied in the vector locus of electric impedance can, of course, be expressed in terms of a corresponding admittance diagram, since admittance is merely the reciprocal of impedance. This is equivalent to saying that, since impedance and admittance are inverse with respect to unity, the admittance vector will describe a locus that is a geometric inversion, with respect to unity, of the corresponding impedance locus. The geometric figure produced by

the inversion of a circle is also a circle, from which it follows that the vector admittance diagram will display a motional circle just as the impedance diagram does. It can also be expected that singular features of the motional-admittance circle, such as the magnitude and inclination of its diameter and the spacing in frequency of points around its contour, will be just as useful in revealing the characteristics of a transducer as the similar information extracted from a motional-impedance circle. It does not follow, however, that precisely the *same* information is obtained when identical procedures of analysis are applied to these two diagrams. The interpretive value of the admittance diagram stems, in fact, from just such differences.

Only the total admittances or impedances presented at the external transducer terminals are accessible for measurement, and it is these observable quantities that are simply related by the unit inversion. A process of subtraction is required in either case in order to exhibit the motional values. Circuit elements that are connected in series, or in parallel, combine differently in the algebraic expressions for impedance and for admittance. As a consequence, it can *not* be assumed that the motional admittance is the reciprocal of the motional impedance. In fact, it turns out that there is no simple universal relation between these motional quantities, in spite of the fact that each is characterized by a circular locus. They do tend to be complementary, however, and it is often worth while to perform the numerical inversions and to plot both diagrams in order to facilitate the analysis of a single series of experimental observations.

The total impedance Z_{ee}, the blocked impedance Z_e, and the motional impedance, are simply related by Eq. (4.1), repeated here for reference;

$$Z_{ee} = Z_e + Z_{mot}; \quad Z_{mot} = \frac{-T^2}{Z_m + Z_L} = \frac{Z_{em}^2}{Z_m + Z_L}. \tag{4.1}$$

The total admittance, the blocked admittance, and the motional admittance, can be defined explicitly, in a similar way, as

$$Y_{ee} \equiv \frac{1}{Z_{ee}}, \quad Y_e \equiv \frac{1}{Z_e}, \quad Y_{mot} \equiv Y_{ee} - Y_e. \tag{4.36}$$

After a modest amount of algebraic manipulation, the motional admittance can then be expressed in the form

$$Y_{mot} = \frac{-Z_{em}^2/Z_e^2}{Z_m + Z_L + (Z_{em}^2/Z_e)}. \tag{4.37}$$

A little more of the same kind of algebraic juggling will allow the efficiency, previously expressed by Eq. (4.16) in the impedance form

$$\eta = \frac{|Z_{ee} - Z_e|}{R_{ee}} \frac{R_L}{|Z_m + Z_L|}, \tag{4.16}$$

to be rewritten in terms of the observable admittances, as follows:

$$\eta = \frac{|Y_{ee} - Y_e|}{G_{ee}} \frac{R_L}{|Z_m + Z_L + (Z_{em}^2/Z_e)|}. \tag{4.38}$$

Note that the mechanical-impedance terms appearing in the denominators of Eqs. (4.37) and (4.38) differ from the corresponding terms in their companion expressions by the addition of the ratio Z_{em}^2/Z_e. Recall also that when the motional-impedance circle was being analyzed, it was assumed that the numerator of Eq. (4.1) would change relatively slowly with frequency, whereupon it was obvious that the maximum motional impedance would occur when the reactive part of $Z_m + Z_L$ vanished, either as a result of frequency variation or of reactance tuning. This condition established the resonance frequency f_R as that for which

$$X_m + X_L = X'_m + X''_m + X_L = 0 \qquad [\text{at } f_R]. \tag{4.39}$$

It is equally valid — and both approximations are good if the mechanical Q is 10 or higher — to assume that the numerator of Eq. (4.37) will not change appreciably within the frequency interval required for the vector admittance to trace out its motional circle. It follows then, that the frequency f_Y, at which the motional admittance has its maximum value, and hence the frequency associated with the motional admittance diameter, is that for which

$$X'_m + X''_m + X_L = \begin{matrix}\text{imaginary} \\ \text{part of}\end{matrix} \left[\frac{-Z_{em}^2}{Z_e}\right] \qquad [\text{at } f_Y]. \tag{4.40}$$

It may be remarked parenthetically that, according to Eq. (4.35), the first term of this equation will just cancel the right-hand member provided $Z_e = Z'_e$, corresponding to $Z''_e = 0$. A more general interpretation of Eq. (4.40) can be advanced, however, in terms of the phase angles characterizing the force factor [cf. Eq. (4.14*a*)] and the blocked impedance. These are defined through the relations

$$Z_{em} \equiv |Z_{em}| e^{-i\beta}, \quad Z_e \equiv |Z_e| j e^{-i\xi} = |Z_e| e^{i\left(\frac{\pi}{2} - \xi\right)}. \tag{4.41}$$

Note the appearance of the factor j in the blocked impedance, where it is introduced in order to make β and ζ take on identical values in the special case for which the "leakage" impedance Z_e'' is negligible and Eq. (4.35) is satisfied.

Several useful relations can now be displayed in terms of these phase angles. For example, the denominator of the motional admittance Eq. (4.37) becomes real at the diametral frequency f_Y at which Eq. (4.40) is satisfied. It follows, then, that the

$$\begin{matrix}\text{dip angle of the diameter of} \\ \text{the motional admittance circle}\end{matrix} = 2(\beta - \zeta), \qquad (4.42)$$

in which the right-hand member is the net phase angle of the numerator of Eq. (4.37). Conversely, the "horizontalness" of the motional-admittance diameter may be used as a criterion of the propriety of neglecting the leakage impedance Z_e''.

The right-hand member of Eq. (4.40) can now be rewritten, with the help of these phase angles, a little trigonometry, and the fundamental relation $e^{-j\phi} = \cos\phi - j\sin\phi$, in the form

$$X_m' + X_m'' + X_L = \frac{|Z_{em}|^2}{|Z_e|}\cos(2\beta - \zeta) \qquad [\text{at } f_Y]. \qquad (4.43)$$

Since the cosine is an even function, it would appear at first glance that Eq. (4.43) would always require the net mechanical impedance to be positive at the admittance frequency f_Y. A trial expansion of Z_e, as written in Eq. (4.41), with the resistances neglected, will indeed confirm this prediction, *provided* the reactive part of Z_e is positive, *as it will always be for electromechanical coupling by way of a magnetic field*, whether the transducer mechanism involves a moving conductor, a moving armature, or magnetostriction. On the other hand, the reactive part of the blocked impedance, X_e, *will always be negative when electric fields provide the agency of electromechanical coupling*, as in piezoelectric or electrostatic transducers. A similar test with Eq. (4.41) will then indicate that, in these cases, π radians must be subtracted from the argument of the cosine in Eq. (4.43), with a consequent reversal of its sign.

The significance of this sign reversal will be apparent when the typical behavior of $X_m + X_L$ is considered. The mechanical system of the transducer, including its load, has been assumed throughout this discussion to have a single degree of freedom. The variation with frequency of its equivalent series reactance, $X_m + X_L$, can, therefore, be represented

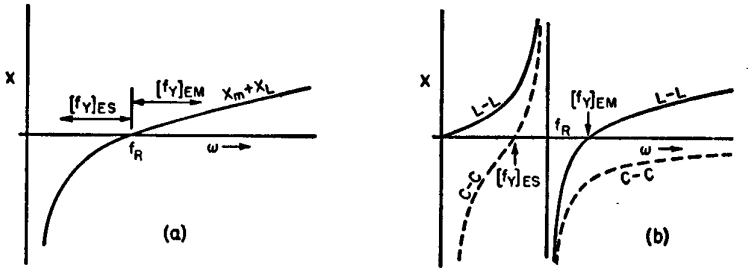

FIG. 4.6. Schematic representations of the typical variation with frequency of (*a*) the total mechanical reactance, and (*b*) the reactance of a 3-element network of type *L–L*, representing electromagnetic coupling, and of type *C–C*, representing electrostatic coupling. This sketch is drawn to scale for $k_{eff}^2 = 0.5$.

schematically as shown in Fig. 4.6(*a*). The algebraic sign of the cosine factor in Eq. (4.43) then dictates the conclusion that f_Y will lie *above* f_R for electromagnetic coupling, but *below* f_R for electrostatic coupling, as indicated by writing

$$[f_Y]_{ES} \leq f_R \leq [f_Y]_{EM}. \qquad (4.44)$$

As viewed from the external blelectric terminals, the ocked reactance, more or less diluted by the leakage reactance, appears effectively to be shunted by the inductance–capacitance combination representing the electromechanical transformation of $X_m + X_L$. This constitutes a 3-element reactance of canonical configuration whose behavior at zero and at "infinite" frequency allows it to be classified either as type *L–L*, for electromagnetic coupling, or as *C–C*, for electrostatic coupling. The occurrence of f_Y either above or below f_R, as expressed by Eq. (4.44), thus conforms to the normal sequence of resonances and antiresonances for typical *L–L* and *C–C* reactance configurations, as shown schematically by the solid and dashed-line curves of Fig. 4.6(*b*).

The frequency interval separating f_Y and f_R is governed, for any specific combination of phase angles β and ζ, by the magnitude of the ratio of the square of the force factor to the blocked impedance, Z_{em}^2/Z_e. In the special case of negligible leakage impedance, to which Eq. (4.35) applies, this quotient is just the term Z_m' that represents the portion of the mechanical impedance that is intrinsically associated with the transduction field. In the following discussions of specific transducer mechanisms, this concept will be used as a basis for defining a *coefficient of electromechanical coupling k*. Beyond this, however, the preceding discussion suggests that

the frequency spread between f_R and f_Y can itself serve as an index of how closely the electric and mechanical meshes are coupled. In these terms, and with due regard for Eq. (4.44), an effective coefficient of electromechanical coupling can be defined by the following pair of relations:

$$k_{\text{eff}}^2 \equiv 1 - \left(\frac{f_R}{f_Y}\right)^2, \quad \text{[for electromagnetic coupling]}$$
$$\equiv 1 - \left(\frac{f_Y}{f_R}\right)^2. \quad \text{[for electrostatic coupling]} \tag{4.45}$$

Return now to the question of operation at maximum efficiency, which will be identified by the subscript E. An exact expression for the maximum efficiency condition was obtained in Eq. (4.22*b*), so this relation can now be recast, in terms of the phase angles used above, in the form

$$X_m + X_L = \frac{|Z_{em}|^2}{|Z_e|} \frac{\sin 2\beta}{2 \sin \zeta} \quad [\text{at } f_E]. \tag{4.46}$$

Three special cases of general interest, corresponding to different values of the two phase angles, can now be identified.

CASE I. $\beta = 0$, $\zeta \neq 0$. These angles characterize a dissipationless transduction mechanism with nonvanishing leakage impedance — a typical situation prevailing with conventional moving-coil transducers. The ohmic resistance of the voice coil constitutes the major part of the "leakage" impedance that is not coupled with the transduction field. According to Eqs. (4.39) and (4.45),

$$[X_m + X_L]_E = [X_m + X_L]_R = 0; \tag{4.47}$$

for which it follows that, in this case, maximum efficiency occurs at resonance so that $f_E = f_R$.

CASE II. $\beta = \zeta \neq 0$. This is the special case, frequently invoked throughout the preceding discussion, in which the leakage impedance is negligible and the force factor and the blocked impedance have the same nonvanishing phase angles defined in Eqs. (4.41). This condition is well met in the magnetostriction ring transducer, and is nearly enough satisfied to represent a useful approximation for many other well-designed transducers of the moving-armature and magnetostriction type. According to Eqs. (4.43) and (4.46),

$$[X_m + X_L]_E = [X_m + X_L]_Y, \tag{4.48}$$

from which it follows that maximum efficiency occurs at the frequency f_Y corresponding to the diameter of the motional-admittance circle. When the dissipative component of Z_e and Z_{em} consists primarily of eddy-current losses, the blocked impedance itself has a locus that is a circle tangent to the reactance axis at the origin of the impedance diagram. When this condition prevails, the locus of maximum efficiency on the impedance diagram is another circle that is tangent to the resistance axis at the origin and passes through the reference value of Z_e. The maximum-efficiency locus determined by graphical construction in Fig. 4.2 is a crude approximation of such a circular locus, but the leakage impedance of the experimental transducer to which Fig. 4.2 pertains is too high to qualify it as a typical example of the case $\beta = \zeta$. When this condition *is* satisfied, however, the circular locus of maximum efficiency in the impedance diagram inverts to become the horizontal diameter of the motional-admittance circle, which become thereby the locus of maximum efficiency. This is one of the features that contributes importantly to the preference for admittance measurements in the electrical analysis of transducers for which maximum efficiency is a dominant design consideration.

CASE III. $\beta = \zeta = 0$. In this special case, the blocked impedance is a pure reactance and the transduction is dissipationless. Electrostatic loudspeakers, and many piezoelectric transducers (especially those employing quartz), meet these conditions reasonably well. The reactance condition for maximum efficiency given by Eq. (4.46) becomes indeterminate in this case. A little reflection will indicate that this is as it should be, since the only dissipative elements left are R_m'' and R_L. As a consequence, the efficiency will always be $R_L/R_m'' + R_L$, regardless of tuning! This is not to say that frequency variation is unimportant, however, but only to point out that its influence is revealed by changes in the input impedance rather than by changes in efficiency. In this respect, the situation closely parallels that of an ideal electric wave filter, in which the *efficiency* is not less in a stop band than in a pass band. Only in the pass band, however, is the input impedance predominantly real, so that real power can be accepted for delivery to the load. This parallel can actually be carried one step further, since the addition of an external reactance opposite in sign to X_e' will convert the equivalent circuit of a transducer of this class into the configuration of a band-pass filter terminated in $R_m'' + R_L$. The nominal width of the pass band that can be obtained in this way then turns out to be proportional to the

effective coefficient of electromechanical coupling, and is, to a first approximation, just equal to the ratio of the frequency separation between the diametral frequencies of f_R and f_Y to their geometric mean.

To summarize the foregoing briefly, the electrical analysis of transducer performance can as often be couched advantageously in terms of admittances as in terms of impedances. For an important class of transducers, the conditions of maximum efficiency present themselves more directly in the admittance diagram. Even when this advantage is not realized, the frequency separation between the diametral frequencies of the admittance and impedance diagrams affords a useful measure of the coefficient of electromechanical coupling. Finally, it is to be added that experimental convenience will often dictate a preference for the use of either an impedance or an admittance bridge for securing the raw experimental data. Thus, an admittance bridge is usually to be preferred for measurements on electrostatic systems, while the impedance bridge is better adapted for studying moving-conductor systems. And however the primary observations are made, the preparation of *both* forms of graphical representation is often helpful in deducing the significant features of transducer performance from the electrical measurements.

CHAPTER 5

Moving-Conductor (Dynamic) Transducer Systems

The modern moving-coil direct-radiator loudspeaker has not been changed in any important functional way since its basic configuration and its basic mode of operation were established by Riegger, Wente, and especially by Rice and Kellogg [1] in the early 1920's. Reliance is still placed on mass control of the motion of a small rigid diaphragm to secure substantially uniform electroacoustic response throughout a broad band of mid-range frequencies. It is the traditional obligation of research investigators and advanced-design engineers, however, to waste no time savoring such modest triumphs but rather to turn at once to the problem of dealing with the marginal factors, qualifying conditions, and other circumstances that control the breakdown of the simple theory in one respect or another. The designer is also obliged to go one step further and to take into account the limitations imposed on both theory and practice by virtue of the physical properties of available materials of construction. It will not be possible in these notes to follow the designer very far down this road, but, by keeping clearly in mind what the designer's problem really is, the analysis of simpler situations can be formulated and discussed with greater realism.

A typical form of moving-coil direct-radiator loudspeaker is shown diagrammatically in Fig. 5.1. A ring-shaped permanent magnet *PM* of high coercive force is welded to a base plate *BP* carrying a soft-iron pole piece *PP*. A cover plate *CP* attached to the other end of *PM* provides an annular air gap in which there is a uniform radial magnetic flux density *B*. As an alternative form of construction that may be superior from the point of view of magnetic leakage, the lower portion of the pole

[1] See notes 210–212 and 207 of Chapter 1.

piece may be made the permanent magnet while the outer ring is made of soft iron. The voice coil, *VC*, is a solenoid of copper or aluminum wire wound on a cylindrical form that is centered in the air gap by a flexible spider *SP* so that the coil assembly is free to move along its axis and to carry with it a paper cone *PC* attached rigidly to the voice-coil form.

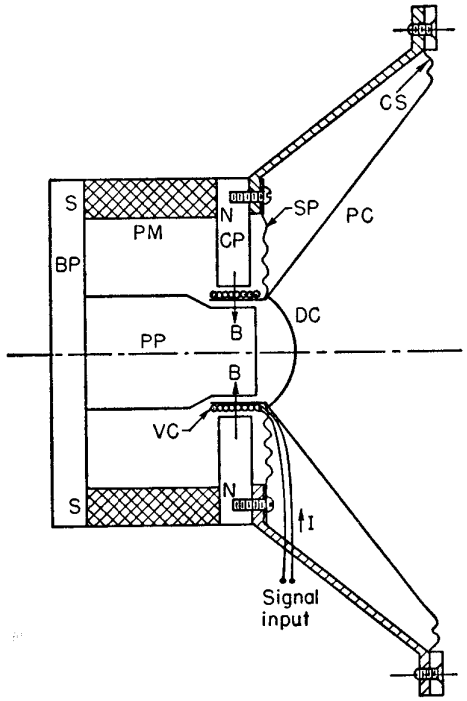

FIG. 5.1. Typical structural features of a loudspeaker of the moving-coil direct-radiator type.

A dome-shaped dust cover *DC* prevents air leakage, helps to keep foreign material out of the air gap, and constitutes a stiffened central section for promoting high-frequency response. The outer edge, or base, of the paper cone is supported flexibly by a "surround," which may consist of a soft material such as thin leather or of a flattened portion of the cone itself. The base of the cone is usefully stiffened by the corrugations *CS*. The cone moves — and thereby radiates sound — as a result of the axial forces generated in the voice coil by interaction of the signal current and the steady radial magnetic field.

There is almost endless opportunity afforded for introducing variations

in the design and construction of each of the functional elements included in the foregoing description. The detailed characteristics of each modification may influence to a greater or lesser degree the over-all performance of the loudspeaker, its efficiency, frequency response, directivity, electric impedance, freedom from distortion, and so on. No attempt will be made here to describe, or even to catalog, all of these effects. Fortunately, the fundamental behavior of this type of transducer mechanism can be studied usefully with the help of an idealized model.

At the outset it will be assumed that the voice coil and all parts of the cone move in phase with the same amplitude and that the mass of the system and the mechanical resistance to its motion can be regarded as lumped constants effective at some reference position selected for the measurement of vibratory velocity, usually at the voice coil. In practice, of course, the cone of a direct-radiator loudspeaker is *not* ideally rigid, and the velocity of transmission for transverse flexural waves along a generator of the paper cone may be low enough to allow several nodal circles and regions of reversed phase to appear within the range of frequency nominally covered by the transducer. Nevertheless, it will be useful to deal with *effective values* of the mechanical constants so that the mechanical impedance of the moving system can be written as $z_m = r_m + j(\omega l_m - 1/\omega c_m)$. The extent to which it is necessary to lean heavily on the term "effective" can then be made explicit by the following definitions of the three mechanical parameters. The resistance r_m represents all the dissipative forces opposing the motion of the mechanical system consisting of voice coil and paper cone, *except* those due to sound radiation; it is an equivalent resistance coefficient such that when multiplied by the velocity v it will represent the total in-phase force reaction, whether the dissipation that gives rise to it actually occurs in the compliant cone support, in the voice-coil centering mechanism, or elsewhere. The equivalent mass l_m is correspondingly defined so as to yield the total inertial reaction force (that is, one that lags the velocity by 90° in phase) when multiplied by the acceleration at the reference point on the voice coil. The effective mass l_m does not, however, include the acoustical accession to inertia, since this will be accounted for as part of the external load. In a similar way, the compliance c_m, or the displacement per unit force, is the reciprocal of the equivalent stiffness of the entire assembly referred to the voice coil as the origin of the coördinates for mechanical displacement.

The electric impedance observed in the absence of any back emf in-

duced by mechanical motion can also be written in the usual way as $Z_e = R_e + j\omega L_e$, where R_e and L_e are the "blocked" values of the resistance and self-inductance of the voice coil. Electromechanical coupling by way of a conductor lying in a transverse magnetic field has already been discussed at some length in Chapter 3. A generalized "black-box" diagram like that of Fig. 2.1 can, therefore, be particularized at once by using Eqs. (3.10) to identify the induced emf E_{Bv} and the mechanical force F_{BI} arising from the interaction of velocity and current, respectively, with the magnetic field. The polarity assigned to these interaction forces as they appear in Fig. 5.2(a) can be chosen with the same degree of

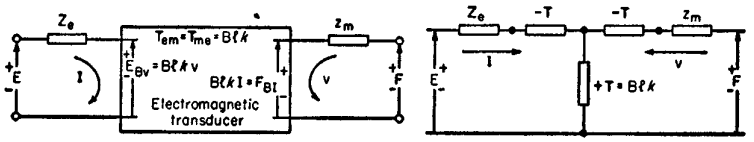

FIG. 5.2. (a) A schematic "black-box" representation of a transducer with electromagnetic coupling, illustrating the choice of algebraic signs for the mechanical forces and emf's of interaction. (b) The canonical two-mesh coupling diagram for the moving-coil transducer.

arbitrariness permitted in establishing a sign convention for mutual inductance in coupled electric circuits. The particular choice indicated in Fig. 5.2 assigns to E_{Bv} the role of a "back emf" that opposes a positive current in the electric mesh when the mechanical velocity is positive. In a symmetrical way, the mechanical reaction force F_{BI} is poled so that it opposes a positive velocity in the mechanical mesh for a positive current in the electric mesh. It has already been established (in the discussion of symmetry advanced in Chapter 3) that the indicated choice of signs leads automatically to conformity with Lenz's law by virtue of including in the defining expressions for E_{Bv} and F_{BI} the space operator k, which embodies algebraically the intrinsic orthogonality of the electromechanical interactions. Equations (3.11) can now be rewritten, for convenient reference, as follows:

$$\begin{aligned} E_{Bv} &= Tv = Blkv, \\ F_{BI} &= TI = BlkI. \end{aligned} \tag{5.1}$$

The basic coupling equations for the electrodynamic transducer can then be written by inspection, with reference to Fig. 5.2(a), in the form

$$\begin{aligned} E &= Z_e I + Blkv, && \text{[volts]} \\ F &= +BlkI + z_m v. && \text{[newtons]} \end{aligned} \tag{5.2}$$

It may be remarked in passing that the first of Eqs. (5.2) is expressed in electrical units and the second in mechanical units, as indicated; and that the transduction coefficient occurs with the same numerical value in either equation when rationalized mks units are used throughout. Thus, the flux density, B, is to be expressed in webers per square meter, and the total length of wire on the voice coil, l, in meters. (See below for further discussion of units and a tabulation of dimensions and cgs/mks conversion factors.)

Equivalent Circuit Representations

With the transduction coefficient identified as (Blk), the standard two-mesh equivalent circuit can be drawn by inspection, as in Fig. 5.2(b), and then can be transformed immediately to any one of a variety of other configurations. The particular form shown in Fig. 5.3, for example, is arranged in conformity with the procedures employed in the preceding chapter; the shunt impedance on the electrical side (represented as the inductance L'_e) represents the portion of the blocked electric impedance Z_e that is perfectly coupled to the magnetic transduction field B; the ohmic resistance and any "leakage" inductance of the voice coil or its leads that is not coupled to the polarizing field is included in the series-connected leakage impedance Z''_e. For the transducer types to be considered in succeeding chapters, the particular configuration exhibited in Fig. 5.3 is especially appropriate, since the shunt-connected

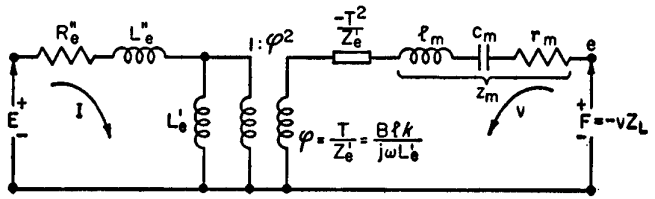

FIG. 5.3. One of the alternative forms for the equivalent circuit of a moving-coil transducer.

reactance element can represent any influence of electromechanical coupling that continues to be reflected in the mechanical circuit even when the external electric terminals are on open circuit. Some such residual coupling effect will be found to be characteristic of all the remaining transducer types; but, for moving-conductor systems conductively coupled to the external circuit, there is no residual coupling,

and it is a free choice as to which circuit element or combination of elements is moved into the shunt position in the process of deriving alternative configurations equivalent to the basic circuit shown in Fig. 5.2(*b*). This unique property of moving-conductor transducers will warrant further discussion a little later. For the moment it is only necessary to observe that different choices for the circuit element to be moved into the shunt position lead to different values for the turns ratio of the ideal electromechanical transformer. After the turns ratio has been established by some particular choice, however, the impedance elements adjacent to the transformer can then be moved freely from one side to the other by simply applying systematically the established impedance (and units) transformation ratio.

An alternative form of the equivalent circuit is shown in Fig. 5.4, in which the whole mechanical-impedance branch, exclusive of the external load, has been moved to a shunt position on the mechanical side of the coupling transformer. This configuration is especially useful for exhibiting the combination of circuit elements that accounts for the unloaded or "vacuum" motional-impedance circle. This may be seen

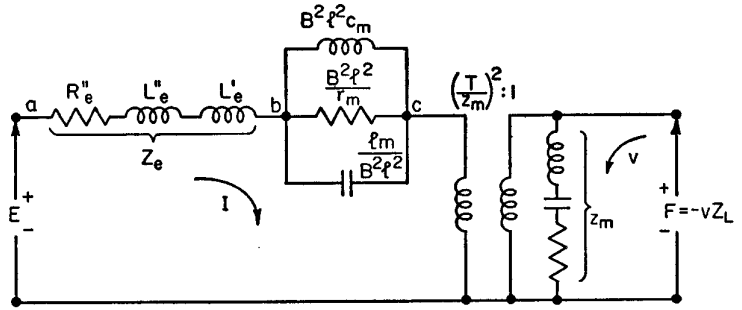

FIG. 5.4. An alternative configuration for the equivalent circuit of a moving-coil transducer.

by noting that the unloaded condition corresponds to a short circuit at the mechanical terminals (that is, to the condition $F = 0$), and that the short circuit reflects through the ideal transformer to provide a direct ground connection for the terminal marked *c*. The series impedance between the points *a* and *c* represents, therefore, the total free impedance Z_{ee}; while the three impedances connected in parallel between points *b* and *c* represent the motional impedance itself.

The values of the circuit elements appearing in Fig. 5.4 are found by evaluating the general expression for the electric driving-point impedance [cf. Eq. (4.1)], which can be written in the form

$$\begin{aligned} Z_{ee} &= Z_e + \frac{-T^2}{z_m} = Z_e + \left[\frac{z_m}{-T^2}\right]^{-1} \\ &= R_e + j\omega L_e + \left[\left(\frac{B^2l^2}{r_m}\right)^{-1} + \left(\frac{B^2l^2}{j\omega l_m}\right)^{-1} + (j\omega B^2l^2c_m)^{-1}\right]^{-1}. \end{aligned} \tag{5.3}$$

The bracketed term on the right has been written as the reciprocal of the sum of three reciprocal impedances in order to suggest that it can be interpreted as the impedance of three elements having the indicated values and connected in parallel. The resistance B^2l^2/r_m can be identified at once as the diameter of the motional-impedance circle, since the inductive and the capacitive branches are in parallel resonance at the frequency that satisfies the relation $\omega_0^2 l_m c_m = 1$. It may also be seen by inspection (or demonstrated by some algebraic manipulation) that the dip angle is zero, corresponding to a horizontal resonance diameter for the motional-impedance circle. This result follows as a consequence of the assumption that there is no dissipative process inherently associated with the transduction field; or, what is equivalent, that the complex force factor, which was defined as the coefficient of *k* or *j* in the transduction coefficient, is in this case real, as may be seen by writing it explicitly in the form

$$Z_{em} = R_{em} = Bl. \tag{5.4}$$

As before, *l* is the total length of the current-carrying voice-coil conductor that interacts with the flux density *B*.

It also follows, though it is a little less obvious, that Fig. 5.4 correctly predicts that the blocked impedance is just Z_e. The blocked condition corresponds to zero velocity in the mechanical mesh, and thus to an open circuit at the mechanical output terminals. This leaves z_m connected in shunt; but when this impedance is "carried through" the coupling transformer, the square of the *k*-factor included as part of *T* in the turns ratio contributes the minus sign that makes the transformed equivalent of z_m just equal and opposite to the motional-impedance branch appearing between the points *b* and *c*. It follows that the net impedance in the electric mesh for this condition is just Z_e, as it should indeed be if the configuration of Fig. 5.4 is to satisfy the conditions of equivalence.

When the load impedance has any other value than that corresponding to open or short circuit, the configuration of Fig. 5.4 offers some algebraic complexity in analysis. It is much more convenient in this case to merge the load impedance Z_L with the mechanical impedance z_m *before* moving their series combination into the shunt position occupied by z_m in Fig. 5.4. At first sight this procedure would appear to complicate still further the turns ratio of the coupling transformer, since the shunt-connected impedance appears in the denominator of the turns ratio. It turns out otherwise, however, for when there is no external applied force except the load reaction, the external terminals can be regarded as permanently short-circuited after the load impedance is merged with the internal mechanical impedance. It follows that this short circuit will be reflected through the coupling transformer as a simple short circuit no matter what the turns ratio is, and, as a welcome result, the much simpler equivalent circuit shown in Fig. 5.5 is obtained. Note that the electromechanical coupling transformer has now disappeared entirely!

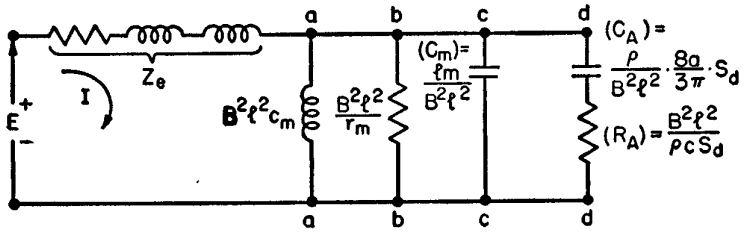

FIG. 5.5. A transformed equivalent circuit for the moving-coil transducer that is well adapted for modeling with an electric-network analog. This is derived from Fig. 5.2(*b*) by merging the load impedance with the self-impedance of the mechanical mesh before making the transformation that introduces an ideal electromechanical coupling transformer.

Prototype Performance Analysis

An extensive discussion of the over-all electroacoustic performance of the transducer can be based on a careful study of the equivalent circuit displayed in Fig. 5.5. First, however, with regard to the manipulations involved in setting up the equivalent circuit itself, it may be noted that the ideal electromechanical transformer has some of the interesting properties of a gyrator. However, in addition to inverting the impedance elements that are reflected through it, it also modifies their scalar magnitude *and* their units of measurement. Thus, the elastic

compliance, c_m meters/newton, which is represented as a capacitance in the mechanical impedance z_m, appears on the electrical side as an inductance $B^2l^2c_m$ henries. As a further example, the two elements appearing in series in the branch *d*–*d* represent a similar inversion of the parallel form of the network that is used to represent the acoustic radiation resistance and the accession to inertia for a piston vibrating in a plane baffle [see Fig. 5.7(*a*)]. These circuit elements are not truly "equivalent" to the radiation impedance in the strict sense in which the word equivalent has been used above, but they offer a simple configuration that constitutes a very reasonable approximation of the impedance represented by the piston functions. And here, as in many other instances, the parallel form is much to be preferred, since it allows the acoustic inertance and resistance to be represented by circuit elements that do not vary with frequency.

The network configuration of Fig. 5.5 provides an excellent basis for studying transducer performance by means of analogous electric-circuit models, since all elements of the system, including the radiation load, have been transformed to appear as conventional electric-circuit elements. It follows that the power delivered to the acoustic load can be found by computing (or by measuring in the electric-circuit model) the electric power dissipated in the resistance element marked (R_A) in the equivalent circuit. Not much has been said so far about the units of measurement for the electrical and mechanical quantities involved in these equivalent-circuit diagrams. Fortunately, not much needs to be said on this subject, since no conversion factors intrude their troublesome exponents when mks rationalized units are used consistently for all quantities involved, whether electrical or mechanical.

The advantages of the homogeneity of mks units are probably felt nowhere more gratefully than in dealing with electromechanical transducers, since it is continually necessary to perform algebraic manipulations involving both kinds of quantities. This homogeneity has its basis in the choice of the joule as the fundamental unit of energy in both electrical and mechanical systems, and in the definition of other units in both systems in such a way that the mechanical joule is numerically equal to the electric joule. A tabular presentation of the basic dimensions and the equivalent units for the physical quantities that are most frequently used in analysis of electromechanical systems is presented in Appendix A. Its utility can be illustrated by verifying explicitly that the electric power $I^2(R_A)$, as computed for Fig. 5.5, does indeed have the

dimensions of power. In pursuing such dimensional questions it is a free choice whether the fundamental dimensions are taken to be charge, mass, length, and time or the combination that is sometimes more convenient for electromagnetic calculations, charge, voltage, length, and time. For either choice the same answer is obtained, as may be shown by writing

$$I^2(R_A) = I^2 \cdot B^2 \cdot l^2 \cdot \rho^{-1} \cdot c^{-1} \cdot S_d^{-1}$$

[Dimensional Equations]

$$\approx \frac{Q^2}{T^2} \cdot \frac{V^2T^2}{L^4} \cdot L^2 \cdot \frac{L^5}{QVT^2} \cdot \frac{T}{L} \cdot \frac{1}{L^2} = \frac{QV}{T}$$

$$= \frac{\text{coulomb volts}}{\text{second}} = \text{watts.} \quad (5.5)$$

$$\approx \frac{Q^2}{T^2} \cdot \frac{M^2}{Q^2T^2} \cdot L^2 \cdot \frac{L^3}{M} \cdot \frac{T}{L} \cdot \frac{1}{L^2} = \frac{ML^2}{T^3} = \frac{\text{joules}}{\text{second}} = \text{watts.}$$

The significance of the foregoing, as it applies specifically to the evaluation of the circuit constants appearing in Fig. 5.5, is that the reactance branches *a–a*, *b–b*, and *c–c* are given directly in henries, ohms, and farads respectively when the magnetic and mechanical constants appearing in the expressions attached to each circuit element are expressed in mks units. This can be illustrated by performing a simple order-of-magnitude calculation. If the mass of the cone and voice-coil system is taken to be 0.0072 kg (7.2 gm) and the average magnetic field B to be 0.9 weber/m^2 (= 9,000 gauss), and if the length of wire comprising the voice coil is about 3.7 m (23 turns, say, on a 2-inch form), then it follows that the capacitor (C_M) appearing between the terminals *c–c* would have a capacitance of about 650 microfarads. If the mechanical resonance frequency is then assumed to be 120 cycles per second, it can be deduced immediately that the branch connected between the terminals *a–a* would have an inductance of about 2.7 millihenries. Such a relatively large value of capacitance and small value of inductance would suggest that the circuit of Fig. 5.5 is a low-impedance circuit, as indeed it should be if the circuit is to be equivalent to the actual loudspeaker as viewed from its electrical terminals. The equivalent radiation load (R_A) can be evaluated in a similar way. Taking the value of ρc for air to be about 420 kg sec^{-1} meter^{-2}, and assuming a diaphragm area $S_d = 0.025$ m^2 (nominal 7-in. diameter), the value of (R_A) turns out to be 1.2 ohms.

In order to carry out experiments on an electric analog of this equivalent circuit, it would usually be desirable to transform the impedance level of the entire circuit by some arbitrary factor (325, for example) in

order to convert the required values of inductance and capacitance to sizes more conveniently available in the laboratory. The freedom to introduce such an arbitrary multiplier rests on the fact that, after the impedance level has been changed, an ideal transformer, with impedance ratio equal to the arbitrary multiplier, can be introduced between the modified circuit and the external electrical terminals. If such a transformer were actually provided, the original impedance conditions prevailing at the input terminals would be completely restored. In practice, however, it is usually simpler to omit the transformer and merely to increase the impressed voltage by the square root of the impedance transformation ratio, thus restoring the original power levels throughout the circuit.

As suggested above, a host of questions concerning the electroacoustical behavior of a dynamic loudspeaker can be, as it were, submitted to the circuit of Fig. 5.5 for answer. A few examples will illustrate this procedure. Consider, for instance, the canonical circumstances specified by Rice and Kellogg as appropriate for obtaining uniform response over a wide frequency range. Operation above the mechanical resonance frequency, that is, under mass control, implies that the impedance of each of the branches *a–a* and *b–b* is high enough for it to be neglected, and that the performance is controlled by the capacitance (C_M) in the branch *c–c*, which represents the total mass of the moving system. The further requirement that the diaphragm be acoustically small is equivalent to requiring that the dimensional constants and the frequency be chosen in such a way that the reactance of (C_A) in the load branch *d–d* will be large in comparison with the radiation load (R_A). Under these conditions, the input current I (which is assumed to be constant in order to yield a constant driving *force*) will divide between the branches *c–c* and *d–d* in accordance with the relative size of the two capacitances. Note, however, that, so long as these conditions remain satisfied, the *fraction* of the input current appearing in the load branch will *not* vary with frequency. It follows then that the current in (R_A), and hence the power dissipated in useful radiation, will indeed be independent of frequency, as predicted. Of course, when the frequency becomes high enough for the impedance of the branch *d–d* to "level off" at the value of the radiation load (R_A), which is equivalent to saying when the diaphragm can no longer be regarded as acoustically small, the "mass branch" *c–c* will begin to divert an increasingly larger fraction of the input current away from the load. The dissipation in the load, which represents the sound radiation, will

then begin to fall off at a rate which can readily be shown to approach 6 db per octave.

In a similar way, at frequencies below that of mechanical resonance, the diminishing reactance of the "stiffness branch" a–a will again cause more and more current to be diverted from the load branch. In this case, however, the sound output diminishes at a rate that approaches 12 db per octave, since the reactance of (C_A) is increasing while the reactance of the shunt diversion path a–a is decreasing. This, then, is the typical behavior of the classical prototype of the mass-controlled small-diaphragm dynamic loudspeaker.

According to the foregoing, uniform acoustic output is obtained above the frequency of mechanical resonance so long as the impedances of the branches c–c and d–d vary in a similar way with frequency. Even when this condition is satisfied, however, the *magnitude* of the acoustic output depends on the magnitude of the total input current and on the relative magnitude of the two indicated capacitances. Moreover, since it can be seen that (C_A) varies with the cube of a, the radius of the diaphragm, it would follow that, if the thickness of the diaphragm were always the same fraction of its radius, the sound output under fixed electrical conditions would be controlled by the *density* of the diaphragm material. In typical practice, the thickness of the paper cone varies more nearly as the square root of the radius, which is to say that small cones are relatively thicker than large ones. On this basis it would be inferred that the small ones would be correspondingly less "responsive" — and presumably less efficient, although a good many other factors would need to be considered before generalizing about efficiencies. Nevertheless, to the extent that the material and dimensions of the paper cone are controlling factors, one is led to the conclusion that the sound output would be enhanced by making the diaphragm as thin as possible and of a very low-density material. To go too far in this direction, however, would be to court trouble from the failure of another assumption, namely, that the diaphragm is rigid and that all parts move in phase at all frequencies of interest. More will need to be said about this later.

Consider now the circumstances that would arise if the barometric pressure of the ambient atmosphere in which the loudspeaker operates were to be drastically lowered. If only the pressure were reduced, without alteration of the constitution of the gas mixture, the impedance level of the load branch d–d would simply vary inversely with the density ρ, which appears in the expressions for both (C_A) and (R_A). The mass of

the moving system, as represented by (C_M), would remain constant, however, so there would be a decrease in the sound-power output corresponding to the decrease in density. If, on the other hand, the loudspeaker were to be operated in a different gaseous atmosphere, the changes in both ρ and the characteristic impedance ρc would need to be considered in assessing the new situation. In hydrogen, for example, the velocity of sound is markedly higher than in air, with the result that the air-to-hydrogen impedance ratio is only about 4:1 in spite of a density ratio of nearly 14:1. As a consequence, the capacitance (C_A) would diminish by a larger factor than that by which (R_A) would increase, and the diaphragm would thus appear to be acoustically smaller in a hydrogen atmosphere than in air. This explains why some trouble is occasionally taken to make use of a hydrogen (or helium) atmosphere in order to extend the frequency range in microphone-calibration experiments.

Representation of the joint acoustical influence of such variables as frequency, dimensions, and gas constitution by embodying them in an equivalent circuit makes it possible to exhibit in very compact form the essence of the analysis made in 1868 by Stokes in his classic paper "On the Communication of Vibration from a Vibrating Body to a surrounding Gas." [2] Long before the pressure reduction mentioned above is carried far enough to be considered a good vacuum, the impedance level of the branch d–d will have become so high that its effect can be entirely neglected. In practice, a reduction of the pressure to a half millimeter of mercury or less is usually sufficient to remove all the noticeable reactions of the acoustic-load branch on the remainder of the circuit. It should not be overlooked, however, that removal of the air in this way will also remove any incidental contribution to the mechanical resistance r_m caused be viscosity or heat losses associated with motion of the air through small air-gap clearances or its compression within the magnet structure. Such losses may be comparable with other internal mechanical losses at low frequencies but they are usually negligible in comparison with the radiation resistance at mid-range and higher frequencies.

An Illustrative Example

The typical behavior of the electrical-input impedance of a "good" 7-inch loudspeaker operating in a vacuum is illustrated in Fig. 5.6 by

[2] Sir G. G. Stokes, *Phil. Trans. Roy. Soc.* (*London*) **158,** 447–463 (1868); also in *Mathematical and Physical Papers*, Vol. 4, pp. 299–324 (Cambridge [Eng.], Cambridge University Press, 1904).

the large circle marked V. By making any convenient alteration of the mechanical constants and then repeating these measurements, in accordance with the procedures discussed in Chapter 4, the three mechanical constants of the loudspeaker can be separately evaluated. Two experi-

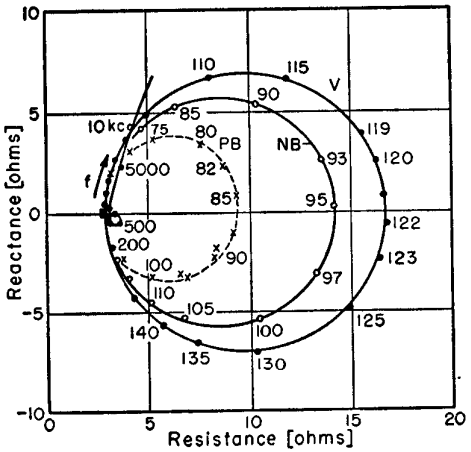

FIG. 5.6. Typical vector-impedance loci for a moving-coil loudspeaker under various conditions of loading.

mental methods of producing a known change in one of the mechanical constants are especially convenient. The most reliable method is that in which the loudspeaker is operated face up in a vacuum chamber both without and with an added mass, which may consist simply of a lead ring (solder wire!) held in position on the conical surface by its own weight. The alternative scheme requires the loudspeaker to be operated in air, first face up, and then face down on a hard surface. In the latter case, the volume of air trapped between the surface of the cone and the flat surface provides an easily calculable increment in the mechanical stiffness of the cone mounting. This method must be used with some caution, however, since the effect of changes in the accession to inertia may not be a negligible factor in determining the resonance frequency of the system.

The magnitude of the mass increment representing the acoustical accession to inertia is often underestimated in casual consideration of the low-frequency behavior of ordinary loudspeakers. The smaller circle, marked *PB* in Fig. 5.6, was obtained with this 7-inch loudspeaker operating in an "infinite" plane baffle [actually mounted in the door separating two rooms]. The resonance frequency under this condition

of loading is seen to have been lowered to about 70 percent of its vacuum value, from which it may be inferred that the mass of air entrained with the diaphragm is in this case almost exactly equal to the mass of the diaphragm and voice-coil assembly itself. To the extent that the experimental conditions conform with the assumptions made in computing the accession to inertia, such an addition of air loading may be regarded as a "convenient alteration of the mechanical constants" and may be made the basis for evaluating the mechanical parameters of the loudspeaker [the illustrative numerical data used above were selected on this basis].

In connection with such calculations, attention should be directed to the factor $8a/3\pi$ that appears in the expression for (C_A) in Fig. 5.5. This factor will be recognized as the characteristic "end correction" used to describe the accession to inertia acting on *one side only* of a rigid piston of radius a vibrating in an infinite plane baffle. When the effect of an infinite baffle is secured by the use of a box or housing that completely encloses the back side of the diaphragm, the air loading on the rear of the diaphragm is accounted for as a change in the effective stiffness of the suspension. This is the situation that was assumed in writing the expressions for (C_A) and (R_A) as they appear in Fig. 5.5. Under the circumstances prevailing for the plane-baffle curve *PB* of Fig. 5.6, however, *both* sides of the diaphragm radiate freely into acoustic half-spaces, and the constants for the load branch must be correspondingly modified by doubling the effective area S_d which appears in the expressions for (C_A) and (R_A).

When a loudspeaker is operated with a baffle that is too small, or without any baffle at all, as illustrated by the curve labeled *NB* in Fig. 5.6, the radiation loading is intermediate between the two cases just discussed. In order to compute the performance in this case, it is necessary to modify the configuration of the load-impedance branch *d–d* of Fig. 5.5. No exact solution is available for the radiation impedance of an unbaffled conical radiator, but the typical behavior of the load impedance for such a radiator can be simulated by the 3-element network shown in Fig. 5.7(*b*). This configuration is derived on the assumption that the specific acoustic impedance (= mechanical impedance *per* unit area) will be the same for the vibrating unbaffled cone as for an oscillating sphere. However, the specific impedance is not the same for all surface elements of the sphere, and when the average specific impedance for the sphere is multiplied by the surface area of the piston, it turns out that the

predicted mechanical resistance is obviously too low, since it is only two-thirds of the limiting value that must always prevail for very high frequencies, at which the radiating surface can, in effect, act as its own baffle. When the constants obtained in this way are renormalized to yield the correct asymptotic behavior of the resistance term, the values of the circuit elements turn out to be as shown in Fig. 5.7(b).

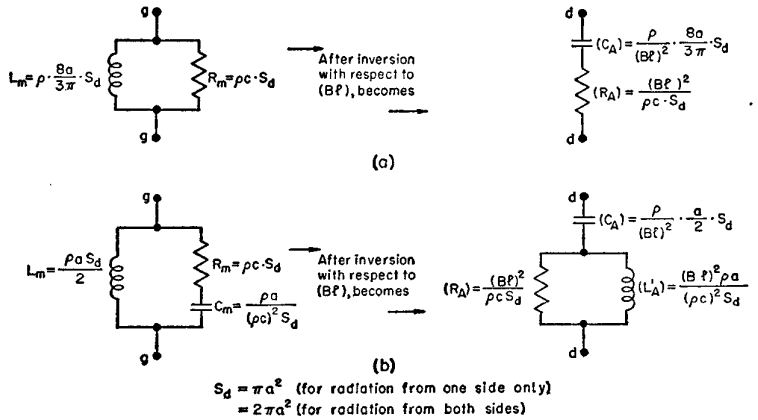

FIG. 5.7. Electric networks that simulate approximately the mechanical impedance due to sound radiation loading of a circular piston: (a) in an infinite baffle, (b) unbaffled.

The same procedure used for obtaining Fig. 5.5 is now to be followed again: the mechanical impedance presented at the terminals g–g is connected at the terminals for the external mechanical load, merged with z_m and moved into the shunt position, and then carried through the electromechanical transformer. It appears then as the modified load branch d–d shown in the right-hand side of Fig. 5.7(b), where it is seen to have a form that corresponds to an impedance inversion with respect to the force factor, (Bl); thus, as a typical example, $R_m(R_A) = (Bl)^2$. In a qualitative sense, the appearance of the inductance (L'_A) in shunt with (R_A) can be explained as a circuit modification introduced to represent the "short-circuiting" of useful radiation at low frequencies by destructive interference between sounds radiated from the front and back sides of the diaphragm.

Before leaving the vector-impedance diagrams of Figs. 5.6, it may be worth while to call attention to the fact that the dip angle is very small — in fact, zero within the limit of experimental error in these measurements.

This fact, coupled with the fact that the motional impedance is substantially greater than the d.c. resistance of the voice coil, causes half of the motional-impedance circle to lie below the R-axis. Readers who encounter this characteristic feature of electromechanical coupling for the first time are entitled to be surprised by the observation that a relatively short length of wire, coiled up and suspended in a steady magnetic field in this particular way, can present at its two ends a negative, or capacitive, reactance over a band of low audiofrequencies covering nearly an octave. It may also be worth noticing that the minor parasitic resonance that shows up in the vacuum circle at a frequency near 500 c/s can just barely be detected in the original data for the "unbaffled" circle, and seems to be suppressed entirely when the loudspeaker is operated with its normal acoustic load.

The vector-impedance curves displayed in Fig. 5.10 were obtained [3] by operating the loudspeaker used for the data of Fig. 5.6 in a bass-reflex enclosure. The transition from one to another of these vector-impedance loci (they can hardly be called circles!) was produced by altering the "tuning" of the enclosure by changing the size of the ports. A comparison of the distribution of frequencies around the locus marked A with the corresponding distribution for the plane-baffle curve PB of Fig. 5.6 will confirm the fact that such an enclosure can indeed produce a useful extension of the response toward lower frequencies — as advertised.

A quantitative understanding of this behavior can be gained most easily by considering how the configuration of the load branch d–d of Fig. 5.5 can be further modified in order to account for the additional effects introduced by the enclosure and by sound radiation from the auxiliary openings in the box. The network configuration displayed in Fig. 5.8(a) can be regarded as a first-order approximation of the acoustic "circuit" [4] for a bass-reflex enclosure. No attempt will be made here [5] to supply the analytical background on which such circuit representations are based, nor to give an exposition of the techniques for composing such networks. A few comments, however, may assist the reader in making the connection between this specific network and the literature dealing with network analogs.

[3] I am indebted to John F. Hersh for the measurements displayed in Figs. 5.6, 5.10 and 5.11. F.V.H.

[4] This method of dealing with mutual impedance in reflex enclosures was suggested to me in April 1950 by Dr. B. M. Oliver (B.T.L.) in a private communication. F.V.H.

[5] See note 6 and related text of Chapter 1.

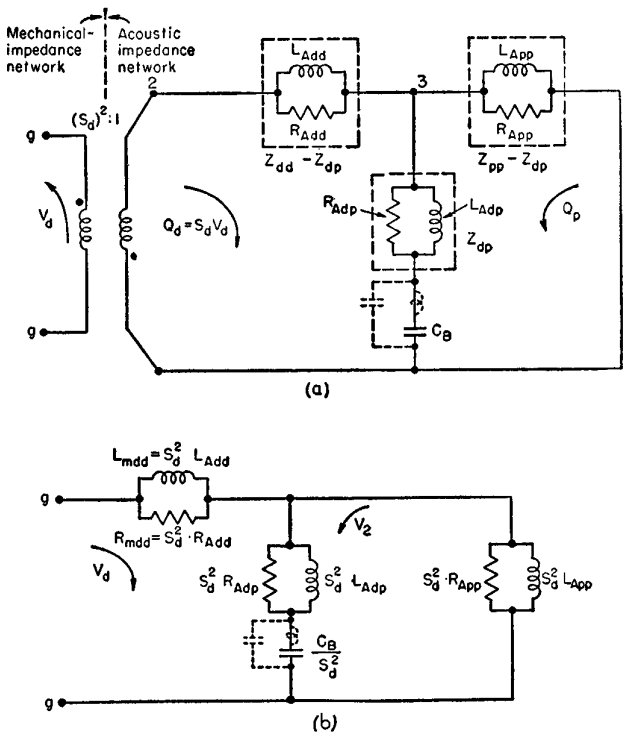

FIG. 5.8. (*a*) An acoustic-impedance network simulating the behavior of a bass-reflex loudspeaker enclosure: C_B, compliance of air enclosed within the box; Q_d, Q_p, volume currents through diaphragm aperture and through port; Z_{dd}, Z_{pp}, acoustic self-impedance presented by the medium at the diaphragm aperture and at the port; Z_{dp}, acoustic mutual impedance between the diaphragm and the port, whose center-to-center distance is g. (*b*) The mechanical-impedance network derived from (*a*) by successive transformations.

The condenser C_B appearing in Fig. 5.8(*a*) accounts for the acoustic compliance of the volume of air enclosed within the box. Its allocation to a shunt-connected branch can be rationalized by observing that continuity requires the volume current Q_d through the diaphragm *either* to be compressed within the box by flowing in the branch containing C_B, *or* to emerge from the port as represented by the current in the branch containing the radiation impedance of the port. The existence of an *either-or* choice for the volume current then demands, as usual, that a

branch point be provided — in this case, the junction marked 3. When it is necessary or desirable to extend the range of validity of such a representation, an additional inductance and capacitance can be associated arbitrarily with the box compliance C_B, as shown by the dashed-line elements, in order to simulate the effect of the first resonance and the first antiresonance of the acoustic impedance presented by the box to the back side of the loudspeaker diaphragm.

The T-configuration of the dotted rectangles enclosing the radiation-impedance elements is arranged to exhibit the mutual acoustic impedance [6] that accounts for the interaction between the two adjacent sound sources representing diaphragm and port. Such mutual-impedance effects have usually been neglected in analyzing the performance of bass-reflex enclosures. However, the use of equivalent circuits as a tool of analysis makes it easy to keep the mutual impedance under observation, and the decision to neglect or not to neglect can be postponed until the final circuit configuration is approached with actual numbers in hand.

The ideal transformer appearing at the left in Fig. 5.8(*a*) functions to convert from acoustic impedance to mechanical impedance by virtue of a "turns ratio" equal to the area of the diaphragm. If the circuit elements appearing on the right in this diagram are carried through the transformer one after the other, the transformer itself finally disappears, leaving the network transformed into the mechanical-impedance network shown in Fig. 5.8(*b*). This is somewhat more complicated than the network used to represent the radiation impedance of the unbaffled cone [cf. Fig. 5.7(*b*)], but it can be dealt with in exactly the same way. It follows then that, after the usual inversion with respect to (Bl), the modified load branch to be "read into" the equivalent circuit of Fig. 5.5 at the terminals *d–d* will take the form shown in Fig. 5.9.

Notice that the first branch, reading from the left in Fig. 5.9, contains the same elements (C_A) and (R_A) that appeared before, as might be expected since sound is still to be radiated as usual from the front surface of the diaphragm. At the right, between the points 7 and 8, appears a similar branch representing the mutual impedance. The branch 4–5–6 represents the inversion of the box compliance, now appearing as the inductance (L_B), and the dashed elements that carry the second approximation to the box impedance. Both this branch and the mutual-

[6] Robert L. Pritchard, "Mutual Acoustic Impedance between Two Circular Disks," *J. Acoust. Soc. Am.* **23,** 143 (A) (January 1951), and same topic *in extenso* in Appendix C of his Doctoral Dissertation, Harvard University, October 1950.

impedance branch provide the coupling to the elements (R'_A) and (C'_A), appearing between terminals 6 and 9. The resistance (R''_A) represents the radiation resistance of the port aperture. The inertial reaction of the incompressible part of the oscillating air flow through the aperture, which is just the "accession to inertia" for the radiating port, is embodied in the capacitance (C'_A).

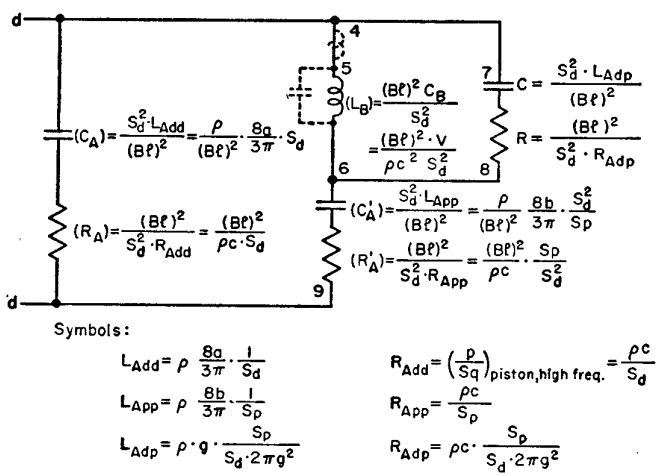

FIG. 5.9. The impedance reflected into the electric mesh (at the d–d terminals of Fig. 5.5) by the electromechanical transformation of the mechanical-impedance network of Fig. 5.8(b).

The significance of "tuning the box" by changing the dimensions of the port will be apparent now, since the value of (C'_A) is seen to depend on the port dimensions. Note first that if the port were entirely closed, making $S_p = 0$, the reactance of (C'_A) and the port radiation resistance (R'_A) would both go to zero. This would reduce the bass-reflex enclosure to a simple closed box whose acoustical influence would be manifested by the added stiffness represented in the circuit by the branch 4–5–6 containing the inductance (L_B). As a small port opening is introduced, the capacitance (C'_A) retreats from its infinite value and series resonance with the residual inductance in the (L_B)-branch occurs at some low frequency. Reference to the general circuit configuration of Fig. 5.5 will recall that such a series resonance will lead to an increase in the fraction of the current I diverted to the load branch, and hence to a

peak in the sound radiation represented by the power dissipated in (R'_A). The vector locus labeled C in Fig. 5.10 corresponds to such an adjustment, and the auxiliary loop in this locus occurring at a low frequency is the manifestation of the series resonance just described. As the area of the port is further increased, the port resonance moves

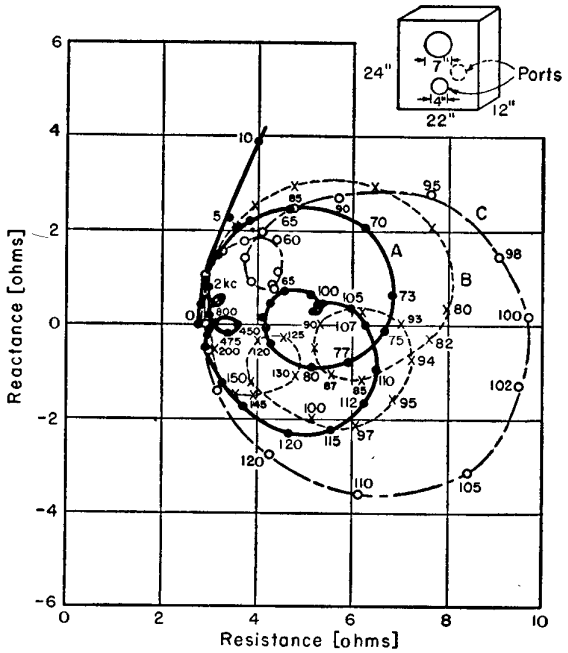

FIG. 5.10. Typical vector-impedance loci illustrating the operation of a moving-coil loudspeaker in a bass-reflex enclosure: curves C, B, and A show stages of increase in the port area and the approach toward "correct tuning" of the enclosure.

upward in frequency and continues to contribute a response peak. The port branch has the further effect of influencing the location of the frequency at which the diaphragm system has its primary mechanical resonance, the effective reactance of the port branch *above* its frequency of series resonance being of the right sign to shift the primary resonance upward. As the port area is increased toward its optimum size, therefore, its effect is to make the original peak appear to have been split into two peaks, one lying above and one below the original resonance frequency.

It is the lower of these two peaks that accounts for the beneficial extension of response toward lower frequencies.

The foregoing description has been focused on the location of critical frequencies of resonance. The height of the associated response peaks depends, of course, on the radiation resistance or other damping associated with each resonance. Examination of the expressions annexed to the various circuit elements appearing in Fig. 5.9 will indicate that enough variables are available to provide the necessary control of these damping terms. The optimum adjustment, of course, is one which makes the two peaks nearly equal and of a height that does not rise objectionably above the level of response at neighboring frequencies. The solid curve *A* of Fig. 5.10 exhibits the typical behavior of the vector impedance under an adjustment that is not far from optimum.

Similar, though slightly less informative, guidance for proper tuning of a bass-reflex enclosure can be drawn from a graph of the variation with frequency of the absolute magnitude of the electric impedance. Three curves of this type are shown in Fig. 5.11. Comparison of the multiple maxima of curve *B* in Fig. 5.11 with the successive loops of the vector locus marked *B* in Fig. 5.10 permits a direct comparison of the quality of information made available by these two experimental procedures. The vector magnitude curves serve especially well the needs

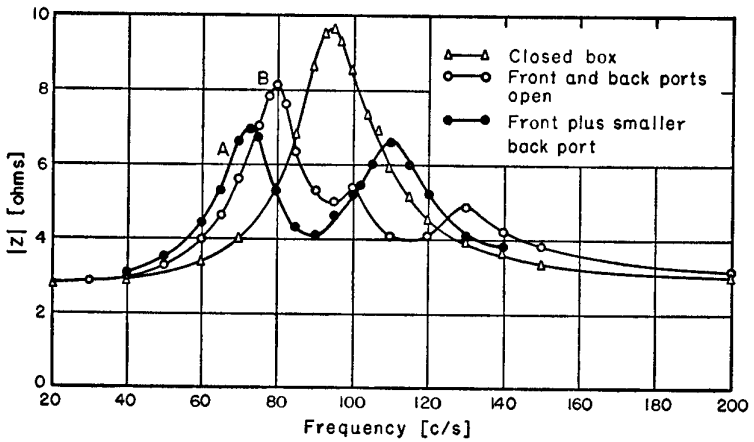

FIG. 5.11. Curves of the absolute magnitude of the electric input impedance of a direct-radiator loudspeaker in a bass-reflex enclosure; curves *A* and *B* correspond to curves *A* and *B* of Fig. 5.10.

of the amateur constructor, since the data can be obtained easily and without elaborate equipment — for example, by the expedient of supplying current to the loudspeaker from a very high-impedance source and simply observing the voltage developed across the input terminals as the frequency is varied.

Virtually all of the foregoing discussion has been devoted to considerations affecting the low frequency response of the loudspeaker. A different, but no less serious, class of problems is encountered in dealing with the response at high frequencies. This is the portion of the spectrum in which the designer is victimized by shortcomings in the physical properties of available materials of construction. The first sign of trouble to appear usually takes the form of a failure of the idealistic assumption that the diaphragm moves as a rigid "piston." This often occurs, and other modes of vibration make their appearance, at frequencies well below those for which the diaphragm begins to be acoustically large. In some respects the failure of this assumption is a blessing in disguise; when the outer portions of the diaphragm move with reduced amplitude at high frequencies, the net effect is a partial approach to the decoupling of different annular zones of the radiator at high frequencies, as contemplated in the "variable-area" schemes advanced by Wegel, Parry, Ringel, Olson, *et al.*[7] Decoupling of the outer zones arises because they are each in turn driven by a mechanical "transmission line" comprising the portion of the cone surface *inside* the driven zone; and since this transmission line has distributed mass and stiffness, it naturally behaves as a low-pass system having a cutoff frequency. Such decoupling does not come as an unmixed blessing, however. Unless special efforts are made to introduce distributed damping for flexural vibrations of the conical surface (and this is attended by its own difficulties), the mechanical driving-point impedance for the cone, its net effective radiating area, and the sound output, will each pass through pronounced maxima and minima as the frequency is increased. Eliminating these irregularities in response throughout the middle and upper range of frequency is one of the major and not yet fully solved problems of modern loudspeaker design.

No complete analytical treatment of this problem has yet been given. A method of attacking it with the aid of equivalent circuits can be suggested, but the fruitfulness of such a mode of attack on this kind of problem is still to be established. In order to mount such an attack,

[7] See notes 213, 215, 217, and 218 of Chapter 1.

the lumped circuit elements appearing in Fig. 5.5 would need to be replaced by the input terminals of a "leaky" transmission line. Such a transmission line would almost certainly be nonuniform, since it would be required to simulate the distributed mass and all the elastic properties of the cone, including the effects of radiation loading. Mawardi [8] has made some progress toward the solution of a simplified problem of this type, but it does not appear likely that a solution specifically applicable to the geometry of construction of a cone loudspeaker will become available soon.

It is possible that some progress might be made in dealing analytically with this situation by replacing the *L–C* circuit representing a diaphragm system having a single degree of freedom with a slightly more complicated network of lumped constants. For example, it might be feasible to use just enough circuit elements to provide a representation of the first few critical frequencies representing the low-order modes of vibration of the cone. At the outset, such a scheme would consist merely in simulating by a network configuration the mechanical behavior made known by other independent measurements. As to *why* such an effort might be useful — perhaps in due course such an electric-circuit model might be able to "talk back" to the designer and to provide clues concerning useful modifications of the mechanical structure from which the model was derived.

The methods of impedance analysis described in Chapter 4 can be used to deduce a good bit of additional information about the performance of the loudspeaker used for the illustrative curves of Figs. 5.6, 5.10, and 5.11. Many of the embellishments of the procedures of impedance analysis are concerned with the phase shift that gives rise to a dip angle, and much of this algebraic complexity obligingly disappears when the dip angle is zero, as in this case. Unfortunately, the usefulness of these procedures for the study of a typical mass-controlled dynamic loudspeaker is restricted by other factors. For example, much of the analysis is based on the assumption of a single degree of mechanical freedom — a condition that in no sense describes the behavior of a system capable of giving rise to a vector-impedance locus like curve *B* of Fig. 5.10! As Wegel once put it, a little ruefully, while observing the queer motion of a too-long driving link in the motor mechanism of a primitive loudspeaker, "to describe that motion in terms of only six

[8] Osman K. Mawardi, "A Physical Approach to the Loudspeaker Problem," *J. Acoust. Soc. Am.* **26**, 1–14 (January 1954).

degrees of freedom would be a gross oversimplification." [9] On the other hand, the general formulation of the analysis might make it useful to study such complicated modes of operation by means of impedance measurements — might, that is, were it not for the fact that the motional impedance is so small a fraction of the total impedance over most of the frequency range of interest that the difficulty of measuring it accurately robs the method of any general utility.

When the motional impedance *can* be measured with satisfactory accuracy, however, the machinery of impedance analysis is both applicable and useful. For example, the vacuum circle of Fig. 5.6 allows the potential efficiency for this loudspeaker to be evaluated as 43 percent. At resonance in the "infinite" baffle, the efficiency realized is only 35 percent. The latter figure is to be regarded as an electromechanical, rather than an electroacoustical, efficiency, since it was assumed that the internal mechanical resistance was not altered in going from vacuum conditions to a normal atmosphere. However, other computations based on these data confirm the suggestion made above that internal air losses may be relatively important at low frequencies. For example, the value of load resistance associated with the 35-percent efficiency is much higher than the load that would be predicted theoretically for radiation from both sides of a rigid piston in a plane baffle. The bass-reflex enclosure improves this load situation: the electromechanical efficiency (still including the parasitic internal losses of undetermined origin), at the low-frequency response peak of curve *A* in Fig. 5.10, turns out to be 43 percent, or just equal to the potential efficiency within the precision limits imposed by reading data from the plotted curves.

As for the efficiency at higher frequencies well removed from such response peaks, the motional impedance could not be (or at least *was* not) determined with enough accuracy to allow a meaningful calculation of efficiency to be made. Estimates of the least magnitude of the motional impedance that could have been observed indicate that the efficiency must have been less than 2 percent, but these are obviously not the circumstances under which impedance analysis shows up to good advantage.

[9] A dark episode in the development of the "good old WE *540AW*," nostalgically remembered by R.L.W. and privately confessed to F.V.H.

CHAPTER 6

Electrostatic Transducer Systems

Electrostatic mechanisms of electromechanical transduction have established a long, if not distinguished, record through more than two centuries of pioneering use in almost every branch of the transducer art. Yet, in spite of ubiquitous appearance on the frontiers of transduction, such systems have only within recent years been able to gain, and hold, command of first preference in any major area of the field. It is difficult to say which is the more remarkable, the consistency with which electrostatic motors and generators have yielded to other transduction mechanisms when they have competed for the same service, or the regularity with which electrostatics has been resurrected for service in special applications.

The fundamental nature of electrostatic forces is direct mechanical action exerted on relatively imponderable electric charges. In this respect these forces contrast sharply with the body stresses that characterize piezoelectricity and magnetostriction, and with the magnetic and electromagnetic forces that act on massive conductors of magnetic flux or electric current. The relatively small magnitude of electrostatic forces, and the ease with which their action can be brought to bear uniformly over extended areas, marks this mechanism of transduction as one of inherently low internal impedance — a force generator of high internal mobility, to put it in terms of the "other" analogy. But since the acoustic impedance of air is likewise low, it follows that there *should* be an essential "rightness" about the employment of electrostatic mechanisms for the transduction of airborne sounds.

Of course, the mobility advantage that goes with utilizing the force reactions of very light charges is wholly lost when the charge-carrying vehicle of force transmission is itself massive in comparison with the acoustic medium. The ever-present limitations imposed by the materials

of construction must, therefore, be overcome before the prospective advantages of the "built-in" impedance match can be realized. It was this obstacle as much as any other that doomed to only modest success the extensive development effort devoted to electrostatic loudspeakers [1] during the decade 1925–1935.

Electrostatic transduction does not die easily, however, and can hardly be expected to do so while the lure of that built-in impedance match continues to beckon the ingenious. The most recent revival of interest has been sparked by the postwar availability of synthetic diaphragm materials so light and thin that their superficial density is comparable with that of a film of air only a few millimeters thick. Even so light a diaphragm as this can not quite be regarded as acoustically negligible; but it *is* now possible to project designs that approach, more closely than ever before, the ideal situation in which electromechanical forces of transduction act directly on the sound-bearing medium without introducing any localized discontinuity in the properties of the medium.

One electrostatic device that has earned a secure place for itself in the transducer art is the condenser microphone. Wente's "uniformly sensitive instrument" [2] of 1917 probably represents the first transducer design in which sensitivity was deliberately traded for uniformity of response, and it was almost certainly the first in which electronic amplification was relied on to gain back the ground lost by eschewing resonance. Its availability — and the availability of the amplifier on which it depended — ushered in a new and thrilling era for the quantitative measurement of acoustical phenomena. The principal changes introduced in the condenser microphone itself during the next three decades consisted of the virtual elimination of the cavity in front of the diaphragm and a drastic reduction in the size of the instrument. As will appear

[1] See, for example, G. Green, "On the Condenser-Telephone," *Phil. Mag.* [7] **2,** 497–508 (September 1926); **7,** 115–125 (1929); V. F. Greaves, F. W. Kranz, and W. D. Crozier, "The Kyle Condenser Loud Speaker," *Proc. Inst. Radio Engrs.* **17,** 1142–1152 (July 1929); C. R. Hanna, "Theory of the Electrostatic Loud Speaker," *J. Acoust. Soc. Am.* **2,** 143–149 (October 1930); P. E. Edelman, "Condenser Loud-Speaker with Flexible Electrodes," *Proc. Inst. Radio Engrs.* **19,** 256–267 (February 1931); Hans Vogt, "Ueber die Erzeugung von Schallvorgängen durch das elektrostatische Feld," *Zeitschrift für technische Physik* **12,** 632–639 (1931), "Der tönende Kondensator," *Elektrotechnische Zeitschrift* **52,** 1402–1407 (12 November 1931); N. W. McLachlan, "The Stretched Membrane Electrostatic Loudspeaker," *J. Acoust. Soc. Am.* **5,** 167–171 (October 1933).

[2] See note 98 of Chapter 1; also E. C. Wente, "The Sensitivity and Precision of the Electrostatic Transmitter for Measuring Sound Intensities," *Phys. Rev.* **19,** 498–503 (*May* 1922).

shortly, it is only the impedance level of the instrument that changes when all its dimensions are altered by the same scale factor; the sensitivity remains the same. Fortunately, improvements in the performance and reductions in the size of preamplifiers have kept pace with these scale changes, although it may represent acoustical vanity to phrase it that way; it could just as well be said that the amplifier developments made these scale changes feasible. In either case, the result is that the modern miniature condenser microphone has become an indispensable tool for the acoustics laboratory, since it can be made so small in size that it produces negligible distortion of the sound field that it measures and so uniform and stable in response that it can serve as a secondary standard for sound-pressure measurements.

The Condenser Microphone — Design Features

The typical condenser microphone comprises a tightly stretched metallic diaphragm exposed to the sound field and a closely spaced counterelectrode, usually relieved by annular and radial grooves. A moderately high polarizing voltage (*ca.* 200 v) is applied through a very high resistance, by virtue of which the charge on the condenser remains substantially constant. When the capacitance is changed by *displacement* of the diaphragm, the voltage difference between the insulated back electrode and the grounded diaphragm changes accordingly, and this change constitutes the output signal. If it is intended that the output be proportional to the *pressure* of the actuating sound wave, the usual relations governing the constant-force excitation of a simple mechanical system indicate that the motion should be *stiffness controlled.* It follows that the frequency of mechanical resonance of the diaphragm must lie at or near the upper limit of the frequency range for which the microphone is expected to exhibit uniform response.

The extent to which the resonance frequency of the diaphragm can be raised by tighter stretching is sharply limited by the ultimate tensile strength of available diaphragm materials. For stainless steel (as employed in the popular WE *640AA*), this limit is approximately 7–8 kc/s. Duralumin, when rolled thin enough for the surface layer hardened by cold work to constitute most of the cross section, permits this limit to be pushed up toward 12 kc/s.[3]

[3] Theodore H. Bonn, "An Ultrasonic Condenser Microphone," *J. Acoust. Soc. Am.* **18,** 496–502 (October 1946).

An alternative method of obtaining a high resonance frequency consists in using a small thick plate as the deflecting diaphragm, the restoring force being furnished by elastic rigidity rather than by stretching. Details of construction of a contemporary high-quality microphone [4] of this type [the Altec-Lansing *Model 21B*] are shown in Fig. 6.1. The

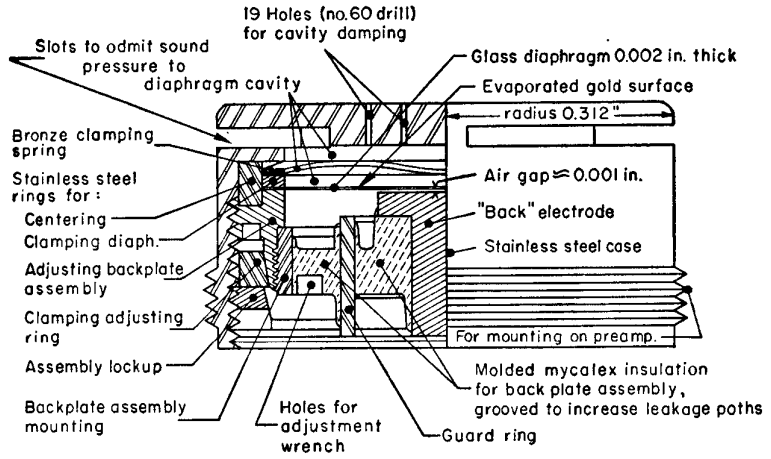

FIG. 6.1. Details of construction of a modern form of condenser microphone. (*Courtesy of Altec-Lansing Mfg. Co.*)

qualifying term "thick" is, of course, used figuratively — in this example the diaphragm is a glass disk only 0.002 in. thick. A very thin film of evaporated gold on the front surface of the diaphragm serves as the mobile electrode, and the interelectrode insulation provided by the glass diaphragm itself guards against short circuit even under blast conditions. At the same time, the relatively high dielectric constant of the glass leads to an effective interelectrode spacing that is not much greater than the thickness of the air film between the inner surface of the diaphragm and the stationary back electrode. With this scheme of construction, it is easy to modify the instrument for the measurement of very high pressure amplitudes (as required for explosion studies, for example) merely by increasing the thickness of the glass diaphragm.

Other expedients are also used to control the dynamic characteristics of the diaphragm. The spacing between the diaphragm and the stationary

[4] John K. Hilliard, "Miniature Condenser Microphone," *J. Soc. Motion Picture and Television Engrs.* **54,** 303–314 (March 1950).

electrode is usually made quite small (*ca.* 0.001 in. = 25 μ [microns]) in order to enhance the ratio of the active or variational capacitance to the fixed, or stray, capacitance between the insulated back electrode and the grounded housing. The presence of so thin a film of air trapped in the narrow air gap can influence materially the motion of the diaphragm, either by adding its stiffness to that of the diaphragm or by damping its motion, depending on whether the air is merely compressed in the air gap or is allowed to flow laterally toward the reservoirs provided by the grooves and cavities cut in the back electrode. In the latter case, a very substantial amount of viscous damping can be provided since the channel for such lateral flow is very narrow. In designing a condenser microphone for maximum uniformity of response, the dimensions and disposition of these grooves in the back electrode are carefully selected [5] to provide just-less-than-critical damping of the principal diaphragm resonance. In this way the upper limit of the range of uniform response can be made to occur somewhat above the frequency of resonance.

When a resonance peak in the response occurring outside the nominal range of coverage can be tolerated, the air-escape reservoirs can be omitted from the back plate and the stiffness of the air used to bolster up the stiffness of the diaphragm itself. This scheme finds its most interesting application in the case in which the diaphragm is made of a thin membrane of modest intrinsic strength for which most of the stiffness is contributed by the film of trapped air. For example, a small diaphragm 9 mm in diameter, made of the thin material described above, and backed up by a shallow cavity 0.5 mm deep, was found to have its principal resonance at 15.5 kc/s.[6] A more spectacular example of how far this line of attack can be carried is furnished by a report [7] of usable output obtained at frequencies as high as 1 Mc/s with a small condenser microphone in which the diaphragm was a thin plastic film and the air gap was only the thin layer of gas occluded on the polished surface of the stationary electrode.

One of the features of the condenser microphone that contributes to its usefulness as a laboratory tool is the relative ease with which its

[5] Irving B. Crandall, "The Air-Damped Vibrating System: Theoretical Calibration of the Condenser Transmitter," *Phys. Rev.* **11**, 449–460 (June 1918).

[6] Made and tested by Theodore J. Schultz, Acoustics Research Laboratory, Harvard University.

[7] Privately communicated by Dr. Erwin Meyer, III Physikalische Institut, Göttingen.

pressure calibration can be established,[8] either by reciprocity methods or by the use of an electrostatic actuator. For free-field use, however, diffraction effects must usually be taken into account even at frequencies well below resonance, and at frequencies above resonance the microphone can seldom be regarded as "small in comparison with the wavelength." Nevertheless, when these diffraction hazards can be adequately dealt with, and when the decrease in its response of 12 db per octave above resonance can be adequately compensated, the "standard" form of condenser microphone can serve usefully over a frequency range extending well up into the ultrasonic.

The Electrostatic Loudspeaker — Design Features

The electrostatic loudspeaker failed to gain wide commercial acceptance, in spite of extensive development activity [9] devoted to it during 1925–1935, for the very sound reason that several serious shortcomings still adhered to its design. Either the diaphragm or the air gap itself had usually been relied on to provide the protective insulation against electrical breakdown, but this protection was often inadequate and limits were thereby imposed on the voltages that could be used and on the specific power output. Close spacings, a film of trapped air, stiff diaphragm materials, and vulnerability to harmonic distortion combined to restrict to very small amplitudes both the allowable and the attainable

[8] A. L. DiMattia and F. M. Wiener, "On the Absolute Pressure Calibration of Condenser Microphones by the Reciprocity Method," *J. Acoust. Soc. Am.* **18**, 341–344 (October 1946); Stuart Ballantine, "Technique of Microphone Calibration," *ibid.* **3**, 319–360 (January 1932); see also L. L. Beranek, *Acoustic Measurements*, Chapter 4 (New York, Wiley, 1949).

[9] For example, Colin Kyle, U. S. Pats. No. 1,644,387 (filed 4 October 1926) issued 4 October 1927, and No. 1,746,540 (filed 25 May 1927) issued 11 February 1930; Ernst Klar (Berlin), German Pat. No. 611,783 (filed 22 May 1926) issued 5 April 1935, and U. S. Pat. No. 1,813,555 (filed 21 May 1927, renewed 14 November 1930) issued 7 July 1931 [insulating spacers, perforated plate coated with a dielectric]; Hans Vogt (Berlin), more than a score of contemporary and relevant German patents, for example, German Pats. No. 583,769 (filed 25 December 1926) issued 9 September 1933 and No. 601,117 (filed 17 May 1928) issued 8 August 1934, and U. S. Pat. No. 1,881,107 (filed 15 September 1928) issued 4 October 1932 [tightly stretched diaphragm between perforated rigid electrodes]; Edward W. Kellogg (G. E. Co.), U. S. Pat. No. 1,983,377 (filed 27 September 1929) issued 4 December 1934 [sectionalized diaphragm with inductances for impedance correction]; William Colvin, Jr., U. S. Pat. No. 2,000,437 (filed 19 February 1931) issued 7 May 1935 [woven-wire electrodes]; D. E. L. Shorter, British Pat. No. 537,931 (filed 21 February 1940, complete spec. 23 January 1941, accepted 14 July 1941) [diaphragm segmentation with external dividing networks for improving directivity and impedance].

diaphragm motion; and as a consequence, large active areas had to be employed in order to radiate useful amounts of sound power, especially at low frequencies. But when large areas were employed, the sound radiation was much too highly directional at high frequencies. Several of the patents cited above [9] bear on one or another of these features, and it is now apparent that an integration of such improvements would have made it possible to overcome almost — but not quite — every one of these performance handicaps. Occurring singly as they did, however, no one of these good ideas was able by itself to rescue the electrostatic units from the burden of their other shortcomings. Taken together, however, with the newly available diaphragm materials and with the important addition of one or two new ideas, the modern form of electrostatic loudspeaker can so completely surmount these former handicaps that it merits careful consideration as a potential competitor for the moving-coil loudspeaker in many applications.

The outstanding performance characteristic of the electrostatic loudspeaker is the unusual smoothness of its pressure response, as exemplified by the relative freedom from peaks and valleys in the curve displaying relative response as a function of frequency. The corresponding regularity of phase promotes the avoidance of waveform distortion in the reproduction of transient signals. Casual tests indicate that such smoothness of response is an important determinant of listener satisfaction, but no systematic study of this subjective aspect of electroacoustics has yet been undertaken.

A second distinguishing feature of the performance of electrostatic transducers is their high intrinsic conversion efficiency. Sound radiation does not need to share the signal energy delivered to the transducer with magnetic-hysteresis losses, eddy-current losses, nor with heat losses in a voice-coil conductor; and since the condenser dielectric is chiefly air, the dielectric losses are, or can be made, significantly lower than for most piezoelectric materials. The widespread — but erroneous — impression that electrostatic devices are "inherently inefficient" stems from a misdirection of emphasis. It is true that the input impedance of an electrostatic transducer is primarily that of a capacitive reactance; and as a consequence, such devices usually operate at a low and variable power factor. The place where dissipation occurs, however, is not in the transducer, but in the internal resistance of the signal source, which must supply the "wattless" component of the condenser charging current. Several interesting proposals have been advanced for dealing

constructively with this problem; and if it can be solved, the electrostatic loudspeaker *and* its signal source will emerge as the most efficient member of the family of electroacoustic energy transducers.

The several preceding discussions of the "variable-area" principle will at once suggest this as a useful approach to the problem of securing the simultaneous advantages of a large area for low-frequency radiation and a small area of comparable acoustical size for high-frequency radiation. The variable-area principle can be introduced effectively in either of two ways: the diaphragm may be segmented and used in conjunction with external electric dividing networks; or a thin conducting film of very high resistance can be utilized for one electrode of the condenser. In the latter case, electrical connection is made at the center or at one corner of this electrode; its high resistance and distributed capacitance then serve the functions of an *R–C* transmission line that enables the diaphragm to act as its own dividing network. In either case, it is important to notice that the principle of active-area variation serves not only to control the increase of directivity at high frequency, but also to reduce the variation of input impedance with frequency.

Other features of the so-called "modern" electrostatic loudspeaker will turn up in the conditions and assumptions on which the following analysis is based. It may be useful to summarize these,[10] however, in the form of a long serial sentence, many of whose parts will be self-explanatory: Distinguishing features of an electrostatic loudspeaker can usefully include (*a*) an extraordinarily light and strong diaphragm material, (*b*) high polarizing voltages — high enough to produce dielectric breakdown were it not for (*c*) complete sheathing of the stationary electrode with an insulating layer having high dielectric strength, (*d*) acoustic transparency of the stationary electrode, (*e*) viscous damping of the stationary electrode to keep it truly stationary, (*f*) subdivision of the diaphragm into elementary vibratory units, or bays, (*g*) systematic variation of the diaphragm stiffness by adjustment of the lateral disposition of spacers, (*h*) systematic variation of the diaphragm separation from the backplate, (*i*) arrangement for the effective area of the dia-

[10] A program of research on electrostatic loudspeakers has been pursued with varying intensity for several years at the Acoustics Research Laboratory, Harvard University. Continuity and many original ideas have been contributed by A. A. Janszen. This summary is taken from an interim report by A. A. Janszen, R. L. Pritchard, and F. V. Hunt, "Electrostatic Loudspeakers," issued as Technical Memorandum No. 17, 1 April 1950. See also A. A. Janszen, U. S. Pat. No. 2,631,196 (filed 5 October 1949) issued 10 March 1953.

phragm to vary automatically with frequency, perhaps with (j) further control of area reduction by electrical segmentation of the stationary electrode.

Electrostatic transducers can be either "single-sided," in which electrostatic forces act on only one side of the vibratile diaphragm, or "push-pull," in which electric forces act on both sides of the diaphragm. Constructional problems are usually simpler for single-sided units, and condenser microphones are almost invariably constructed in this way. Since the same electromechanical analysis will serve to describe the performance of either microphone or loudspeaker, the single-sided case will be dealt with first. The question of harmonic distortion will need to be considered carefully; and since electrostatic forces are inherently quadratic, some care must be taken to establish criteria for the control of this hazard. However, since the analytical machinery needed to deal with the nonlinear-distortion problem is relatively more cumbersome, the fundamental-frequency mode of operation for a single-sided unit will be considered first.

The Single-Sided Electrostatic Transducer

Consider first the mechanical mesh of the system described by the diagrammatic sketches of Fig. 6.2, and begin by recalling the elementary expressions for the force of attraction between oppositely charged condenser plates and for the capacitance of a parallel-plate condenser, to which can be added the basic relation between the charge on and the voltage across any condenser. These relations can be written

$$f_e = \frac{-q^2}{2\epsilon_0 S}; \quad C = \frac{\epsilon_0 S}{d+x}; \quad q = Ce_c. \tag{6.1}$$

The minus sign appears in the expression for the mechanical force of electrical origin f_e because this stress is a tension and acts in the negative x-direction. Using the notation defined by the schematic diagram of Fig. 6.2(b), the differential equation for the motion of the diaphragm can be written at once by setting the sum of the applied external (acoustic) force and the force of electrostatic attraction equal to the sum of all the mechanical reaction forces arising from diaphragm motion; thus,

$$\begin{aligned} f_A + f_e &= l_m\ddot{x} + r_m\dot{x} + \frac{1}{c_m}x, \\ f_A &= l_m\ddot{x} + r_m\dot{x} + \frac{x}{c_m} + \frac{q^2}{2\epsilon_0 S}. \end{aligned} \tag{6.2}$$

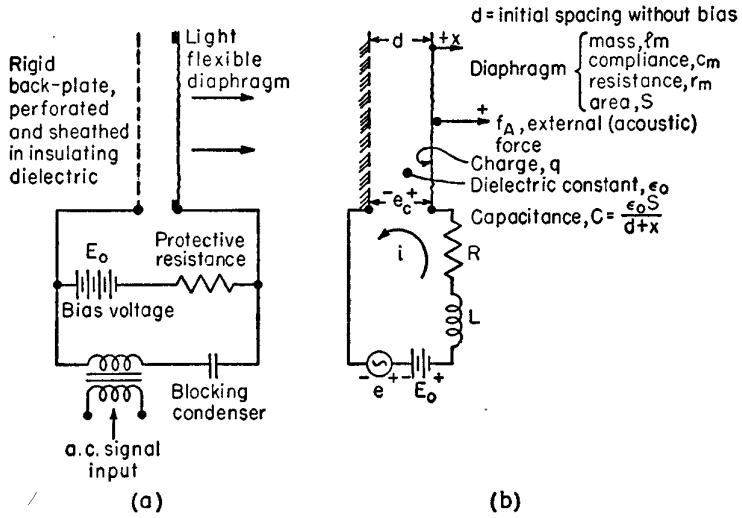

FIG. 6.2. (a) Electric circuitry for isolating the signal source and the biasing circuit for a single-sided electrostatic loudspeaker. (b) Schematic diagram establishing the nomenclature for analyzing the performance of a single-sided electrostatic transducer.

The differential equation for the electric mesh can be written in a similar way by setting the sum of the impressed polarizing and signal voltages equal to the voltage "drops" across the electric impedances; thus,

$$\begin{aligned} E_0 + e &= L\ddot{q} + R\dot{q} + \frac{q}{C}, \\ E_0 + e &= L\ddot{q} + R\dot{q} + \frac{q(d+x)}{\epsilon_0 S}. \end{aligned} \tag{6.3}$$

The presence of the q^2 term in Eq. (6.2) and of the xq term in Eq. (6.3) brands these as nonlinear differential equations. The nonlinearity is of a mild variety, however, and a valid first-order solution can be approximated by "linearizing" the equations at the outset. This amounts to neglecting the product of the variational part of q multiplied by itself or by x. For well-behaved physical systems (and this one is), another approach can be used which has the advantage of making it possible to evaluate the distortion products generated by the nonlinearity. This procedure involves assuming that each of the variables can be expanded in a Fourier series. When these series are introduced in Eqs. (6.2) and

(6.3), pairs of equations can be extracted that will describe the behavior of the systems at the zero, fundamental, and harmonic frequencies. This procedure will be carried through in detail later.

It will be useful to consider first, however, just the conditions of equilibrium and the fundamental-frequency mode of operation. For this purpose, only the first-order terms of the Fourier series will be required, and these can be written most conveniently as the sum of two conjugate exponentials. The assumed form of the solution can then be expressed by the following four equations:

$$\begin{aligned} x &= x_0 + \tfrac{1}{2}x_1 e^{j\omega t} + \tfrac{1}{2}x_1^* e^{-j\omega t}, \\ q &= q_0 + \tfrac{1}{2}q_1 e^{j\omega t} + \tfrac{1}{2}q_1^* e^{-j\omega t}, \\ f_A &= \tfrac{1}{2}F_1 e^{j\omega t} + \tfrac{1}{2}F_1^* e^{-j\omega t}, \\ e &= \tfrac{1}{2}E_1 e^{j\omega t} + \tfrac{1}{2}E_1^* e^{-j\omega t} = E_1 \cos \omega t. \end{aligned} \tag{6.4}$$

Inspection of Eqs. (6.2) and (6.3) reveals that the square of q and the product xq will also be required. These can be written out explicitly with the help of Eqs. (6.4) as follows:

$$\begin{aligned} q^2 &= q_0^2 + q_0 q_1 e^{j\omega t} + q_0 q_1^* e^{-j\omega t} + \begin{bmatrix}\text{terms in higher}\\ \text{powers of } \omega\end{bmatrix}, \\ xq &= x_0 q_0 + \tfrac{1}{2}(x_0 q_1 + x_1 q_0) e^{j\omega t} + \tfrac{1}{2}(x_0 q_1^* + x_1^* q_0) e^{-j\omega t} + \begin{bmatrix}\text{terms in higher}\\ \text{powers of } \omega\end{bmatrix}. \end{aligned} \tag{6.5}$$

The following abbreviations will also prove useful:

$$C_0 \equiv \frac{\epsilon_0 S}{d + x_0}; \quad z_m \equiv j\omega l_m + r_m + \frac{1}{j\omega c_m}; \quad Z_e = j\omega L + R + \frac{1}{j\omega C_0}; \tag{6.6}$$
$$j\omega x_1 = v_1; \quad j\omega q_1 = I_1.$$

It is now only necessary to proceed systematically to introduce the assumed form of the variables established by Eqs. (6.4) and (6.5) into Eqs. (6.2) and (6.3). After a little algebraic manipulation and rearrangement, this pair of equations can be written as follows:

$$\begin{aligned} E_0 + \tfrac{1}{2}E_1 e^{j\omega t} + \tfrac{1}{2}E_1^* e^{-j\omega t} &= \frac{q_0(d + x_0)}{\epsilon_0 S} \\ &+ \tfrac{1}{2}e^{j\omega t}\left[\left(j\omega L + R + \frac{1}{j\omega C_0}\right) j\omega q_1 + \frac{q_0}{j\omega \epsilon_0 S} j\omega x_1\right] \\ &+ \tfrac{1}{2}e^{-j\omega t}\left[\left(j\omega L - R + \frac{1}{j\omega C_0}\right) j\omega q_1^* + \frac{q_0}{j\omega \epsilon_0 S} j\omega x_1^*\right]; \end{aligned} \tag{6.7}$$

$$\begin{aligned} \tfrac{1}{2}F_1 e^{j\omega t} + \tfrac{1}{2}F_1^* e^{-j\omega t} &= \frac{x_0}{c_m} + \frac{q_0^2}{2\epsilon_0 S} \\ &+ \tfrac{1}{2}e^{j\omega t}\left[\left(j\omega l_m + r_m + \frac{1}{j\omega c_m}\right) j\omega x_1 + \frac{q_0}{j\omega \epsilon_0 S} j\omega q_1\right] \\ &+ \tfrac{1}{2}e^{-j\omega t}\left[\left(j\omega l_m - r_m + \frac{1}{j\omega c_m}\right) j\omega x_1^* + \frac{q_0}{j\omega \epsilon_0 S} j\omega q_1\right]. \end{aligned} \tag{6.8}$$

In order that this pair of equations may be satisfied at all instants of time, the coefficients of the exponentials having like powers of ωt must individually satisfy each equation. As a consequence, two pairs of equations can be extracted from Eqs. (6.7) and (6.8), one representing the steady or zero-frequency solution and one representing the solution for the assumed fundamental frequency ω.

The steady terms in Eqs. (6.7) and (6.8) can be collected as follows:

$$E_0 = \frac{q_0(d + x_0)}{\epsilon_0 S} = \frac{q_0}{C_0}, \tag{6.9a}$$

$$0 = \frac{x_0}{c_m} + \frac{q_0^2}{2\epsilon_0 S}. \tag{6.9b}$$

The first of these merely yields the unexciting information that the normal relation between charge and voltage holds with regard to the bias condition. The second contains more interesting information concerning the equilibrium position, or static deflection, of the diaphragm under the influence of polarization. If the polarizing charge q_0 is expressed in terms of the more easily measurable polarizing voltage, it turns out to be necessary to solve a cubic equation in order to compute the equilibrium displacement x_0. This will be discussed below at greater length.

Consider next the fundamental-frequency mode of operation. Since the positive and negative exponentials in Eqs. (6.7) and (6.8) have conjugate coefficients, they can be combined to yield explicitly a real cosinusoidal function; but alternatively, and more simply, it can be recognized by reference to Eqs. (6.4) that the coefficient of $e^{j\omega t}$ alone carries complete information about the complex amplitude of the cosine function. Using either method, and with the help of the notation defined by Eq. (6.6), one obtains the two electromechanical equations in the canonical form

$$E_1 = Z_e I_1 + \frac{q_0}{j\omega \epsilon_0 S} v_1, \tag{6.10a}$$

$$F_1 = \frac{q_0}{j\omega\epsilon_0 S} I_1 + z_m v_1. \tag{6.10b}$$

It can be seen at once that the transduction coefficient is symmetric and may be written explicitly in the alternative forms:

$$T_{em} = T_{me} = T = \frac{q_0}{j\omega\epsilon_0 S} = \frac{E_0}{j\omega(d + x_0)} \quad \left[\frac{\text{volts}}{\text{meter/second}} = \frac{\text{newtons}}{\text{ampere}}\right] \tag{6.11}$$

The appearance of the time-phase quadrature factor j is to be duly noted. The force factor, or coefficient of j, is real in this case, since no dielectric dissipation was included in the expression for the relation between the current into and the voltage across the capacitance C. It is also to be noted that, since the angular frequency ω appears in the denominator of T, the transduction coefficient itself can be represented as the reactance of a condenser C_{em}, whose value is defined explicitly through

$$T = \frac{1}{j\omega C_{em}}; \quad C_{em} \equiv \frac{\epsilon_0 S}{q_0} = \frac{d + x_0}{E_0}. \tag{6.12}$$

With the help of Eqs. (6.10) and (6.12), the equivalent-circuit diagram can be drawn at once as shown in Fig. 6.3(a), wherein the transduction

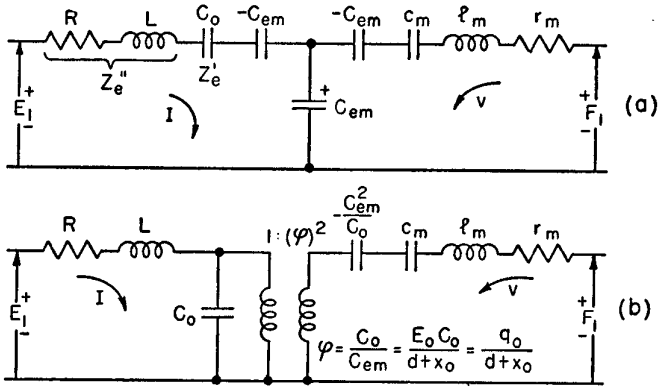

FIG. 6.3. Typical equivalent electric circuits for an electrostatic transducer.

coefficient is represented explicitly as a capacitance. The ideal electromechanical coupling transformer can then be introduced in the usual way by moving the equilibrium capacitance C_0 into the shunt position as shown in Fig. 6.3(b). The turns ratio of this ideal transformer is, as

usual, the quotient of the transduction coefficient divided by the impedance moved into the shunt position; and since in this case these are like reactance elements, the turns ratio is real. It follows, incidentally, that such a transformer would permit direct "modeling" with an analogous electric circuit. Alternative expressions for the turns ratio, and its dimensions, are shown in the following equation:

$$\phi = \frac{T}{Z_e'} = \frac{C_0}{C_{em}} = \frac{C_0 E_0}{d + x_0} = \frac{q_0}{d + x_0} \quad \left[\frac{\text{newtons}}{\text{volt}} = \frac{\text{amperes}}{\text{meter/second}}\right] \tag{6.13}$$

One of the most notable features about the equivalent circuit of Fig. 6.3(b) is the appearance of a negative capacitance, representing a negative mechanical compliance, on the mechanical side. As discussed in the preceding chapter, the shunt position for the static electric capacitance C_0 is mandatory in this case because the influence it has on the effective mechanical impedance will always be present so long as a fixed polarizing voltage is maintained across the condenser, even though the electrical terminals are otherwise on open circuit. Thus, when an external force acts to move the diaphragm from its position of mechanical equilibrium in the direction of reduced spacing, the force is opposed by the mechanical stiffness but is assisted by the increase of electrostatic attraction due to reduced spacing, and vice versa. The amount by which the effective mechanical compliance is modified as a result of the presence of a polarizing voltage can be evaluated by merging the positive and negative compliances shown in Fig. 6.3(b) into an effective mechanical compliance c_m', whose value is given by

$$c_m' = \left[(c_m)^{-1} + \left(\frac{-C_{em}^2}{C_0}\right)^{-1}\right]^{-1} = \frac{c_m}{(1 - k^2)}. \tag{6.14}$$

The numeric k is identified as the *electromechanical coupling coefficient* and is defined explicitly through

$$k^2 \equiv \frac{c_m C_0}{C_{em}^2} = c_m C_0 \left(\frac{E_0}{d + x_0}\right)^2. \tag{6.15}$$

If the diaphragm is to be mechanically stable, it is obvious that k^2 must be equal to or less than 1, since if this were not true, the net effective compliance would become infinite or negative and the diaphragm would collapse into contact with the fixed electrode. This stability condition is equivalent to requiring that

$$k^2 \leq 1; \quad \frac{1}{c_m} \geq \frac{C_0 E_0^2}{(d + x_0)^2} = \frac{E_0^2 \epsilon_0 S}{(d + x_0)^3}. \tag{6.16}$$

It is useful to compare this condition with Eq. (6.9*b*), which is a static force equation from which the equilibrium displacement x_0 can be obtained. Equation (6.9*b*) can be rewritten, for comparison, in terms of the polarizing voltage and the spacing:

$$\frac{-x_0}{c_m} = \frac{q_0^2}{2\epsilon_0 S} = \frac{C_0^2 E_0^2}{2\epsilon_0 S} = \frac{E_0^2 \epsilon_0 S}{2(d+x_0)^2} = E_0^2 \frac{\epsilon_0 S}{2d^2}\left(1+\frac{x_0}{d}\right)^{-2}. \qquad (6.17)$$

This equation cannot be solved explicitly for the equilibrium displacement x_0, because the equation is cubic in this variable, but a graphical

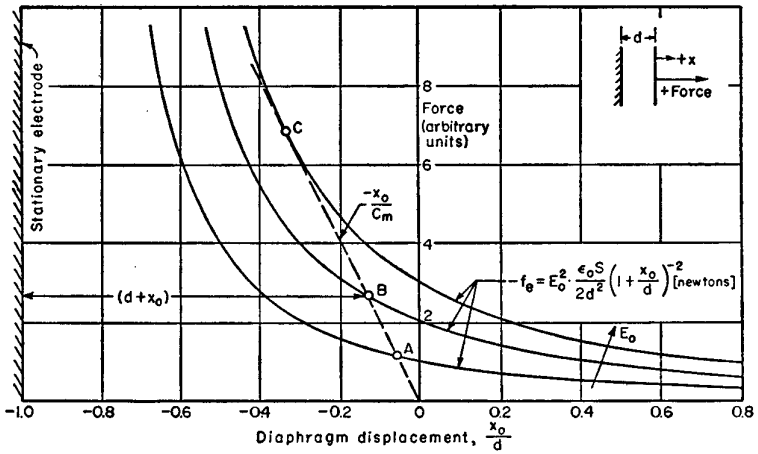

FIG. 6.4. Typical variation of the elastic- and electric-force components that determine the initial displacement under bias and the conditions of static equilibrium for a single-sided electrostatic transducer.

solution can easily be found. In the typical experimental situation, the polarizing voltage is the independent variable, in which case the situation will correspond to that illustrated in Fig. 6.4, where the dashed straight line represents the elastic restoring force given by the left-hand member of Eq. (6.17). The family of parabolic curves represents the electrostatic-attraction force given by any of the right-hand members of the serial Eq. (6.17) for different values of E_0. The intersection of the straight line with any one of these parabolic curves, as at A, B, or C, determines a corresponding equilibrium value of the normalized displacement x_0/d, which will always be negative since the positive x-direction was selected to be opposite to that in which the diaphragm is drawn by the polarizing voltage.

An instability boundary is reached when the parabolic curve for $-f_e$ just comes tangent to the straight line, as at C. Of course, the slope of the parabolic curve and of the straight line must be the same at the point of tangency, as may be verified analytically by observing that the derivative of Eq. (6.17) with respect to x_0 yields the limiting equality relation of Eq. (6.16). As a further consequence of the geometrical relations exhibited by these curves, the upper limit for x_0 can be generalized by solving Eq. (6.17) for the reciprocal compliance and comparing the result with the inequality requirement of Eq. (6.16). Thus:

$$\frac{1}{c_m} = \frac{-E_0^2 \epsilon_0 S}{2(d+x_0)^2 x_0} \geq \frac{E_0^2 \epsilon_0 S}{(d+x_0)^3}. \qquad (6.18)$$

It follows then, from Eq. (6.18), that the stability criterion can be expressed by the simple requirement that

$$\frac{-x_0}{d} \leq \frac{1}{3}. \qquad (6.19)$$

In order to solve Eq. (6.17) graphically in a practical case, the magnitude of the compliance c_m must be known. The simple form of expression for the restoring force appearing on the left-hand side of Eq. (6.17) embodies the assumption that this compliance is constant, corresponding to a linear restoring force. If the normalized equilibrium displacement x_0/d can be measured directly, this assumption can be submitted to test. It turns out that this can be done quite simply, merely by measuring the capacitance at some moderately high frequency well separated from any diaphragm resonance so that the measurement will not be significantly affected by any residual motion of the diaphragm. Then, by defining the equilibrium capacitance in the absence of polarization as C_{00}, the capacitance with polarization as C_0, and the difference between these as ΔC, the following relations can readily be established:

$$C_0 \equiv \frac{\epsilon_0 S}{d+x_0}; \quad C_{00} \equiv \frac{\epsilon_0 S}{d}; \quad \Delta C \equiv C_0 - C_{00}; \qquad \frac{-x_0}{d} = \frac{\Delta C}{C_0}; \quad \left(1+\frac{x_0}{d}\right) = \frac{C_{00}}{C_0}. \qquad (6.20)$$

A test of this kind was carried out [11] with an experimental electrostatic loudspeaker unit (abbreviated ESLU hereafter, for convenience) and

[11] I am indebted to A. A. Janszen and J. F. Hersh for the experimental measurements shown in Figs. 6.5, 6.7, 6.12, and 6.14. F.V.H.

gave the results shown in Fig. 6.5. The experimental ESLU consisted of a single "bay" comprising a thin circular diaphragm 5 inches in diameter, sandwiched between two stationary electrodes. The diaphragm material was Saran (vinylidene chloride), having a measured superficial density of 0.03 kg/m^2, a nominal thickness of 12μ, and an elastic modulus

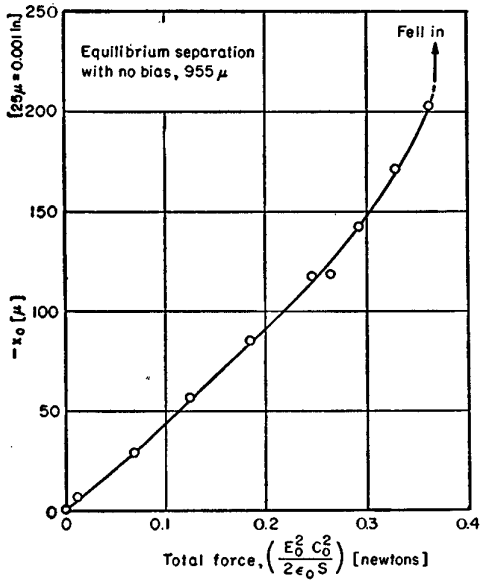

FIG. 6.5. Measurements showing typical values of diaphragm displacement, as a function of the electrostatic force due to the bias voltage, for a single-sided electrostatic loudspeaker; displacements inferred from measured change of capacitance.

of 3.5–5.5 $\times$ 10^8 newtons/m^2. The fixed electrodes were made acoustically transparent by perforations and each was completely sheathed in a sprayed-on plastic film of high dielectric strength. The two stationary electrodes were 4.5 inches in diameter and each was mounted in such a way that its separation from the vibratile diaphragm could be nicely adjusted. By altering the external connections, this experimental ESLU could be used for tests of either single-sided or push-pull operation.

The initial slope of the displacement-force curve of Fig. 6.5 is seen to be linear, within the precision of measurement, thus confirming the appropriateness of this convenient assumption. This linearity also suggests that the diaphragm, while it was not intentionally stretched any more tightly than seemed necessary in order to guard against wrinkling, must nevertheless have been under sufficient tension to make it behave

as a *stretched* membrane, since it is for this case that theory predicts a linear restoring force. If the *supported*-membrane mode of operation is used, that is, if the diaphragm is mounted so that it is under no tension except that arising from deflection, the restoring force can be expected to vary with the cube of the deflection, according to the relation

$$(f_m/S) = \alpha\left[\frac{Y_0 h}{a^4}\right]x^3; \quad x \gg 2h \tag{6.21}$$

where (f_m/S) is the force per unit area applied normal to the equivalent flat plate, x is the average displacement of the plate, Y_0 is Young's modulus of the membrane material, $2h$ is the thickness of the membrane material, $2a$ is the distance between supports (for example, for a circular membrane supported circumferentially, $2a$ would be the diameter of the mounting circle), and α is a numerical constant depending primarily on the geometry, but including also the effect of Poisson's ratio.

In some experimental ESLU's that have been tested, the diaphragm has appeared to behave as if it were partially "supported" and partially "stretched," but no attempt has been made to resolve the restoring force systematically into linear and cubic components. In order to do this, it would probably be necessary to take into account the nonplanar shape of the deflected diaphragm and the corresponding variation of electrostatic force on different annular zones.

It is easy to show that, for the case of a cubic restoring force, a stability limit of $\frac{3}{5}$ would be imposed on the equilibrium displacement $-x_0/d$, instead of the limit $\frac{1}{3}$ predicted by Eq. (6.19) for the linear case. In practice, "fall-in" usually occurs at values of $-x_0/d$ substantially less than the theoretical limit. For example, in the test shown in Fig. 6.5, fall-in occurred at a value of $-x_0/d$ of about 0.22. It was not determined whether this premature collapse was caused by the perturbing forces introduced by the signal used for capacitance measurement, by transient vibratory or acoustic forces, or by the fact that the curvature of the diaphragm allows its central portion to reach the critical spacing while the average spacing deduced from capacitance measurements is still less than the critical value, but the latter cause seems most likely.

A convenient method for assessing the electromechanical coupling is also provided by measurements of the kind shown above. If the mechanical compliance given by the equality standing on the left in Eq. (6.18) is substituted in the defining relation [Eq. (6.15)] for the coupling coefficient, the latter can be written in the form

$$k^2 = 2\,\frac{C_0(-x_0)}{\epsilon_0 S} = \frac{2(-x_0)}{d + x_0}. \qquad (6.22a)$$

Then, in terms of the quantities defined by Eq. (6.20), the coupling coefficient can be evaluated by any of the following alternative relations:

$$k^2 = 2\left(\frac{C_0}{C_\infty} - 1\right) = 2\,\frac{\Delta C}{C_\infty} = 2\,\frac{-x_0/d}{1 + (x_0/d)}. \qquad (6.22b)$$

A graphical representation of Eq. (6.22*b*) is shown in Fig. 6.6 by a curve giving the coefficient of electromechanical coupling as a function of the ratio of the change in capacitance arising from polarization to the equilibrium capacitance without polarization. Equation (6.22*b*) can also be used, in conjunction with the data for Fig. 6.5, to study the variation of the electromechanical coupling coefficient with polarizing

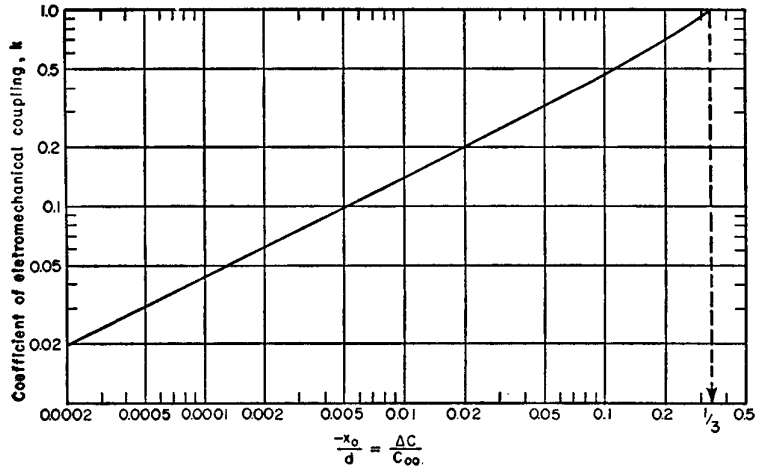

FIG. 6.6. The coefficient of electromechanical coupling for a single-sided electrostatic loudspeaker as a function of the change in capacitance produced by application of the polarizing voltage.

voltage. This relation is shown in Fig. 6.7 along with the relation between the normalized equilibrium displacement and polarizing voltage. It is notable that even for polarizing voltages no greater than 80 percent of the fall-in limit the magnitude of the coupling coefficient is substantially in excess of that obtained with even the most active of magnetostrictive or piezoelectric materials. More conservative values of

polarization, such as half the fall-in limit, can still yield coupling coefficients of the order 0.25.

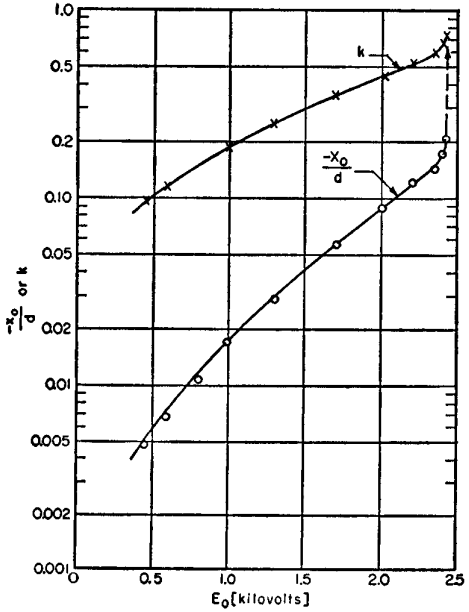

FIG. 6.7. The electromechanical coupling coefficient and the equilibrium displacement under polarization, displayed as a function of bias voltage for an experimental electrostatic loudspeaker unit.

The Push-Pull Electrostatic Loudspeaker

A variety of different circuit arrangements can be used to provide double-sided operation of an electrostatic loudspeaker, but the configuration shown [12] in Fig. 6.8 has been found to have novel advantages. It will be observed that the two stationary electrodes flanking the vibratile diaphragm are each at ground potential, except for the a.c. signal voltage. The latter is assumed to be divided equally between the two meshes containing the "active" condensers C_a and C_b, as it would normally be if the signal is delivered at the terminals of a center-tapped coupling transformer as indicated. One of the practical virtues of this circuit

[12] Carlo V. Bocciarelli of the Philco Corp. suggested this circuit to us and argued qualitatively the advantages of "constant-charge" operation. The analysis given below shows the performance to be even better than predicted. The circuit itself, though not its unusual virtues, has been proposed in various patents and other publications dating back at least to H. Riegger's disclosure in German Pat. No. 398,195 (filed 10 March 1920) issued 2 July 1924.

arrangement is that the electrode bearing the high polarizing voltage is prevented from becoming a shock hazard by the protective housing formed by the rugged stationary electrodes. As before, the electric-impedance elements L_a, R_a, L_b, and R_b are included for generality. The resistance R_0 in the common leg of the circuit serves as the high resistance designated as "protective" in Fig. 6.2(a). The impedance in this branch is common to the two meshes and, as will be seen later, it turns out to have an important influence on the performance of the ESLU.

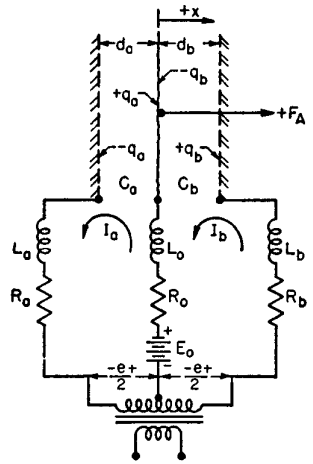

FIG. 6.8. Schematic diagram establishing the nomenclature for analysis of the push-pull electrostatic loudspeaker.

By way of whetting interest in the analysis to follow, one remarkable feature of the push-pull ESLU can be described at the outset in qualitative terms. It is customary to regard electrostatic devices as inherently nonlinear, since the tractive force between condenser plates maintained at a constant potential difference varies inversely as the square of their separation. Consider, however, the situation presented by Fig. 6.8, and assume that a large charge has been placed on the mobile diaphragm. If the charging circuit is now disconnected — or, what is equivalent, if R_0 is made so large that the time constants R_0C_a and R_0C_b are very long — then the force acting on the diaphragm will be determined only by the magnitude of the unvarying charge on the diaphragm and by the electric field established by the signal voltage between the stationary electrodes, and will be *independent of the position* of the diaphragm in the space between these electrodes. As a consequence, many of the

limitations previously regarded as "inherent" to electrostatic systems will *not* limit the performance of an ESLU in this mode of operation. For example, in so far as linearity requirements are concerned, it will no longer be necessary to restrict the allowable motion of the diaphragm to a small fraction of the initial separation. Moreover, the restriction on the allowable ratio of signal voltage to polarizing voltage will also disappear. Confirmation of these remarkable performance features will constitute the objective of the following analysis.

Three basic equations will be required to describe the electromechanical system of Fig. 6.8 — one for the single mechanical mesh and one each for the two electric meshes identified by subscripts a and b. With the help of Eqs. (6.1)–(6.3) above, these can readily be written by inspection. Alternatively, the energy functions can be formulated so that Lagrangian equations can be written in the appropriate variables. By either procedure, the basic equations emerge as

$$F_A = z_m v - F_e$$
$$= l_m\ddot{x} + r_m\dot{x} + \frac{x}{c_m} - \left[\frac{q_b^2}{2\epsilon_0 S} - \frac{q_a^2}{2\epsilon_0 S}\right], \tag{6.23}$$

$$+E_0 + \frac{e}{2} = (L_a + L_0)\ddot{q}_a - L_0\ddot{q}_b + (R_a + R_0)\dot{q}_a - R_0\dot{q}_b + \frac{q_a}{C_a}, \tag{6.24a}$$

$$-E_0 + \frac{e}{2} = (L_b + L_0)\ddot{q}_b - L_0\ddot{q}_a + (R_b + R_0)\dot{q}_b - R_0\dot{q}_a + \frac{q_b}{C_b}. \tag{6.24b}$$

The letter symbols and the algebraic signs used in these expressions are defined by Fig. 6.8. The following definitions are also implied:

$$C_a = \frac{\epsilon_0 S}{d_a + x}; \quad i_a = \dot{q}_a; \quad C_b = \frac{\epsilon_0 S}{d_b - x}; \quad i_b = \dot{q}_b; \quad d_a + d_b = 2d. \tag{6.25}$$

Solutions of these nonlinear differential equations can be sought, as before, by assuming that each of the variables can be expressed in the form of a Fourier series, which can be written most conveniently in complex exponential form, as follows:

$$x = \sum_{-\infty}^{+\infty} \frac{1}{\epsilon_n} x_n e^{jn\omega t}, \tag{6.26a}$$

where $|\, x_n \,|$ is the peak amplitude of the nth harmonic, $x_{-n} = x_n^*$, and ϵ_n is the Neumann factor and has the value 1 if $n = 0$, but the value 2 if $n \neq 0$;

$$q_{a,b} = \sum_{-\infty}^{+\infty} \frac{1}{\epsilon_n} q_{a,b;n} e^{jn\omega t}, \tag{6.26b}$$

$$F_A = \sum_{-\infty}^{+\infty} \frac{1}{\epsilon_n} F_n e^{jn\omega t} - F_0, \tag{6.26c}$$

$$e = \frac{E_1}{2} e^{j\omega t} + \frac{E_1}{2} e^{-j\omega t} = E_1 \cos \omega t. \tag{6.26d}$$

The last equation announces that reference phase is established by the impressed signal voltage, and that this signal is a pure cosinusoid (fundamental frequency only, as indicated by the subscript on E_1). The various derivatives of x and q, and their product, that occur in Eqs. (6.23) and (6.24), can be written explicitly as

$$\begin{aligned}
&\dot{x} = \sum \frac{1}{\epsilon_n} jn\omega x_n e^{jn\omega t}; \quad \dot{q}_{a,b} = \sum \frac{1}{\epsilon_n} jn\omega q_{a,b;n} e^{jn\omega t}, \\
&q^2 = \sum_n \sum_m \frac{1}{\epsilon_n \epsilon_m} q_n q_m e^{j(n+m)\omega t}, \\
&xq = \sum_n \sum_m \frac{1}{\epsilon_n \epsilon_m} x_n q_m e^{j(n+m)\omega t}, \\
&\ddot{x} = \sum \frac{1}{\epsilon_n} (-n^2\omega^2) x_n e^{jn\omega t} = \sum \frac{1}{\epsilon_n} (jn\omega) jn\omega x_n e^{jn\omega t}, \\
&\ddot{q} = \sum \frac{1}{\epsilon_n} (-n^2\omega^2) q_n e^{jn\omega t} = \sum \frac{1}{\epsilon_n} (jn\omega) jn\omega q_n e^{jn\omega t}.
\end{aligned} \tag{6.27}$$

This set of relations corresponds to Eqs. (6.4) and (6.5) used above, but the summations appearing in Eqs. (6.27) will furnish the complete series expansion for each of these physical variables instead of just the fundamental-frequency terms that were used in the simpler analysis carried through before. When Eqs. (6.26) and (6.27) are introduced in Eqs. (6.23) and (6.24), each of the latter will consist of an infinite sum of terms of the generic form $H_N e^{jN\omega t}$. As usual, if these two equations are to be satisfied at all instants of time, each of the separate equations like (6.23) and (6.24) that are made up of just the coefficients H_N of like order N must individually be satisfied. Each coefficient H_N, however, is itself composed of a summation of terms in x_n, q_n, or both, whose subscripts have the same algebraic sum N. In general, therefore, a complete solution for *any* of the physical variables of order N would require the solution of an infinite set of simultaneous algebraic equations. Fortunately, these series converge rapidly enough in practice for a useful,

and generally adequate, approximation to be achieved while still neglecting in each series, for a particular N, all terms in $N+2$ or higher. For example, the products $q_1 q_1^*$ and $q_2 q_2^*$ would belong in the series for $N = 0$ (since $q_1^* = q_{-1}$); but since they are of order 2 and 4, respectively, they can be safely discarded. This procedure can be illustrated by writing out in full all the terms to be retained in the expressions for q^2 and xq:

$$\begin{aligned}
q_{a,b}^2 = q_0^2 &+ e^{j\omega t}\tfrac{1}{2}[2q_1 q_0 + \begin{cases} q_2 q_1^* + q_1 q_2^* + \cdots \\ \text{neglected} \end{cases} \\
&+ e^{j2\omega t}\tfrac{1}{2}[+\tfrac{1}{2} q_1^2 + 2q_2 q_0 + \begin{cases} q_3 q_1^* + \cdots \\ \text{neglected} \end{cases} \\
&+ e^{j3\omega t}\tfrac{1}{2}[2q_3 q_0 + q_2 q_1 + \begin{cases} q_4 q_1^* + \cdots \\ \text{neglected,} \end{cases}
\end{aligned} \tag{6.28a}$$

$$\begin{aligned}
xq_{a,b} = x_0 q_0 &+ e^{j\omega t}\tfrac{1}{2}[x_0 q_1 + x_1 q_0 + \cdots] \\
&+ e^{j2\omega t}\tfrac{1}{2}[\tfrac{1}{2} x_1 q_1 + x_2 q_0 + x_0 q_2 + \cdots] \\
&+ e^{j3\omega t}\tfrac{1}{4}[2x_3 q_0 + 2x_0 q_3 + x_2 q_1 + x_1 q_2 + \cdots].
\end{aligned} \tag{6.28b}$$

The appropriate subscript a or b is to be prefixed before the numerical index for each of the quantities on the right in Eqs. (6.28a,b) in order to identify the corresponding quantities for the two electric meshes. Finally, at long tedious last, Eqs. (6.28a,b) and like expansions for the other quantities given in Eqs. (6.27) are to be substituted in the three basic Eqs. (6.23), (6.24a), and (6.24b). Three equations each can then be extracted from the resulting algebraic mess (!), for $N = 0, 1, 2, 3$. These correspond respectively to the zero-frequency or static equilibrium situation, and to operation at the fundamental frequency and at the second and third harmonic frequencies. In expressing these results, the abbreviations defined by Eqs. (6.6) and (6.12) can be collected and extended, as follows:

$$\begin{aligned}
&T_{an} = \frac{q_{a0}}{jn\omega\epsilon_0 S} = \frac{E_0}{jn\omega(d_a + x_0)}; \quad T_{bn} = \frac{q_{b0}}{jn\omega\epsilon_0 S} = \frac{-E_0}{jn\omega(d_b - x_0)}; \\
&C_{ema} = \frac{d_a + x_0}{E_0}; \quad C_{emb} = \frac{d_b - x_0}{E_0}; \quad C_{a0} = \frac{\epsilon_0 S}{d_a + x_0}; \quad C_{b0} = \frac{\epsilon_0 S}{d_b - x_0}; \\
&Z_{ean} = \left(jn\omega L_a + R_a + \frac{1}{jn\omega C_{a0}}\right); \quad Z_{ebn} = \left(jn\omega L_b + R_b + \frac{1}{jn\omega C_{b0}}\right); \\
&z_{mn} = \left(jn\omega l_m + r_m + \frac{1}{jn\omega c_m}\right); \quad F_{An} = -z_{Ln} v_n; \\
&jn\omega q_{an} = I_{an}; \quad jn\omega q_{bn} = I_{bn}; \quad jn\omega x_n = v_n; \\
&z_{Ln} = \text{mechanical impedance presented by radiation loading at the } n\text{th harmonic frequency.}
\end{aligned} \tag{6.29}$$

An Aside: Harmonic Distortion Products for the Single-Sided ESLU

It is timely now to take another look at the electromechanical circuit of Fig. 6.8, and to observe that if the connection to the right-hand stationary electrode is broken, so that the b-mesh is removed, the remaining a-mesh corresponds exactly to the single-sided case considered above. By the same token, Eqs. (6.23) and (6.24a) reduce to the equivalent of Eqs. (6.2) and (6.3) if q_b and its derivatives are set equal to zero, and if $(L_a + L_0)$ is identified with L of Eq. (6.3) and $(R_a + R_0)$ with R. The relations needed for a study of harmonic distortion in the single-sided ESLU can be marshaled, therefore, in terms of this reduced form of Fig. 6.8. The extension to the push-pull case can then be made simply by replacing the terms omitted from Eq. (6.24a) and adding Eq. (6.24b).

$N = 0.$

$$0 = \frac{x_0}{c_m} + \frac{q_{a0n}^2}{2\epsilon_0 S}$$
$$E_0 = \frac{q_{a0}(d_a + x_0)}{\epsilon_0 S} = \frac{q_{a0}}{C_{a0}}. \tag{6.30a}$$

$N = 1.$

$$0 = (z_{m1} + z_{L1})v_1 + T_{a1}I_{a1},$$
$$E_1 = T_{a1}v_1 + Z_{ea1}I_{a1}. \tag{6.30b}$$

$N = 2.$

$$-\frac{q_{a1}^2}{4\epsilon_0 S} = (z_{m2} + z_{L2})v_2 + T_{a2}Ia_2,$$
$$-\frac{x_1 q_{a1}}{2\epsilon_0 S} = T_{a2}v_2 + Z_{ea2}I_{a2}. \tag{6.30c}$$

$N = 3.$

$$-\frac{q_{a2}q_{a1}}{2\epsilon_0 S} = (z_{m3} + z_{L3})v_3 + T_{a3}I_{a3},$$
$$-\frac{(x_2 q_{a1} + x_1 q_{a2})}{2\epsilon_0 S} = T_{a3}v_3 + Z_{ea3}I_{a3}. \tag{6.30d}$$

Note first that the "impressed," or "forcing," quantities appearing on the left in Eqs. (6.30c) and (6.30d), which are written here as they emerge from the algebraic "mess" referred to above, can be expressed in terms of the corresponding currents and velocities by using the elementary relations $j\omega q_a = I_a$ and $j\omega x = v$. The tactical advantage gained by discarding the terms in $(N + 2)$ and higher will now become apparent. The fundamental-frequency components of velocity and current can be found by solving Eq. (6.30b), since the only forcing function is the impressed signal E_1. With v_1 and I_1 in hand, the forcing functions for the

second-harmonic components of velocity and current are known, and Eq. (6.30c) can be solved for v_2 and I_2. Then, with v_1, v_2, I_1, and I_2 known, the third-harmonic components can be evaluated from Eq. (6.30d), and so on. The fact that these harmonic components *can* be evaluated in this way does not gainsay the fact that there are too many physical variables involved to make it easy to interpret the results in general terms. The quantity that is probably of most interest is the ratio of the second-harmonic velocity to the velocity at the fundamental frequency. By a tedious procedure of the sort often referred to euphemistically as "a little algebraic manipulation," the relative second-harmonic velocity can be expressed in the form [13]

$$\frac{v_2}{v_1} = \left(\frac{E_1}{4E_0}\right)\left(\frac{z'_{m1}}{z'_{m2}}\right)(1 + \gamma)(1 + 3\gamma), \tag{6.31a}$$

where z'_{m1} and z'_{m2} are total effective mechanical impedances at the corresponding frequencies, including the radiation load and the negative stiffness contributed by polarization, and γ is a complex quantity that represents the ratio of this electromechanical component of negative stiffness to the total mechanical impedance. Alternatively, this complex quantity can be expressed as the product of two ratios,

$$\gamma = -\left(\frac{x_1}{d + x_0}\right)\left(\frac{\sqrt{2}E_0}{E_1}\right). \tag{6.31b}$$

An upper bound for the distortion predicted by Eq. (6.31a) can be stated in terms of the absolute magnitudes of these ratios, in the form

$$\left|\frac{v_2}{v_1}\right| \leq \left|\frac{E_1}{4E_0}\right| \cdot \left|\frac{z'_{m1}}{z'_{m2}}\right| (1 + 4\,|\gamma| + 3\,|\gamma|^2). \tag{6.31c}$$

A sample calculation using the upper limits often quoted for ESLU operation, namely, $E_1/E_0 \leq \frac{1}{4}$, $x_1/d \leq 1/20$, will confirm the conclusion that these restrictions on signal voltage and allowable diaphragm excursion are by no means conservative.

Returning now to the push-pull ESLU, it can be remarked at the outset that the harmonic distortion generated during push-pull operation of almost any quasi-linear system affords an agreeable contrast with the distortion products arising in single-sided operation. In the present instance, however, the comparison will turn out to be spectacular.

[13] This compact form of summarizing the results on second-harmonic distortion for the single-sided ESLU was devised by R. L. Pritchard; see note 10.

By returning to the algebraic wars and completing the substitution of Eqs. (6.28) and (6.27) into Eqs. (6.23), (6.24*a*) and (6.24*b*), the electromechanical equations for the push-pull ESLU can be marshaled as follows:

$N = 0.$

$$0 = \frac{x_0}{c_m} + \frac{q_{a0}^2 - q_{b0}^2}{2\epsilon_0 S},$$

$$E_0 = \frac{q_{a0}}{\epsilon_0 S}(d_a + x_0) = \frac{q_{a0}}{C_{a0}}, \qquad (6.32a)$$

$$-E_0 = \frac{q_{b0}}{\epsilon_0 S}(d_b - x_0) = \frac{q_{b0}}{C_{b0}}.$$

$N = 1.$

$$0 = (z_{m1} + z_{L1})v_1 + T_{a1}I_{a1} - T_{b1}I_{b1},$$

$$\left(\frac{E_1}{2}\right)_a = T_{a1}v_1 + (Z_{ea1} + Z_{01})I_{a1} - Z_{01}I_{b1}, \qquad (6.32b)$$

$$\left(\frac{E_1}{2}\right)_b = -T_{b1}v_1 - Z_{01}I_{a1} + (Z_{eb1} + Z_{01})I_{b1}.$$

$N = 2.$

$$\frac{q_{b1}^2 - q_{a1}^2}{4\epsilon_0 S} = (z_{m2} + z_{L2})v_2 + T_{a2}I_{a2} - T_{b2}I_{b2},$$

$$-\frac{x_1 q_{a1}}{2\epsilon_0 S} = +T_{a2}v_2 + (Z_{ea2} + Z_{02})I_{a2} - Z_{02}I_{b2}, \qquad (6.32c)$$

$$+\frac{x_1 q_{b1}}{2\epsilon_0 S} = -T_{b2}v_2 - Z_{02}I_{a2} + (Z_{eb2} + Z_{02})I_{b2}.$$

$N = 3.$

$$\frac{q_{b2}q_{b1} - q_{a2}q_{a1}}{2\epsilon_0 S} = (z_{m3} + z_{L3})v_3 + T_{a3}I_{a3} - T_{b3}I_{b3},$$

$$-\frac{x_1 q_{a2} + x_2 q_{a1}}{2\epsilon_0 S} = +T_{a3}v_3 + (Z_{ea3} + Z_{03})I_{a3} - Z_{03}I_{b3}, \qquad (6.32d)$$

$$\frac{x_1 q_{b2} + x_2 q_{b1}}{2\epsilon_0 S} = -T_{b3}v_3 - Z_{03}I_{a3} + (Z_{eb3} + Z_{03})I_{b3}.$$

Static Equilibrium: $N = 0$

The zero-frequency Eqs. (6.32*a*) will, as before, yield information about the conditions of static equilibrium. For this case, the time constants R_0C_a and R_0C_b are of no consequence since the charges q_{a0} and q_{b0} will eventually adjust themselves to bring both C_a and C_b to the full bias voltage E_0. The q's can be eliminated then from the first of Eqs. (6.32*a*), by using the other two relations, whereupon the equilibrium condition can be written as

$$-\frac{x_0}{c_m} \equiv F_{m0} = -F_{e0} \equiv \frac{q_{a0}^2 - q_{b0}^2}{2\epsilon_0 S} = \frac{E_0^2 \epsilon_0 S}{2}\left\{\frac{1}{(d_a + x_0)^2} - \frac{1}{(d_b - x_0)^2}\right\}. \qquad (6.33)$$

Note carefully the algebraic signs attached to F_{m0}, the elastic restoring force acting *on* the diaphragm, and to the electrical force F_{e0}. Equilibrium requires, of course, that the sum of these be zero, which is just what Eq. (6.33) says. As before, this is a cubic in x_0, so a graphical solution would appear to be indicated; but it will be useful to consider first the general behavior of the electrical force F_{e0}. At this point it will be prudent to insist temporarily on structural symmetry so that it can be assumed that $d_a = d_b = d$. The electrical-force part of Eq. (6.33) can then be manipulated into the following form:

$$F_{e0} = \frac{E_0^2 \epsilon_0 S}{2}\left\{\frac{1}{(d - x_0)^2} - \frac{1}{(d + x_0)^2}\right\} = E_0^2 \epsilon_0 S \frac{2x_0 d}{(d^2 - x_0^2)^2} = \frac{2E_0^2 \epsilon_0 S}{d^2}\left[\frac{\delta}{(1 - \delta^2)^2}\right] = \frac{2E_0^2 \epsilon_0 S}{d^2}[\delta + 2\delta^3 + 3\delta^5 + \cdots], \qquad (6.34)$$

where $\delta\,[\equiv x_0/d]$ has been introduced as an abbreviation for the normalized displacement coördinate. It is at once apparent that the equilibrium Eq. (6.33) is satisfied by $x_0 = \delta = 0$; which is to say that there will be no shift of diaphragm position when bias voltage is applied. It is also apparent that the electrical force is linear for small displacement, and that it acts *in the direction of the displacement.* It constitutes, therefore, a *negative stiffness* whose magnitude is given by the derivative of F_{e0} with respect to x_0. If the electrical stiffness is defined as $1/c_e$, it can be evaluated readily from Eq. (6.34) as

$$\frac{1}{c_e} \equiv \frac{dF_{e0}}{d(-x_0)} = -\frac{dF_{e0}}{d\delta}\cdot\frac{d\delta}{dx_0}, \qquad \left(-\frac{1}{c_e}\right) = \frac{2E_0^2 \epsilon_0 S}{d^3}(1 + 6\delta^2 + \cdots) \qquad (6.35)$$

The typical equilibrium conditions prescribed by Eq. (6.33) are exhibited graphically in Fig. 6.9. The elastic force F_{m0} and the electrical force F_{e0} are shown by the solid-line curves; the electrical force is shown

also with reversed sign (dashed curve) so that its intersection with the straight line representing F_{m0} can display the equality demanded by Eq. (6.33). Note that all three solutions of the cubic equation are in evidence; but note also that the two intersections marked A are not only unstable but also inaccessible, since the electrical negative stiffness will

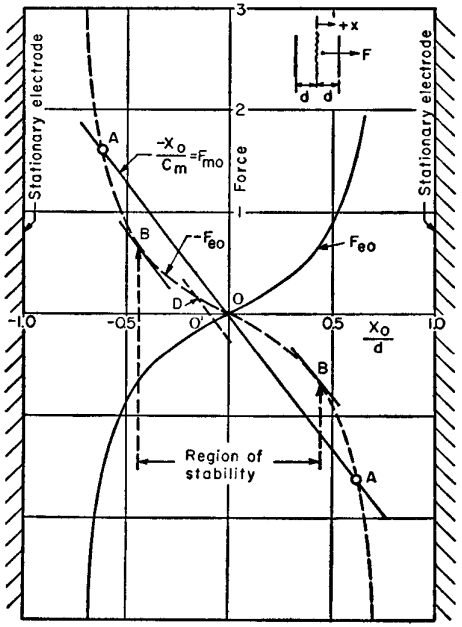

FIG. 6.9. Typical variation of the electric and mechanical forces affecting static equilibrium for the push-pull electrostatic loudspeaker.

have exceeded the mechanical positive stiffness, and "fall-in" will have ensued, before the points A can be reached. The boundaries of the region of stability are indicated by the points marked B, at which the *slope* of the $(-F_{e0})$-curve matches that of F_{m0}. These points can be located analytically by first expressing the fact that the mechanical stiffness must exceed the electrical negative stiffness, and then by solving for the critical value of δ in the limiting equality. Thus, with c_e given by Eq. (6.35),

$$\frac{1}{c_m} \geq \left(\frac{-1}{c_e}\right),$$
$$\frac{1}{c_m} \geq \frac{2E_0^2\epsilon_0 S}{d^3}(1 + 6\delta^2 + 15\delta^4 + \cdots). \tag{6.36}$$

Note how this result compares with the corresponding criterion for the single-sided case given by Eq. (6.16) above. By introducing the (theoretical) critical limit $x_0 = -d/3$, Eq. (6.16) can be solved for the value of E_0 at which fall-in would occur; this yields

$$(E_0)_{\text{crit.,s.s.}} = \left(\frac{8}{27} \cdot \frac{d^3}{c_m\epsilon_0 S}\right)^{\frac{1}{2}}. \tag{6.37a}$$

In the push-pull case, the diaphragm remains undeflected in spite of increasing bias, but its stiffness is progressively neutralized and fall-in would occur for the value of E_0 given by Eq. (6.36) with δ set equal to zero, namely,

$$(E_0)_{\text{crit.,p.p.}} = \left(\frac{1}{2} \cdot \frac{d^3}{c_m\epsilon_0 S}\right)^{\frac{1}{2}} \doteq 1.30\,(E_0)_{\text{crit.,s.s.}} \tag{6.37b}$$

It was observed experimentally for the single-sided ESLU that the diaphragm fell in at values of δ that were only $\frac{2}{3}$ of the theoretical limit, but since both critical voltages are likely to be influenced in a similar way by the perturbations that hasten diaphragm collapse, the advantage in this respect would appear to remain with the push-pull case.

The generality sacrificed by requiring that $d_a = d_b$ can now be recouped. If a little asymmetry were introduced — by moving the mounting frame for the diaphragm a little to the left, for example, so that $d_a < d_b$ — the effect would be to shift correspondingly the neutral axis-crossing point O' for the F_{m0} curve, as shown by the short dashed line drawn parallel to F_{m0} in Fig. 6.9. The equilibrium prescribed by Eq. (6.33) would then occur at D, the new intersection of F_{m0} and $(-F_{e0})$; and this point will always lie farther from the central position than the distance to which O' was shifted by the structural asymmetry. The extent to which the asymmetry is exaggerated in this way depends on the relative slopes of these curves, that is, on the extent to which the mechanical stiffness is neutralized by the negative electrical stiffness. The boundaries of the region of stability are still located symmetrically with respect to the mid-point between the stationary electrodes, however, so that one effect of the structural shift is to reduce the effective width of the stable region.

For single-sided operation, diaphragm collapse was found to occur always at a particular critical value of $-x_0/d$. In the push-pull case, on the other hand, the slope of the F_{e0}-curve increases progressively on either side of the central position and may yield a critical value of x_0/d

that is either large or small depending on the bias voltage [cf. Eq. (6.36)]. This effect may be measured, as before, by defining a coefficient of electromechanical coupling in terms of the relative values of the mechanical and electrical contributions to stiffness. Equation (6.14), the defining relation for the coupling coefficient k, can easily be transposed to the form

$$k^2 = \frac{(-1/c_e)}{(1/c_m)}. \tag{6.38a}$$

The initial value of the electrical stiffness can be found by setting $\delta = 0$ in Eq. (6.35); and when this is introduced in Eq. (6.38a), the coupling coefficient becomes

$$k^2 = \frac{2E_0^2\epsilon_0 S c_m}{d^3} = \frac{2c_m C_{00}}{(d^2/E_0^2)} = \frac{2c_m C_{00}}{C_{em}^2}. \tag{6.38b}$$

The introduction of C_{em} in this expression anticipates the identification of the transduction coefficient that will turn up in connection with the fundamental mode of operation.

One basic feature of the foregoing deserves reëmphasis. When the diaphragm is displaced by some external agency, the electrical forces indicated by the F_{e0} curve of Fig. 6.9 can come into play only in so far as it is possible for electric charge to flow to or from the diaphragm in the amount required to keep the condensers C_a and C_b charged just to the bias voltage E_0. For example, if the time constant R_0C_a were very long, and if an external force acted suddenly to deflect the diaphragm to a position even beyond the point marked A in Fig. 6.9, the initial effect would be an increase in C_a and a drop in the voltage across C_a (with corresponding converse changes for C_b). Instability and fall-in would *not* manifest itself until enough time had elapsed for the charge on C_a to rebuild its voltage back toward E_0 far enough to reach the critical voltage for the assumed diaphragm displacement. It follows that diaphragm excursions of *any* extent will not precipitate static instability or fall-in provided their "dwell time" in the unstable region is short in comparison with the time constants.

The foregoing can be summarized briefly by two statements: (*a*) the stability criterion given by Eq. (6.36) *must* be observed in order to assure the stability of *static* equilibrium; (*b*) but instability will not be precipitated even by large excursions occurring under dynamic conditions at frequencies for which the half-period is negligible in comparison with

the time constant of the biasing circuit, that is, for frequencies that satisfy the criterion

$$f \gg \frac{1}{2R_0C_{a,b}}. \tag{6.39}$$

The Push-Pull ESLU at Fundamental Frequency: $N = 1$

The set of equations for $N = 1$ [Eqs. (6.32b)] display an agreeable symmetry. The two electric meshes are coupled by the common impedance Z_{01}, and each is coupled to the single mechanical mesh by a (symmetric) transduction coefficient. A three-mesh configuration such as that shown in Fig. 6.10(a) would appear to satisfy these coupling requirements, but one must always set up such trial circuits with caution until it is verified that all the algebraic signs and the assumed

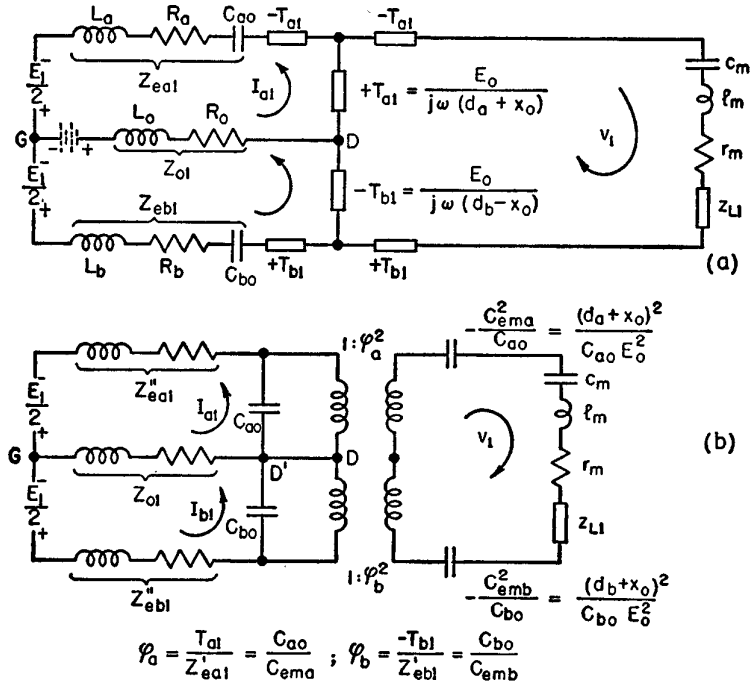

FIG. 6.10. (*a*) The basic equivalent circuit for the push-pull electrostatic loudspeaker; (*b*) transformation of the equivalent circuit of (*a*).

directions of all currents are self-consistent. The basic test, however, is to write out explicitly the three-mesh equations for the alleged equivalent circuit and compare these with the "original." If they agree, the equivalence is established. Figure 6.10(*a*) passes this test, so one may proceed at once to transform it to the configuration shown in Fig. 6.10(*b*). The structural symmetry might be better suggested in the mechanical mesh if the mechanical-impedance elements and the load impedance were each divided into two parts and disposed symmetrically about the mid-line of the circuit diagram. Nothing would be gained by this, however, since this is an equivalent circuit, not a pictorial diagram. The essential feature of the mechanical mesh is that two forces act on a *single* mass element that has a *single* velocity, and this is just what the mesh diagram displays.

Two important conclusions can be drawn from a qualitative study of this equivalent circuit. If structural symmetry has been preserved, so that $C_{a0} = C_{b0}$, and if the external electric impedances are also symmetrical, so that $Z''_{ea1} = Z''_{eb1}$, then the charging arm containing Z_0 will correspond to the "detector" diagonal of a balanced bridge and *no* variational current will appear in the bias supply circuit. By the same token, no variational voltage at fundamental frequency will appear between the diaphragm D and the mid-point of the signal-supply circuit marked G; the signal currents I_{a1} and I_{b1} will be exactly equal, and there will be no variation of the net electric charge on the diaphragm at fundamental frequency. In such a case, which can be identified as "*balanced* push-pull," the impedance Z_{01} can be made infinite without causing any change. Moreover, when $C_{a0} = C_{b0}$, the turns ratio of each electromechanical transformer becomes the same. The connection D–D' can then be broken, the two condensers and the two transformers can be merged, and the equivalent circuit for the balanced case can finally be redrawn in the simplified form shown in Fig. 6.11(*a*). This circuit conforms exactly with that of Fig. 6.3(*b*) except for the capacitance facing the signal source, which is halved in the push-pull case since the generator "sees" C_{a0} and C_{b0} in series. There *are* important differences, however, with regard to linearity and stability.

It is a simple matter, of course, to eliminate the coupling transformer by successively carrying through each element on the right; and as before the transformer eliminates itself when nothing else is left on the mechanical side except a short circuit. The all-electric circuit of Fig. 6.11(*b*) shows the result of this operation. Insertion of realistic

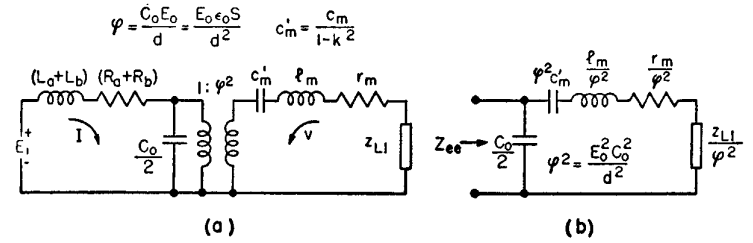

FIG. 6.11. (*a*) Simplified equivalent circuit for the balanced push-pull electrostatic loudspeaker. (*b*) Network representation of the electric input impedance seen at the terminals of the push-pull ESLU.

numbers for the quantities appearing in this diagram will confirm the fact that electrostatic devices are often of very high impedance. An impedance transformation by a factor of perhaps as much as 10^{-4} would make this configuration easier to study in the laboratory with an electrical model. No attempt has been made yet to exploit this line of attack on the design problem for electrostatic loudspeakers.

It is to be observed that a negative stiffness term makes its customary appearance, as exemplified by the negative compliance $(-C^2_{ema}/C_{a0})$ shown in Fig. 6.10(*b*), and notwithstanding the preceding discussion of this feature as it applied to the conditions of static equilibrium. Is there a contradiction here? The answer is no, and the reason is instructive. In the static case, the equilibrium position was central and the stability question revolved around the force reactions arising when the diaphragm was displaced mechanically. The conclusion was drawn that no electrical forces could act to neutralize the mechanical stiffness *if* no variational charge could be delivered by the bias source, and that the delivery of such variational charge could be prevented in practice by building a long time constant into the bias circuit. In the course of normal operation of a push-pull ESLU at fundamental frequency, the position in which the diaphragm would be in equilibrium is shifted systematically by the electric charges delivered by the signal source to the stationary electrodes. For mechanical perturbations about such a shifted position of electrical equilibrium, the situation is similar to that displayed by Fig. 6.9 with respect to the central equilibrium position. But now there is a "stiff" source to maintain the voltage difference between the fixed electrodes, namely, the signal source. As a result, the same negative stiffness that appeared statically about the neutral point is now mani-

fested about the position of dynamic equilibrium. This conclusion does *not*, however, cancel out any of the benefits of working with a fixed net charge on the moving electrode. The position of dynamic equilibrium can still move far into the region of *static* instability, carrying its *dynamic* negative stiffness along with it, as it were, so long as it moves back out into a safe "static" region before the bias charge has time to catch up with it.

As suggested above, the criterion for dynamic stability turns out to be exactly the same as that found previously in the static case. This can be demonstrated readily by computing the value of the net effective mechanical compliance c'_m, which appears in the simplified diagram of Fig. 6.11(a) as a diagrammatic abbreviation for the series combination of c_m and the two negative compliances appearing in Fig. 6.10(b). For the balanced case this may be written

$$\frac{1}{c'_m} = \frac{1}{c_m} - \frac{2}{C_{em}^2/C_0} = \frac{1}{c_m}\left(1 - \frac{2c_mC_0}{C_{em}^2}\right) = \frac{1-k^2}{c_m}, \tag{6.40}$$

where the coupling coefficient, k, has the same value it had in Eq. (6.38b),

$$k^2 = \frac{c_m(2C_0)}{C_{em}^2} = \frac{2c_mC_0E_0^2}{d^2}. \tag{6.38b}$$

The foregoing can be summarized by saying that push-pull operation at the fundamental frequency does not differ significantly from single-sided operation, except that the two active condensers present themselves in series to the signal source, but act in parallel with respect to the coefficient of electromechanical coupling. It turns out, very conveniently, that the necessary condition for the stability of static equilibrium is sufficient to guarantee dynamic stability in the balanced case, even for large diaphragm excursions.

Impedance Analysis of ESLU Performance

Analysis of the performance of an electrostatic transducer by means of electric-impedance measurements is hampered by many of the same experimental difficulties that appeared in the case of the moving-coil loudspeaker. The electrical-measurement problem can be presented in terms of the all-electric network of Fig. 6.11(b). The "motional" circuit elements, each transformed by the electromechanical impedance ratio $1/\phi^2$, appear in shunt with the "static" capacitance between the signal electrodes, $\frac{1}{2}C_0$. The relatively larger susceptance of the latter swamps

the motional elements, just as the voice-coil resistance swamped the motional impedance of the dynamic loudspeaker throughout its mid-frequency range of uniform response. But it is also true, as it was in the case of the dynamic loudspeaker, that impedance measurements made near resonance, and perhaps under artificial load conditions, can serve the useful purpose of furnishing information about the basic functional parameters that control the performance of the transducer at other frequencies and under more normal load conditions.

Figure 6.12 displays a family of impedance and admittance diagrams obtained by operating the experimental ESLU described above under different load conditions and with different polarizing voltages. The effect of increasing the force factor is strikingly illustrated by the way these circles "bloom" with an increase of bias voltage. Varying the coefficient of electromechanical coupling in this way constitutes another useful and "convenient alteration of one of the physical parameters," and allows the physical constants of the loudspeaker to be deduced by analysis of the electrical measurements.

The vacuum circle also serves, as before, to provide a useful reference load condition. The structural provisions for altering the electrode spacing made it difficult to estimate reliably a "theoretical" value for the accession to inertia, but a comparison of the diametral frequencies of the impedance circles for vacuum and for air loading, identified as ω_{ZV} and ω_Z respectively, indicates that the acoustical loading accounts for about 85 percent of the total mass of the resonating system that gives rise to these "air" circles. In spite of this preponderance of air loading, the radiation resistance is low enough to yield Q-factors of the order of 13–18, as can be inferred from the quadrantal frequencies of the impedance circles.

It should be noted that operating a small single-bay ESLU without a baffle, at these frequencies, represents an artificial load condition. As a matter of fact, it is only when such a unit is isolated that resonance circles like these can be observed. When several similar units are used in conjunction — to serve as a woofer, for example — the composite diaphragm system can be and usually is designed so that it is at least critically damped by the useful radiation load throughout the frequency range in which such resonances could occur. The feasibility of such a design rests on the fact that the specific radiation resistance presented to a small diaphragm increases with the square of its linear dimensions, whereas the reactive loading only increases linearly.

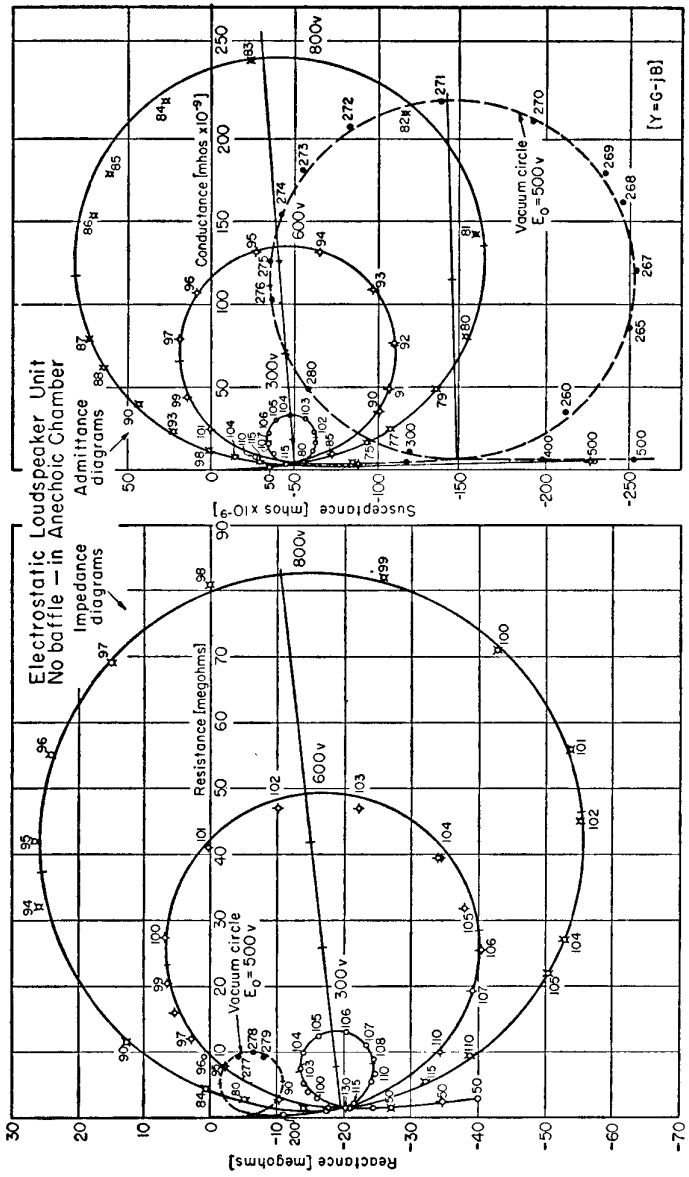

FIG. 6.12. Impedance and admittance diagrams for an experimental, single-bay, electrostatic loudspeaker unit operating under various conditions

The transformed equivalent circuit of Fig. 6.11(*b*) can be used as a vehicle for analyzing the fundamental-frequency behavior of the electrostatic loudspeaker, either analytically or experimentally. In this respect, Fig. 6.11(*b*) is the electrostatic counterpart of Fig. 5.5, which furnished a similar basis for discussing the example of electromagnetic coupling furnished by the dynamic loudspeaker. Moreover, these two circuit configurations stand in a *duality* relation to one another. This is exemplified by observing that the inductive circuit elements representing the blocked impedance in the electromagnetic case appeared in series with the shunt-connected motional elements, whereas in the electrostatic case represented by Fig. 6.11(*b*) the capacitance representing the blocked impedance appears in shunt with the series-connected motional elements. The existence of such a duality relation is one of the features that makes it possible to discuss the electrical analysis of transducer performance in terms of the generalizations advanced in Chapter 4.

The circuit of Fig. 6.11(*b*) is simple enough to encourage a direct verification of some of these generalizations. For example, it is straightforward to show that the diametral "impedance" frequency ω_Z should be independent of the coupling coefficient, and equal to ω_0, the frequency of mechanical resonance in the unbiased condition as defined by $l_m c_m \omega_0^2 = 1$. The stubborn refusal of preliminary measurements to confirm this invariance finally [14] led to consideration of the effects of stray capacitance, which can be defined as the "inert" part of the total capacitance between either stationary (signal) electrode and the diaphragm (a.c.-ground plane).

The required separation of C_0 into "active" and "stray" components must be made with due regard for the fact that it has been tacitly assumed throughout the preceding analysis that the diaphragm behaves as a *flat* piston, all parts of which move with the same displacement. In practice, on the other hand, the diaphragm is nearly always a membrane clamped at its edges — in this case a circular membrane whose curve of deflection can probably be approximated by a parabola, although no direct investigation of this has been carried out. Minor details of construction, such as the amount by which the stationary electrode extends beyond the edges of the diaphragm and the fraction of the diaphragm surface to which a conductive coating is applied, make it difficult to precalculate the stray capacitance accurately. The total, or "static,"

[14] I am further indebted to J. F. Hersh for demonstrating the importance of considering the stray capacitance in this connection. F.V.H.

capacitance can, however, in principle at least, be written as $C_0 = C_0' + C_0''$ where the active component C_0' and the stray component C_0'' are defined in terms of corresponding effective areas by the relation

$$C_0 = C_0'' + C_0' = \frac{\epsilon_0 S''}{d} + \frac{\epsilon_0 S'}{d + x}. \tag{6.41}$$

In terms of the foregoing concepts, the circuit of Fig. 6.11(*b*) can be redrawn, as in Fig. 6.13, to show explicitly that it is only the active

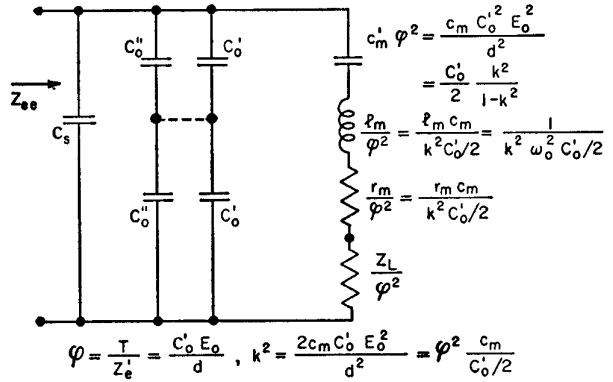

FIG. 6.13. A modification of the all-electric network of Fig. 6.11(*b*), showing the components of the stray capacitance.

capacitance C_0' that appears in the turns ratio of the electromechanical transformer and in the coupling coefficient. Note also that an additional stray component C_s has been indicated in Fig. 6.13 in order to account for the inert capacitance between the leads and between portions of the stationary electrodes that may extend beyond the active diaphragm.

When the variation of ω_Z is reëxamined by analysis of Fig. 6.13, it can readily be shown that

$$\omega_Z^2 = \omega_0^2 \left(1 - k^2 \frac{C_s + \frac{1}{2}C_0''}{C_s + \frac{1}{2}C_0}\right). \tag{6.42}$$

It follows that ω_Z^2 is a linear function of k^2, and hence of E_0^2. A graph of the ω_Z data from Fig. 6.12 confirms this prediction, and its extrapolated intercept yields a value of ω_0, the unbiased resonance frequency, that agrees with the mechanical resonance frequency determined by direct mechanical stimulation of the diaphragm.

No complications like those described above arise in considering the variation of the diametral frequency of the admittance circles. All the stray components of capacitance are subtracted as part of the blocked admittance, leaving the motional admittance to be characterized by the series-connected motional elements. It is then easy to see by an examination of Fig. 6.13 that

$$\omega_Y^2 = \omega_0^2 (1 - k^2) = \omega_0^2 \left(1 - \frac{2c_m C_0'}{d^2} E_0^2\right). \tag{6.43}$$

A graph of the values of ω_Y^2 deduced from the admittance circles of Fig. 6.12 confirms the predicted linear variation with E_0^2, yields an intercept that agrees with the value of ω_0 determined previously, and has a negative slope that yields one determination of the important ratio k/E_0.

An independent measure of the coupling coefficient can be made available by performing an auxiliary experiment similar to the one on which Figs. 6.5 and 6.7 were based. Since there is no static deflection under bias for the balanced push-pull case, this test must be carried out by applying the bias voltage to one side only. The effective value of k^2 for the push-pull case is then to be taken as twice the value found by using Fig. 6.6, as may be deduced from a comparison of Eqs. (6.15) and (6.38*b*).

The measurements of static deflection under single-sided bias can also be used to deduce a static value for the diaphragm compliance, which turns out to be 0.79×10^{-3} m/newton in this example. The effective mass of the vibrating system, which can be computed by using this compliance in conjunction with the mechanical resonance frequencies, is found to be about 0.37 gm with no air loading, and about 2.8 gm for unbaffled operation with air loading on both sides of the diaphragm.

Several other features of incidental interest can be inferred from further study of these circle diagrams. For example, the maximum and minimum values of either conductance or resistance may be used to compute the potential efficiency, as given by Eq. (4.30) or its counterpart in admittance form. The minimum values correspond to the blocked condition in each case, and are independent of bias voltage. The maximum values, on the other hand, vary approximately as the square of the bias voltage. As a consequence, the potential efficiency increases with increasing bias voltage, varying in this example from about 59 percent for $E_0 = 300$ v to 82 percent for $E_0 = 800$ v. Further analysis of the circuit of Fig. 6.13 leads to the prediction that the diameters of the motional-impedance and motional-admittance circles should each in-

crease with the square of the bias voltage. The diameters scaled from Fig. 6.12 do fall on straight lines when plotted against E_0^2, thus confirming this prediction; and the slopes of these straight lines provide two more numerical data involving the physical constants of the ESLU.

It should be apparent from the foregoing that the family of impedance and admittance diagrams shown in Fig. 6.12, when combined with the data from an auxiliary test of static deflection under single-sided polarization, provide a generous surplus of information that allows most of the relevant functional constants to be determined by two or more independent computations. Such opportunities for cross checking sometimes lead to what can be called "experimental embarrassment"(!), but the data presented appear to have enough internal consistency to provide firm support for the theoretical analysis of ESLU performance. It may be useful to add, however, that a good bit of care is called for in making reliable bridge measurements of impedances in the 1–100 megohm range, at frequencies in the neighborhood of 100 c/s.

Harmonic Distortion in the Push-Pull ESLU

The analysis of harmonic distortion arising in the push-pull operation of an electrostatic loudspeaker begins with an inspection of the set of Eqs. (6.32*c*), for the case $N = 2$. It is at once apparent that each of the forcing functions appearing on the left is expressed in terms of only the fundamental-frequency components of charge and displacement. One can proceed, therefore, as in the examination of the corresponding distortion problem for the single-sided case, to assume that these are known and to solve for the second-harmonic amplitudes that appear on the right in Eqs. (6.32*c*). These forcing functions can be interpreted more easily if the charges and the displacement are converted to currents and velocity. When this is done, and when the second and third of Eqs. (6.32*c*) are added together, the following pair of equations is obtained:

$$\begin{aligned} \frac{(j\omega q_{b1})^2 - (j\omega q_{a1})^2}{-4\omega^2\epsilon_0 S} &= \frac{I_{b1}^2 - I_{a1}^2}{-4\omega^2\epsilon_0 S} \\ &= (z_{m2} + z_{L2})v_2 + T_{a2}I_{a2} - T_{b2}I_{b2}, \\ \frac{x_1(q_{b1} - q_{a1})}{2\epsilon_0 S} &= \frac{v_1(I_{b1} - I_{a1})}{-2\omega^2\epsilon_0 S} \\ &= (T_{a2} - T_{b2})v_2 + Z_{ea2}I_{a2} + Z_{eb2}I_{b2}. \end{aligned} \tag{6.44}$$

One is entitled to say "Ah!" at this point because this is the first installment of the climax toward which these algebraic labors have been

directed. If structural symmetry is preserved, so that $C_{a0} = C_{b0}$, it will follow that the two transduction coefficients defined in Eqs. (6.29) will be equal in magnitude and opposite in sign. Thus, for the balanced push-pull case, $T_{an} = -T_{bn}$. It is then easy to deduce explicitly from Eqs. (6.32*b*) that the two fundamental-frequency components of current, I_{a1} and I_{b1}, are equal, as already argued above on grounds of symmetry. As a consequence, the left-hand member of each of Eqs. (6.44) is zero and the only solution (other than one corresponding to free oscillation at the frequency 2ω) is that calling for

$$v_2 = 0 = I_{a2} + I_{b2}. \tag{6.45}$$

Of course, for the second harmonic to vanish in a balanced push-pull system is no novelty; in such cases it is usually the third harmonic that causes trouble. The physical plausibility of the fact that the second-harmonic currents must be equal and opposite, if they exist at all, can be defended, for example, on the grounds that the driving voltage E_1 is constrained by hypothesis to contain no components of other than fundamental frequency even if $R_a = R_b = 0 = L_a = L_b$. By putting Eq. (6.45) and the symmetry conditions into Eqs. (6.32*d*), or by a further argument based on symmetry, one can then proceed to show that $I_{a3} = I_{b3}$. These current relations — opposite even components and like odd components — are typical of this kind of symmetrical configuration and can be formalized by writing [15]

$$I_{an} = (-1)^{n+1}I_{bn}. \tag{6.46}$$

In a way that can now be recognized as typical, each of the forcing functions appearing on the left in Eqs. (6.32*d*) which govern the third-harmonic variables, contains only the velocity and current variables of lower order. Introducing Eq. (6.45) and the symmetry conditions in Eqs. (6.32) then leads to a welcome simplification, which can be enhanced by assuming that $R_a = R_b = 0 = L_a = L_b$, so that

$$Z_{ean} = Z_{ebn} = 1/jn\omega C_{a0} = Z_a/n.$$

The realistic assumption that $Z_{0n} = R_0$ is also helpful, and after the usual "algebraic manipulation," the third-harmonic velocity ratio can be expressed as

$$\frac{v_3}{v_1} = I_{a2} \cdot \frac{1}{2E_0} \cdot \frac{z_1}{z_3} \cdot Z_a \cdot \left[\frac{1 + 2(T_a^2/Z_a z_1)}{1 - \frac{2}{3}(T_a^2/Z_a z_3)}\right], \tag{6.47}$$

[15] I am obliged to Robert B. Goldman, of the Research Division, Philco Corp., for reminding me of this relation, and for correcting thereby a mistake I had made in an earlier version of this analysis. F.V.H.

where z_1 and z_3 represent the total mechanical impedances, including radiation loading, at the frequencies of the fundamental and third harmonic, respectively. Note in particular the linear dependence of the *third*-harmonic velocity ratio on the *second*-harmonic current. Any artifice for reducing this component of current, such as the use of high impedance or "constant current" source, for example, will also abate the third harmonics. It is even more useful to observe that, since the even order components of current are *additive* in the central branch containing R_0 and the bias source, the simple expedient of increasing R_0 will serve to reduce I_{a2} to any desired extent. This behavior can be displayed explicitly by solving Eqs. (6.32*b*) and (6.32*c*) for I_{a2}, which turns out to be expressible in the form

$$I_{a2} = \frac{E_1}{2Z_a[1 - 2(T_a^2/Z_a z_1)]^2} \cdot \frac{E_1}{E_0} \cdot \frac{1}{1 + j\tau} \cdot \frac{T_a^2}{Z_a z_1}, \tag{6.48}$$

where $\tau = 4\omega R_0 C_a$. This value of τ is larger than the time-constant ratio used in Eq. (6.39) by the factor 4π. It follows that the second-harmonic currents (and hence the third-harmonic velocity) will already have been reduced to less than a tenth of their values for a "stiff" bias circuit if the criterion for dynamic stability is satisfied at least as strongly as with an equality in Eq. (6.39).

It is further to be noted that I_{a2} (and hence v_3) are shown by Eq. (6.48) to be directly proportional to the ratio of the motional impedance term T_a^2/z_1 to the blocked impedance Z_a. This suggests that it is the motion of the diaphragm at fundamental frequency that gives rise to the second-harmonic current, rather than any inherent nonlinearity of the transduction coefficient. Trouble might be expected at the frequency of mechanical resonance, when $z_1 \rightarrow r_1$, but even in this case a third-harmonic crisis is prevented by the presence of the z_1-factor in the numerator of Eq. (6.47). In general, however, this motional-to-blocked impedance ratio is so very much less than unity (and more's the pity, for other reasons!) that the third and higher odd harmonics can safely be neglected, even for large values of the excitation ratio E_1/E_0.

This is a very gratifying result, but it is also unusual enough to warrant some discussion. Its plausibility can be argued in the following qualitative terms. In most communication systems where nonlinearity is encountered — for example, in vacuum-tube amplifiers, transformers with iron cores, moving-armature transducers, or the phonograph recording-playback process — the intrinsic nonlinearity does not follow a simple law of variation and many terms in a power-series expansion are required

to describe the functional relations with precision. Push-pull operation in such cases is frequently employed for the sake of canceling out the even-order distortion terms, but odd-order terms in the original functional relation are not thereby eliminated. The electrostatic loudspeaker is fundamentally different in this respect, because its nonlinearity in the single-sided case stems from the simple quadratic nature of electrostatic forces; and since the dielectric involved is only air, there are no other nonlinearities to deal with, as there would be, for example, in a balanced-armature magnetic transducer. As the preceding analysis indicated, the magnitude of each order of distortion for the single-sided ESLU is controlled by the magnitude of the next lower order. In the push-pull ESLU, this process of building on the next lower harmonic order can be forestalled by controlling at the outset the second-harmonic components of velocity and current through the joint action of structural symmetry and a long time constant for the bias supply circuit.

When structural symmetry is not preserved, one can expect that the portion of the active capacitance that is *not* balanced will generate harmonics of all orders in much the same way that it would if that portion were operating as a single-sided ESLU. It can also be predicted, on this basis, that the magnitude of the second-harmonic velocity will be proportional to the capacitance differential, $C_{a0} - C_{b0}$; but to solve Eqs. (6.32*b*) and (6.32*c*) explicitly for v_2/v_1 in the general case involves substantial algebraic complexities. In lieu of this, the results of an experimental test of these predictions concerning harmonic distortion are exhibited in Fig. 6.14. The fixed electrodes of the experimental ESLU described above were mounted so that their spacings could easily be varied, thus allowing the structural symmetry to be altered systematically. In order to make the test reasonably severe (indeed, in order to arouse enough distortion to measure conveniently), the peak a.c. signal voltage on each half of the push-pull unit was made to exceed the d.c. bias voltage by about 10 percent, and a relatively low fundamental frequency was selected ($2\pi a/\lambda \doteq 0.17$) so that the amplitude of diaphragm motion would be substantial. The sound pressure was measured in the anechoic chamber with a standard (condenser!) microphrone on the axis at a distance of about 0.15 m. The upper curve of Fig. 6.14(*b*) shows the relative magnitude of the second-harmonic sound pressure as a function of the relative unbalance, for the case of a "stiff" bias circuit. As predicted by the preceding qualitative argument, the second harmonic diminishes with the degree of unbalance, and is seen to be less than 1 percent when the capacitance unbalance does not exceed 8 percent.

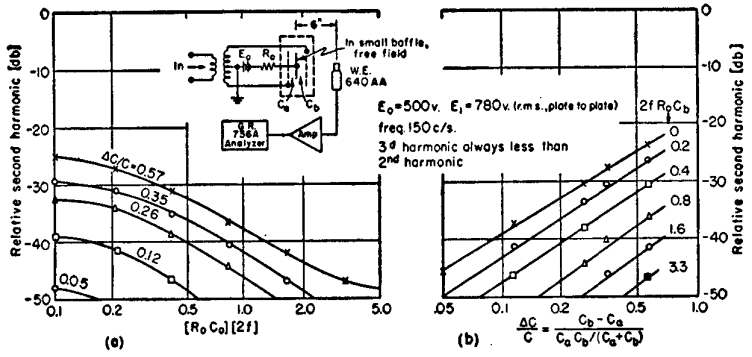

FIG. 6.14. Experimental confirmation of the reduction of harmonic distortion by improvement of "balance" in the push-pull ESLU.

The prediction that it is the equality of the signal currents that controls the reduction of the second harmonic is tested by the expedient of forcing this equality by progressively increasing the resistance R_0 in the bias supply circuit. The appropriate measure of this resistance is the quantity $2fR_0C_0$, the ratio of the time constant of the charging circuit to the half period. It is apparent that the criterion for dynamic stability under large excursions, as set forth by Eq. (6.39), is adequate to assure control of the production of the second, as well as the third and higher harmonics. This conclusion is illustrated explicitly by the curves of Fig. 6.14(*a*), in which the same data are used to display the second harmonic as a function of the time-constant ratio, with the capacitance unbalance as a parameter. The requirement that the ratio of the charging-circuit time constant to the half period should be "large in comparison with unity" is obviously not a stringent one, since a value no larger than unity for this ratio is sufficient to reduce the second harmonic to less than 0.5 percent for a capacitance unbalance as large as 25 percent.

If the foregoing discussion of electrostatic loudspeakers appears to have been as much concerned with raising new questions concerning design procedures as with answering old questions, this perhaps is as it should be. One thing at least can be said now with some certainty — such loudspeakers do have a number of very promising performance characteristics, and they can now be freed from many of the limitations that formerly restricted their field of use.

CHAPTER 7

Moving-Armature (Magnetic) Transducer Systems

The attraction and release of an iron armature under the control of current in the windings of an electromagnet represents the oldest technique in the art of electrical communication that still survives in widespread use. Unlike moving-coil systems, which have dominated their sector of the field for only the last three decades, or electrostatic systems, which have not yet gained more than a tenuous grip on acceptance, moving-armature transducers took over the telephone-receiver field at the outset and have dominated this application since the very beginnings of telephony. The same tractive principle, in addition to performing this electroacoustical function, serves to operate many hundreds of millions of relays now used for switching and control functions throughout the telephone system and elsewhere.

The magnetic-circuit configuration shown in Fig. 7.1(*a*) is sometimes described as *monopolar*, since it uses only a single central air gap traversed by magnetic flux which must return through the diaphragm and the magnetic path formed by the enclosure itself. This arrangement is

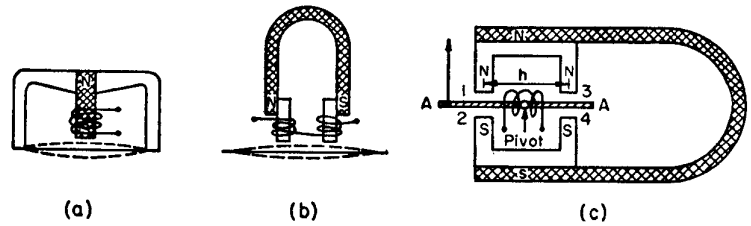

FIG. 7.1. Schematic representations of three typical moving-armature transducer configurations: (*a*) monopolar; (*b*) bipolar; (*c*) balanced-armature.

subject to several magnetic handicaps, the most obvious of which is the difficulty of reducing eddy currents. The construction is very simple, however, and it is still used in some applications.

The possibility of achieving a much-improved magnetic circuit is provided by the bipolar configuration illustrated schematically in Fig. 7.1(*b*). This functional arrangement was universally used in telephone receivers for almost three-fourths of a century, although a wide variety of structural variations were introduced from time to time. Many of these variations were concerned with the shape and disposition of the permanent magnet and the pole pieces, but the most significant improvements came as a result of substituting improved magnetic materials [1] throughout the magnetic circuit. For example, the permanent-magnet function was taken over by Remalloy or one of the members of the Alnico series as soon as these materials became available. The pole pieces are required to carry a.c. flux as well as the steady polarizing flux, a service for which 45-Permalloy (45 percent nickel, 55 percent iron) is well adapted. The diaphragm itself is the bottleneck in this magnetic circuit, since it must be light and thin in order to serve its acoustical function, and yet must operate at very high flux density in the magnetic circuit. The most useful material for satisfying both the mechanical and the magnetic requirements of diaphragm service turned out to be Permendur, an iron-cobalt-vanadium alloy that is capable of retaining high variational permeability at high flux density.

The balanced-armature mechanism illustrated schematically in Fig. 7.1(*c*) has likewise been rendered in a wide variety of structural modifications. Many of these have been concerned with changes in the method of pivoting the armature AA. In one typical variation, shown in Fig. 7.2(*a*), the rocking motion of the armature is replaced by the flexure of a magnetic armature clamped rigidly between nonmagnetic spacers at the end marked P. The pole pieces at this end of the armature appear to provide a shunt path for flux from the polarizing magnet, but it is necessary to tolerate this in order to provide a low-reluctance path for the a.c. flux established by the signal current. When it is worth while to attempt to reduce losses still further, the pole pieces can be laminated and the separation of a.c. and d.c. flux made more complete by blocking the a.c. flux path to the permanent magnet with a heavy copper ring around each leg of the structure, as indicated by the loop marked

[1] V. E. Legg, "Survey of Magnetic Materials and Applications in the Telephone System," *Bell System Tech. J.* **18,** 438–464 (July 1939).

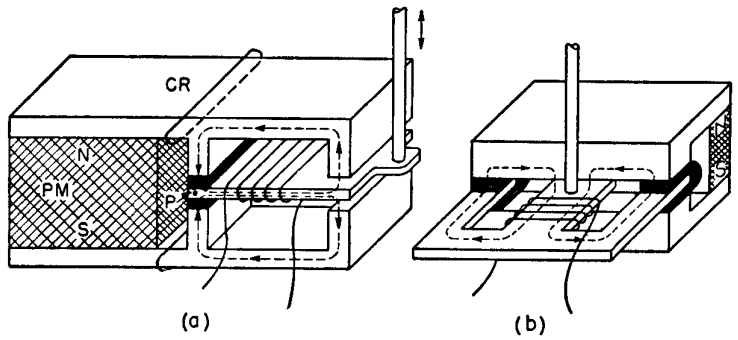

FIG. 7.2. (*a*) A modified balanced-armature configuration using a single pair of variable gaps; (*b*) a rearrangement of (*a*) yielding an improvement in the magnetic flux paths. (*Courtesy of Shure Brothers, Inc.*)

CR. A useful modification of this structure [2] is shown in Fig. 7.2(*b*), where it can be seen that both a.c. and d.c. magnetic circuits have been improved by the expedient of moving the signal coil outside the permanent-magnet structure. In this case, most of the a.c. flux path lies in a thin E-shaped lamination of which the center leg constitutes the moving armature.

The newest member of the moving-armature transducer family is the ring-armature receiver, two stages in the evolution of which are shown in Fig. 7.3. In its final form, this could be called a semibalanced-armature

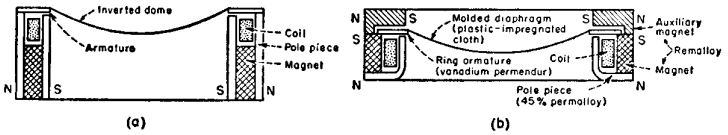

FIG. 7.3. Two stages in the evolution of the ring-armature receiver. [After Mott and Miner, reference 3.] (*Courtesy of the Bell System Technical Journal.*)

system, since it exhibits many of the typical performance features of balanced systems. In spite of this family resemblance, however, the ring-armature mechanism probably deserves to be classified as a basically new configuration. The considerations that guided the design of the instrument shown in Fig. 7.3(*b*), and a thorough analysis of its

[2] Benjamin B. Bauer, "A Miniature Microphone for Transistorized Amplifiers," *J. Acoust. Soc. Am.* **25,** 867–869 (September 1953); also U. S. Pat. No. 2,454,425 (filed 23 December 1943) issued 23 November 1948.

performance, have been described recently in an excellent paper by Mott and Miner.[3] In view of the availability of this very able analysis of an advanced type of moving-armature transducer, the remainder of this chapter will be confined to the elementary theory of such transducers and to the general features of electric circuits associated with ferromagnetic materials.

The basic feature of moving-armature transducer systems is the tractive force that always acts to close the air gap in a magnetic circuit. The classical problem of dealing analytically with such forces was dealt with by Maxwell in terms of stresses that he held to be characteristic of the magnetic field itself. The compressive, or "Maxwell," stress can be expressed in terms of the total force F acting on an element of surface S normal to the magnetic field vector, where F is given by

$$F = -\frac{B^2 S}{2\mu_0} = -\frac{\phi^2}{2\mu_0 S} \text{ [newtons]}. \tag{7.1}$$

In this equation, B is the magnetic induction in webers per square meter, ϕ is the total flux in webers, and μ_0 is the permeability of free space and has the value $\mu_0 = 4\pi \times 10^{-7} = 1.257 \times 10^{-6}$ henries/meter. Before making use of this expression for the electromechanical analysis of a typical moving-armature transducer, it will be useful to review briefly the fundamental physics of the magnetic circuit.

The Magnetic Circuit

The "Ohm's law" of magnetic circuits is often written (and less often justified) as

$$\phi \text{ [flux, webers]} = \frac{\mathfrak{F} \text{ [magnetomotive force, ampere turns]}}{\mathfrak{R} \text{ [reluctance, ampere turns/weber]}}, \tag{7.2}$$

where

$$\mathfrak{F} = \oint \mathbf{H} \cdot d\mathbf{l}, \tag{7.3}$$

the line integral around the magnetic circuit of the magnetic field strength $\mathbf{H}$ [ampere turns/meter], and

$$\mathfrak{R} \equiv \frac{\text{length of flux path [meters]}}{\mu\mu_0 \times \text{cross-sectional area of flux path [square meters]}}. \tag{7.4}$$

[3] E. E. Mott and R. C. Miner, "The Ring Armature Telephone Receiver," *Bell System Tech. J.* **30**, 110–140 (January 1951).

In the latter expression μ is the relative (dimensionless) permeability of the material composing the magnetic path. If a continuous magnetic path is made up of sections having different areas or permeabilities, as in the case of an air gap in a ferromagnetic circuit, the total reluctance is to be computed by adding (as for a "series" connection) the reluctance of each individual portion of the circuit.

An important caution is always to be observed in using the simplified form of Eq. (7.2) for magnetic circuits. In electric circuits, there is an enormous conductivity ratio ($\sim 10^{20}$) between ordinary conductors (copper) and the usual insulating medium around the conductors (air or solid dielectrics), the current is strongly confined to the conducting path, and Ohm's law $I = E/R$ can be applied with precision. On the other hand, in the magnetic circuit, even with ferromagnetic "conductors," the permeability ratio is not so high but what a significant amount of leakage flux usually exists outside the nominal magnetic circuit. Specification of a particular magnetic circuit and a particular flux path in Eqs. (7.3) and (7.4) emphasizes that it has been assumed that such a magnetic circuit can be defined. It follows that the total flux ϕ given by Eq. (7.2) is just that confined to the specified magnetic circuit and does *not* include the leakage flux. Equations (7.2), (7.3), and (7.4) could be replaced by more elaborate integral expressions that would permit the leakage flux to be evaluated numerically, or analytically when the geometry is simple enough and when the characteristics of the magnetic materials are known well enough. Such solutions are usually painful and tedious, however, and corrections for leakage flux are more often made on the basis of empirical data or experimental model tests. The design of practical magnetic circuits for producing high flux density in an air gap is, in fact, largely a problem of accounting properly for the leakage flux, especially in magnetic circuits using permanent magnets.

The Composite Magnetic Circuit

Before carrying this any further, consider Fig. 7.4, which represents the typical behavior of a magnetic circuit. The ordinates represent ϕ_m, the total flux through the magnetic circuit, that is, the flux that is confined to the definable magnetic path of length l_m and cross-sectional area S_m. The abscissa represents the magnetomotive force $\mathfrak{F}$ associated with ϕ_m. When attention is to be centered on the properties of a magnetic *material*, it is more useful to plot the magnetic induction B against the magnetic-field vector H. In the present case, however, attention is

focused on the *circuit*, so the representation is given in terms of the variables appearing in Eq. (7.2).

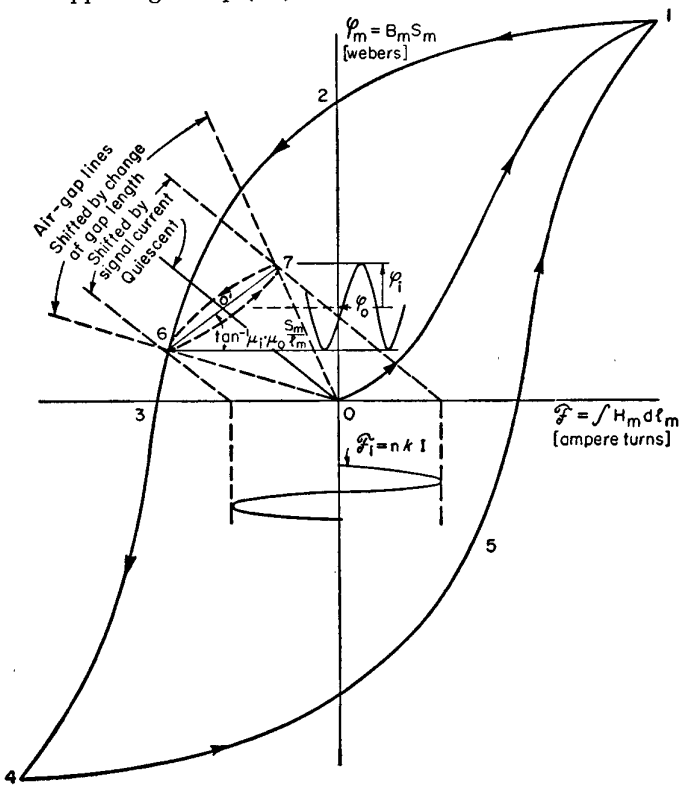

FIG. 7.4. A typical hysteresis loop showing a stabilized minor hysteresis loop.

The terminology used to describe the condition of a magnetic material can be introduced by describing a typical excursion around the hysteresis loop shown in Fig. 7.4. Suppose, for example, that the diaphragm of the receiver shown in Fig. 7.1(*a*) is allowed to make contact with the pole piece, effectively removing the air gap; and that a magnetomotive force $\mathcal{F}$ can be set up by the current in the winding. If the magnet was initially demagnetized, the flux variation with $\mathcal{F}$ will first follow the *normal magnetization curve* from 0 to 1. If the current is now reduced, ϕ_m decreases along the upper branch of the hysteresis loop 1–2, and would

remain indefinitely at the value corresponding to the *remanent* flux if the current is interrupted as it reaches zero. When the current is increased in the opposite direction, ϕ_m follows the descending branch 2–3 of the hysteresis loop; this portion of the loop is called the *demagnetization* curve, and, when the variation is expressed in terms of B and H, it represents the data usually furnished for permanent-magnet materials. As the (reversed) current is still further increased, the flux reverses direction and follows the descending branch 3–4.

Finally, going through the foregoing sequence of current variations in the opposite direction elicits a flux variation described by the ascending branch 4–5–1 of the hysteresis loop. Successive reversals of magnetizing current producing equal positive and negative values of $\mathcal{F}$ cause the same *normal hysteresis loop* 1–2–3–4–5 to be traced recurrently, and the magnetic material is then said to be in a *cyclic condition*. When the material is being thus magnetized symmetrically and cyclically, the *remanent flux density* at $\mathcal{F} = H = 0$ is called B_R, the *residual induction;* the corresponding value of negative H_m required to reduce B_m to zero is called H_c, the *coercive force*. When the material has previously been carried to saturation, the residual induction $(B_R)_{sat}$ is called the *retentivity*, and the corresponding coercive force is called the *coercivity*.

Minor hysteresis loops will be traced out (always lying wholly on the *inside* of the major loop) if the course of variation of $\mathcal{F}$ is reversed before reaching either limit of the major loop. Thus, if ϕ_m is following the descending branch 1–2–6, and the course of $\mathcal{F}$ reverses at 6, ϕ_m does not retrace the descending branch from 6 to 2 but follows the ascending (lower) branch 6–7 of the minor loop. On reversal of this minor excursion of $\mathcal{F}$, ϕ_m follows the descending (upper) dotted curve from 7 to 6, and then continues along the original major loop from 6 to 3 to 4, and so on.

If, instead of supplying a negative magnetizing force by means of reversed current in the winding, the current circuit is left open and the residual induction is reduced by introducing a large air gap (for example, by removing the diaphragm), the flux will again follow the demagnetization curve to some point such as 6; but in this case the negative value of $\mathcal{F}$ is represented by the magnetic potential drop across the large effective air gap between the pole pieces. This magnetic potential drop is represented graphically by the *negative air-gap line* 0–6, which is straight by virtue of the linear relation between H and B in air. If the diaphragm is now replaced, moved close to the pole pieces so that the effective air gap is reduced to less than normal (but not to zero), and then removed

again, the flux will again trace out the minor hysteresis loop 6–7–6. Minor hysteresis loops are lens-shaped, as shown, and do not exhibit the reverse curvature characteristic of the major loop, provided the loop does not cross the vertical axis ($\mathfrak{F} = 0$). If it is assumed for the moment that the minor loop can be approximated by the straight line 6–0′–7 drawn between its tips, then the slope of this line would determine the *incremental permeability*.

Assuming that the current was interrupted when the circuit was at the point 2, and that it has been brought to the point 6 by removing the diaphragm, let the diaphragm now be returned to its normal position with an air gap of length l_g, and assume that this brings the flux to some intermediate position 0′ on the simplified minor loop. *This is the normal "quiescent" operating point for the electromechanical system.* In this condition the permanent-magnet circuit is said to be *stabilized*. Any magnetic variations about the operating point 0′ — whether arising from a signal current i or from small variations in the length of the air gap, as indicated by the dashed lines in Fig. 7.4 — will now take place *reversibly* along the minor loop 6–0′–7 so long as the flux changes do not exceed either the upper or the lower limits of the minor loop.

It would be better, of course, to say *around*, rather than *along*, the minor loop. The assumption made above that the minor hysteresis loop can be approximated by the straight line 6–0′–7 obviously goes too far to be realistic. A better approximation is afforded by assuming that the lenticular shape of the minor hysteresis loop can be approximated by a narrow ellipse. Even an ellipse does not provide a very close match in shape at the pointed tips of the minor loop, but it has the advantage of yielding a simple physical interpretation of the behavior. For example, assume that H varies in response to a sinusoidal magnetizing current, while B takes on the corresponding values dictated by the empirical B–H relation that *is* the minor loop. The difference in shape between the ellipse and the minor loop will then appear as higher harmonics of B generated by the nonlinearity of the magnetic relation. It follows that the ellipse *is* a good approximation to exactly the extent by which harmonics of B can be neglected. However, an even more important consequence of recognizing the ellipse as a fundamental-frequency approximation of the minor loop is that it puts in evidence the physical basis for a *phase shift* between H and B.

To put this another way, an ellipse whose major axis occupies the position 6–0′–7 in Fig. 7.4 can be regarded as a Lissajous figure generated

by two sinusoidal variations at right angles and with a phase difference that is a simple function of the ratio of the minor to major axes of the ellipse. It will still be useful to allow the symbol μ_i and the term "incremental permeability" to stand for the slope of the straight line 6-0′–7 that defines the axis of the minor loop, but it must be understood that a mathematical expression of the relation between increments of B and of H will require that the incremental permeability be multiplied by a complex hysteresis factor $\bar{\chi}$; thus,

$$\frac{\Delta B}{\mu_0 \Delta H} = \mu_i \bar{\chi}; \quad \bar{\chi} = \bar{\chi}_0 e^{-j\beta} = \bar{\chi}_R - j\bar{\chi}_I. \tag{7.5}$$

As suggested above, the same minor loop trajectory will be followed whether the magnetic changes are instigated by the addition of a signal component of magnetomotive force or by a change in the length of the air gap. The complex hysteresis factor $\bar{\chi}$ is, therefore, to be associated with incremental variations of B and H however they are produced.

When the incremental permeability appears in expressions for the inductance of a coil whose core consists of a magnetic material, the *imaginary* part of $\mu_i\bar{\chi}$ will give rise to a dissipative term in the "reactance" of the coil; in short, it is in this way that a component of resistance is introduced in the electric circuit to account for the cyclic energy loss that occurs for each transit around the minor hysteresis loop.

The foregoing relations have been described in nonmathematical terms in order to direct emphasis toward the physical basis for the phase angle associated with the incremental permeability. This is a case in which a phase shift arises as a consequence of the geometric shape of the "path of operation" on the B–H plane. Thus B can be said to "lag" behind H only in a graphical sense based on the symbolism of rotating vectors. The "lag" does *not* derive from any mechanism fundamentally associated with time delay, and it is independent of frequency, at least below those frequencies at which eddy-current shielding of the interior of the magnetic material must be taken into account.

In analytical practice it will always be assumed that the magnetic circuit has been brought to the cyclic condition and that the path of operation connecting B and H is stabilized. It will then be possible to ignore (or to take for granted) the details of magnetic behavior described above, and to summarize the effect of the ferromagnetic circuit by simply accepting the "complexness" of the incremental permeability as one of the characteristic properties of the magnetic medium.

The Transduction Coefficient for Moving-Armature Magnetic Systems

According to Eq. (7.1) above, the mechanical force F acting on an armature forming one boundary of an air gap of length $(d+x)$ and transverse area S_g can be expressed conveniently in terms of the total flux ϕ_g threading the air gap; thus, to repeat Eq. (7.1) for reference,

$$F = -\frac{B_g^2 S_g}{2\mu_0} = -\frac{\phi_g^2}{2\mu_0 S_g}. \tag{7.1a}$$

The negative sign appears in Eq. (7.1*a*) as a consequence of choosing the outward direction as positive for displacement and force, as indicated by the sketch of Fig. 7.5. One could proceed at this point to follow

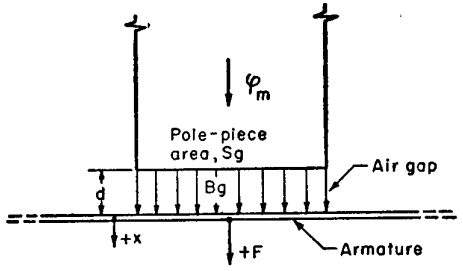

FIG. 7.5. Sketch establishing nomenclature for discussing magnetic and mechanical interactions associated with an air gap.

exactly the same analytical routine used in the preceding chapter for dealing with the electrostatic loudspeaker. This would involve writing the differential equations for the mechanical and electric meshes, introducing the expansion of each variable in a Fourier series, and then the marshaling of the pairs of equations describing the behavior at zero, fundamental, and harmonic frequencies. In this case, however, use will be made of the more elementary (and less powerful) procedure of finding directly the approximate values of the interaction force, previously designated $F_{B,I}$, and the emf of interaction, $E_{B,v}$. With these in hand, the electromechanical coupling equations can be written by inspection.

Begin, then, with the assumption that the total magnetic flux can be represented as the sum of a fixed polarizing flux ϕ_0 and a variational component ϕ_i arising from the (variational) signal current. The polarizing flux, in turn, can be assumed to arise from the action of a polarizing magnetomotive force $\mathfrak{F}_0$ representing either the ampere turns of a steady polarizing current or the "built-in" magnetomotive force of a permanent

magnet. By making use of the basic Eqs. (7.2) and (7.4), the total flux may be expressed in the following forms

$$\phi_{\text{total}} = \phi_0 + \phi_i = \frac{\mathfrak{F}_0 + \mathfrak{F}_i}{\mathcal{R}_{\text{total}}} = \frac{\mathfrak{F}_0 + Nki}{\dfrac{l_m}{\mu_m \mu_0 S_m} + \dfrac{d+x}{\mu_0 S_g}},$$

$$\phi_0 + \phi_i = \frac{\mathfrak{F}_0}{\dfrac{d+x}{\mu_0 S_g}(1+\delta_m)} + \frac{Nki}{\dfrac{d+x}{\mu_0 S_g}(1+\delta_m)}; \tag{7.6a}$$

$$\delta_m = \frac{l_m}{(d+x)} \cdot \frac{S_g}{S_m} \cdot \frac{1}{\mu_m}. \tag{7.6b}$$

Note that the space operator $\boldsymbol{k}$ appears, as usual (cf. Chapter 3), in the relation $\mathfrak{F}_i = Nki$ in order to give expression to the intrinsic orthogonality between H and i. The denominator of Eq. (7.6*a*) is written to indicate that the total reluctance is primarily that of the air gap; the correction term δ_m accounts for the reluctance contributed by the ferromagnetic portion of the circuit. The correction term having been displayed in this way, it will now be assumed that the relative permeability μ_m is high enough to allow δ_m to be neglected, which is equivalent to assuming that *all* the reluctance is concentrated in the air gap. Equation (7.6*a*) then provides the point of departure for evaluating the mechanical forces due either to an electric current or to diaphragm motion, and the emf induced by a change in the air gap.

Consider the latter problem first. It was pointed out in the discussion of Eq. (3.11) that the induced emf in a coil threaded by a time-varying magnetic flux is given by

$$E = NSk\dot{B} = Nk\dot{\phi}. \tag{7.7a}$$

This relation can be expressed in terms of a typical transduction coefficient by rewriting Eq. (7.7*a*) in the form

$$E_{B,v} \equiv T_{em} v = Nk \frac{\partial \phi}{\partial x} \frac{dx}{dt}; \tag{7.7b}$$

from which the definition of the transduction coefficient emerges as

$$T_{em} \equiv Nk \frac{\partial \phi}{\partial x}. \tag{7.7c}$$

The total flux ϕ is expressed by Eq. (7.6*a*) as a function of two independent variables: i, the signal current, and x, the variable component

of air-gap length. Since the induced emf given by Eqs. (7.7*a*) and (7.7*b*) is observable as an open-circuit voltage, the x-derivative of ϕ was written as a partial derivative in order to imply that the x-variation of ϕ should be computed with $i = 0$. This partial derivative can be evaluated at once from Eq. (7.6*a*) and inserted in the expression for the transduction coefficient, Eq. (7.7*c*), yielding

$$\left(\frac{\partial\phi}{\partial x}\right)_{i=0} = \frac{-\mathcal{F}_0\mu_0 S_g\bar{\chi}}{(d+x)^2} = -\frac{\phi_0\bar{\chi}}{d+x};$$

$$T_{em} = -\left(\frac{N\phi_0\bar{\chi}}{d+x}\right)k. \tag{7.8}$$

Observe that the physical situation implied in computing this derivative is exactly that contemplated in the preceding discussion of minor hysteresis loops. The complex hysteresis factor $\bar{\chi}$ must therefore be introduced as a multiplier in Eq. (7.8) in order that the mathematical expression shall include the phase displacement that arises when the incremental variations of ϕ are constrained to follow the trajectory defined by a stabilized minor hysteresis loop.

The converse transduction coefficient can be evaluated in a similar way by referring to Eq. (7.1*a*) and by again making use of the fact that the total flux is a function of the two variables x and i. The following equations state the premise:

$$F_{\text{total}} = \frac{-\phi_{\text{total}}^2}{2\mu_0 S_g};$$

$$dF = \frac{\partial F}{\partial x}dx + \frac{\partial F}{\partial i}di;$$

$$dF = \frac{\partial F}{\partial \phi}\frac{\partial \phi}{\partial x}dx + \frac{\partial F}{\partial \phi}\frac{\partial \phi}{\partial i}di. \tag{7.9}$$

The interaction force, like the induced electromotive force, is an open-circuit quantity and is to be evaluated for zero velocity, that is, with $dx = 0$. Moreover, the differentials of force and of current can now be regarded as the amplitudes of small variational components; and since the fundamental-frequency mode of operation is being considered, the amplitude of these harmonic variational components can be identified with the subscript 1; thus $dF \equiv F_1$ and $di \equiv I_1$.

The evaluation of the interaction force and the mechanoelectrical transduction coefficient can then proceed, using Eq. (7.6*a*) and Eq. (7.9), as follows:

$$F_{B,I} \equiv T_{me}I_1 = \frac{\partial F}{\partial \phi}\frac{\partial \phi}{\partial i}I_1$$

$$= -\frac{\phi_0}{\mu_0 S_g}\cdot\frac{\bar{\chi}NkI_1}{(d+x)/\mu_0 S_g} = -\frac{N\phi_0\bar{\chi}}{(d+x)}kI_1. \tag{7.10}$$

Note that the complex hysteresis factor $\bar{\chi}$ has again been introduced in evaluating the i-derivative of ϕ. Comparison of Eqs. (7.8) and (7.10) leads to

$$T_{me} = -\left(\frac{N\phi_0\bar{\chi}}{d+x}\right)k = T_{em}. \tag{7.11}$$

It will be observed that the transduction coefficients are identical and that the force factor — a coefficient of k in this case — is complex by virtue of the hysteresis factor. Reference to Eqs. (4.14) will then support the interesting prediction that the phase-displacement angle characterizing the hysteresis factor is just half the dip angle to be expected in the motional-impedance circle for a moving-armature transducer of the kind under consideration.

Before proceeding to assemble the equivalent circuits pertaining to the different configurations shown in Figs. 7.1 to 7.3, consider the other term in the differential of the force, given by the last of Eqs. (7.9). This force increment is also to be computed after first setting $\phi_i = 0$; then using Eqs. (7.6*a*) and (7.9) yields

$$dF = -\frac{\phi_0}{\mu_0 S_g}\frac{\partial \phi}{\partial x}dx = \frac{-\phi_0}{\mu_0 S_g}\left(-\frac{\mathcal{F}_0\mu_0 S_g\bar{\chi}}{(d+x)^2}\right)dx$$

$$= +\frac{\phi_0^2\bar{\chi}}{\mu_0 S_g(d+x)}dx. \tag{7.12}$$

Equation (7.12) indicates that one effect of the polarizing field is to give rise to a mechanical force acting *in the direction of the displacement* that calls it forth. It constitutes, therefore, a *negative stiffness* that will be designated $1/c_e$, as in the case of the electrostatic loudspeaker. In that case, however, it was possible to disconnect the polarizing source, whereupon the charge was fixed and the negative stiffness disappeared. The magnetic circuit can not be "opened up" in this way, and the negative stiffness will be in evidence whenever ϕ_0 is, without regard to terminal conditions in the electric mesh — in fact, even without regard to whether there *is* an electric mesh. As a consequence of these facts,

the mechanical impedance of the armature system (or diaphragm) is to be written as

$$z_m = z_m'' + z_m' = \left(j\omega l_m + r_m + \frac{1}{j\omega c_m}\right) + \frac{1}{j\omega c_e}, \tag{7.13a}$$

where c_e is taken from Eq. (7.12) with due regard for signs (see Fig. 7.5); thus

$$\frac{1}{c_e} \equiv -\left(\frac{dF}{dx}\right)_{i=0} = -\frac{\phi_0^2}{\mu_0 S_g (d+x)}. \tag{7.13b}$$

There is one more component of force that deserves brief notice. If the relation $\phi = \phi_0 + \phi_i$ is introduced directly in Eq. (7.9), the total force can be written as

$$F_{\text{total}} = \frac{1}{2\mu_0 S_g}(\phi_0^2 + 2\phi_0\phi_i + \phi_i^2). \tag{7.14}$$

The first term in the parenthesis represents the steady pull on the armature whose variation with x gives rise to the negative stiffness discussed in the last paragraph. When ϕ_i is assumed to be cosinusoidal, the last term in Eq. (7.14) will yield, in addition to a negligible second-order contribution to the steady force [this is the term in $N = 2$ that was neglected, along with higher order terms, in Eqs. (6.28)], a second-harmonic force F_2 whose relative magnitude can easily be evaluated. For example, if $\phi_i = \phi_I \cos \omega t$, then $\phi_i^2 = \frac{1}{2}\phi_I^2 (1 + \cos 2\omega t)$. It follows at once that the relative value of F_2 is

$$\frac{F_2}{F_1} = \frac{\phi_I}{4\phi_0}. \tag{7.15}$$

It would not be valid to interpret Eq. (7.15) as a quantitative measure of the relative magnitude of the second harmonic of the diaphragm motion or of the sound radiation; these will depend, in addition, on the relative magnitudes of the mechanical impedance and the radiation loading at the two frequencies involved. Since these impedance ratios will be influenced by resonances and other factors, no generalizations can be drawn on the basis of Eq. (7.15) alone.

With the transduction coefficient in hand [Eq. (7.11)], and with the effective mechanical impedance defined by Eq. (7.13a), the typical electromechanical coupling equations can be written as

$$\begin{aligned} E &= (Z_e'' + Z_e')I + Tv, \\ F &= TI + (z_m'' + z_m')v. \end{aligned} \tag{7.16}$$

The situation presented now is exactly the one to which Chapters 3 and 4 were addressed. For the most part, reliance will be placed on this previous discussion, and the details of analyzing the performance of this particular transducer system by impedance methods will not be repeated. However, the moving-armature system has some features in common with magnetostriction transducers, and it will be useful to consider a few of these at this point.

The electric impedance appearing in Eq. (7.16) is written as the sum of two components, one of which, Z_e'', includes all the ohmic resistance of the winding and the reactance associated with all the leakage flux that does not play a part in producing stress across the air gap. The other term Z_e' is sometimes called the "core impedance" and accounts for the reactance associated with all the air-gap flux. This component of impedance can be evaluated explicitly in terms of the assumptions already made concerning the magnetic circuit, as follows:

$$\begin{aligned} Z_e' &= j\omega L_e' = j\omega L_0 \bar{\chi}, \\ L_e' &\equiv \frac{N\Delta\phi}{\Delta(ki)} = \left[\frac{N^2\mu_0 S_g}{(d+x)}\right]\bar{\chi}. \end{aligned} \tag{7.17}$$

Note that the usual definition $L = N\phi/I$ has been modified to take account of the fact that it is the *variations* of ϕ that are involved in this case, and of the fact that care is being taken to keep track of the space relations between H and I.

It can now be shown, by direct substitution from Eqs. (7.11) and (7.17), that the electromechanical contribution to the mechanical stiffness can be expressed as a function of the transduction coefficient and the core impedance by the surprisingly simple expression

$$\frac{1}{j\omega c_e} = \frac{T^2}{Z_e'}. \tag{7.18}$$

Equations (7.17) and (7.18) can now be introduced into the electromechanical coupling equations (7.16) so that they become

$$\begin{aligned} E &= (Z_e'' + Z_e')I + Tv, \\ F &= TI + \left(z_m'' + \frac{T^2}{Z_e'}\right)v. \end{aligned} \tag{7.19}$$

The equivalent circuit corresponding to these equations can be drawn at once in the form shown in Fig. 7.6(a). When Z_e' is moved into the shunt position, in the process of transforming the circuit of Fig. 7.6(a)

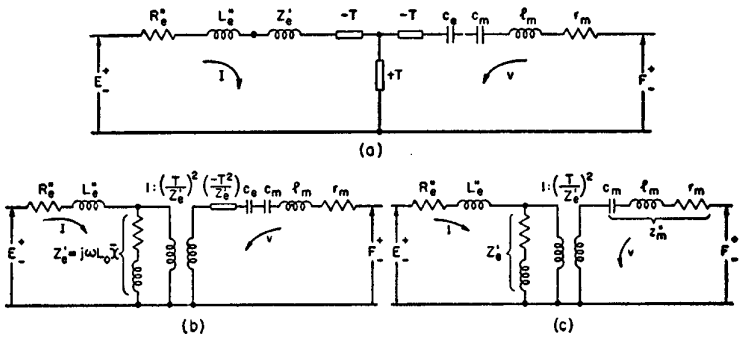

FIG. 7.6. (*a*) The basic equivalent circuit for a moving-armature transducer. The mechanical compliance of electric origin denoted by c_e represents the negative stiffness associated with the polarizing flux. (*b*) Intermediate stage of transformation of (*a*). (*c*) The transformed configuration of the equivalent circuit of (*a*).

in the usual way, the impedance element $(-T^2/Z'_e)$ that appears on the other side of the electromechanical transformer turns out to be just what it takes to cancel c_e! The circuit of Fig. 7.6(*b*) can be redrawn then in the simpler form shown in Fig. 7.6(*c*).

At first glance, this manipulation of the equivalent circuit would appear to have canceled out the electrical (negative) compliance. This is not so, however; it is still there, in the form of the core impedance appearing in shunt on the other side of the ideal transformer, where it remains effective even if the external electric terminals are on open circuit. The circuit of Fig. 7.6(*c*) is therefore a competent representation of the moving-armature system, and the discussions of Chapter 4 are relevant and applicable. Since it was in connection with studies of just such a "moving-armature" system that the concept of motional impedance had its origin, the *first* motional-impedance circle [4] is offered in Fig. 7.7 as an illustration of the performance described by this analysis.

In evaluating the transduction coefficient used above [Eq. (7.11)], a single air gap was considered. For the typical bipolar configuration, the numerical value of T needs merely to be doubled. A somewhat different situation prevails in the balanced-armature configuration. It proves to be useful, and instructive, in analyzing such situations, to replace the magnetic-"circuit" configuration by an electric-circuit analog. Figure 7.8 shows such an equivalent-circuit representation of the balanced-armature

[4] See note 5, Chapter 2.

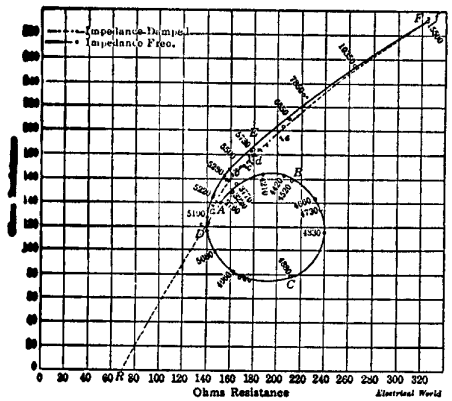

Fig. 6—Vector Impedance Diagram of Bipolar Bell Receiver, Damped and Free, at Different Frequencies.

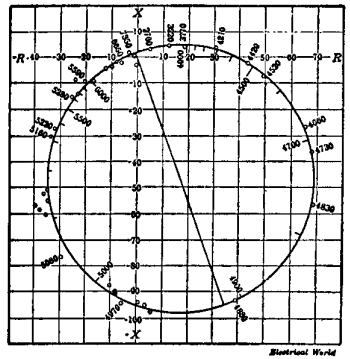

Fig. 7—Circular Graph for Bipolar Bell Receiver with 0.3 Volt at Terminals.

FIG. 7.7. The *first* motional-impedance diagrams, reproduced with the original captions from the Kennelly and Pierce paper of 1912. (See reference 5 of Chapter 2.)

structure of Fig. 7.1(*c*). When the a.c. signal is zero, the transverse branch (representing the armature) remains in place as a short-circuit path for the d.c. polarizing flux. On the other hand, an inductive choke is introduced in series with $\mathcal{F}_0$ in order to prevent any a.c. flux from "flowing" in the polarizing circuit [eddy-current shielding fulfills this function in the actual structure]. Thanks to the inherent symmetries, it is not difficult to solve for the a.c. and d.c. components of "current" in each of the four reluctance branches, and thus to evaluate flux components in each gap. In terms of the notation established by Fig. 7.8

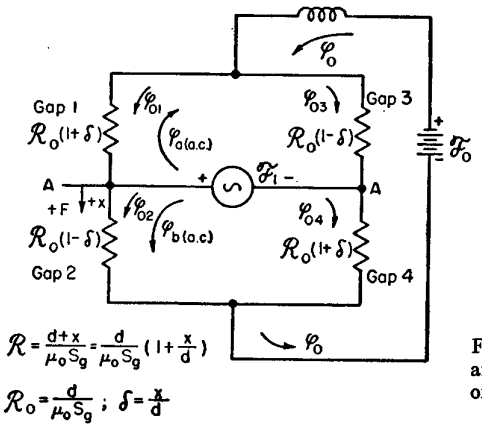

FIG. 7.8. An electric-network analog of the magnetic circuit of a balanced-armature transducer.

with reference to the structure of Fig. 7.1(*c*), the two a.c. components of flux are equal and have the magnitude given by

$$\phi_{a(\text{a.c.})} = \phi_{b(\text{a.c.})} = \frac{\mathfrak{F}_i}{2\mathcal{R}_0}. \tag{7.20a}$$

The steady polarizing flux is then found to divide among the four branches according to this pattern:

$$\begin{aligned} \phi_{01} = \phi_{04} &= \tfrac{1}{2}\phi_0(1-\delta), \\ \phi_{02} = \phi_{03} &= \tfrac{1}{2}\phi_0(1+\delta). \end{aligned} \tag{7.20b}$$

Combining these components according to the indicated direction arrows, and using the total flux for each gap in the basic force equation (7.1), yields an evaluation of net forces that constitute a torque couple whose moment is

$$\text{Torque [newton meters]} = h\,\frac{\phi_0^2}{2\mu_0 S_g}\,\delta + h\left[\frac{\phi_0 N \bar{\chi} k}{2d}\right] I_1, \tag{7.21}$$

where h is the distance between air-gap centers as indicated in Fig. 7.1(*c*). Note that the hysteresis factor has appeared again in making the connection between $\mathfrak{F}_i$ and ϕ_i. The bracketed factor in the last term of Eq. (7.21) identifies the transduction coefficient for the balanced-armature system, and indicates that the force factor is exactly the same as for the monopolar case analyzed above when interpreted in terms of the total polarizing flux and total air-gap length. In a similar way, the first term of Eq. (7.21) will yield, on differentiation with respect to $(-x)$, a

negative electromechanical contribution to stiffness which also corresponds to that found for the monopolar case [cf. Eq. 7.13(*b*)].

The similarity is maintained, therefore, between this case and that of the push-pull electrostatic loudspeaker; operation in the fundamental-frequency mode is essentially the same for single-sided and for push-pull excitation. The differences appear in the stability conditions and in the distortion products. In the present instance the quadratic nature of the basic force equation is just as "pure" as it was in the electrostatic case, but the nonlinear relation between ϕ_i and the signal current restricts the push-pull magnetic system to the elimination of only even-order distortion products.

It is not immediately obvious (or is it?) that the magnetic circuit of the ring-armature receiver (Fig. 7.3) closely resembles the balanced magnetic circuit of Fig. 7.2(*a*). Studying the cross-sectional diagram and the electric analog of the magnetic circuit shown in Fig. 7.9 will

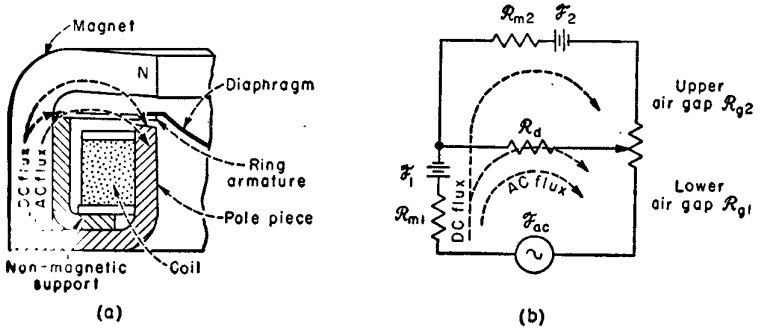

FIG. 7.9. Structural details and an electric-network analog of the magnetic circuit of the ring-armature transducer. [After Mott and Miner, reference 3.] (*Courtesy of the Bell System Technical Journal.*)

make the similarity more apparent, however. The electric analog makes it relatively easy to deduce that balance can be achieved by properly proportioning the relative strengths of the two magnets and the relative reluctances of the two air gaps. The latter adjustment can be made by the simple expedient of allowing the armature to float in an off-center position. In the engineering design of the receiver, a modest degree of unbalance is deliberately introduced so that a steady component of force across the lower gap will be available to hold the armature against its annular seat.

It is a disadvantage of the ring-armature configuration that the pole piece, the permanent magnet, and the ring armature itself, are each in the form of a large short-circuited turn that is closely coupled to the signal winding. As a consequence, the real part of the blocked impedance $(Z_e'' + Z_e')$ includes a component of resistance that represents the losses

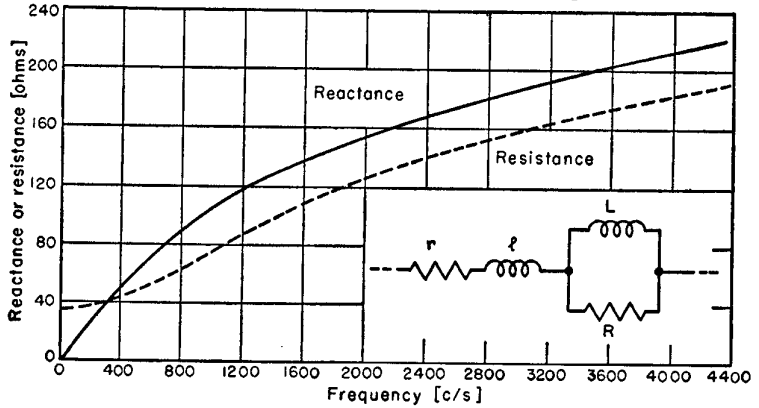

FIG. 7.10. The blocked impedance as a function of frequency for the ring-armature transducer. The inset shows an equivalent electric network that can closely simulate the observed variation of impedance. [After Mott and Miner, reference 3.] (*Courtesy of the Bell System Technical Journal.*)

due to eddy currents induced in these parasitic coupled circuits. The nature and relative magnitudes of this component and of the other loss factors account for the typical frequency behavior of the blocked impedance shown in Fig. 7.10.

The energy losses exacted by hysteresis were accounted for above by introducing a complex multiplier annexed to the incremental permeability. The effect of coupled eddy-current circuits can be handled in a similar way by using a complex *eddy-current factor* to modify appropriately the reactance and resistance of the associated signal winding. Such a factor will need to be evaluated analytically when dealing with the high-frequency losses in magnetostriction transducers with laminated cores, but it is sufficient here merely to account for the low-frequency variation of eddy-current losses with the square of frequency. A parallel combination of R and L turns out, very conveniently, to exhibit impedance components that do behave at low frequencies in just the proper way to account for these eddy-current effects. The simple network shown in the inset of Fig. 7.10 thus proves to be adequate to simulate the

blocked impedance of the ring-armature receiver over the entire frequency range of interest.

It may be recalled that the complex hysteresis factor $\bar{\chi}$, which appears in the L_e' part of the blocked impedance, appears also in the transduction coefficient as a multiplier that makes the force factor complex. When the blocked impedance reveals the effect of a coupled eddy-current circuit, it can be expected that a similar effect will manifest itself in the force factor. Typical behavior of this sort is exhibited in Fig. 7.11.

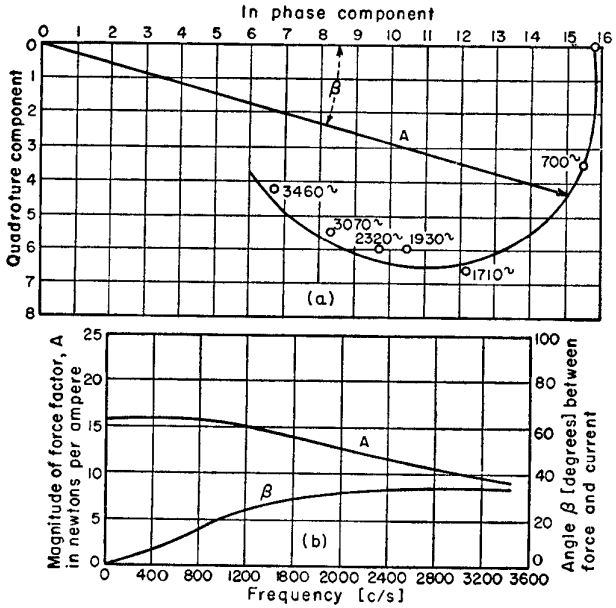

FIG. 7.11. Variation with frequency of the magnitude and phase angle of the force factor for the ring-armature transducer. [After Mott and Miner, reference 3.] (*Courtesy of the Bell System Technical Journal.*)

Wegel [5] showed in 1921 that the presence of a single eddy-current circuit would lead to a semicircular locus for the tip of the vector force factor, with the center of the circle on the real axis. The departure from this condition shown in Fig. 7.11 exemplifies the fact that more than one eddy-current circuit is coupled to the signal coil in this example.

[5] See note 1, Chapter 2.

The functional purpose of a telephone receiver, or earphone, is to establish cyclic pressure variations within a small closed cavity comprising the ear canal. Its useful acoustic load, therefore, can be represented as the stiffness reactance of the ear coupling chamber, which is identified as S_C in the equivalent circuit of Fig. 7.12 and in the sectional drawing of the receiver. It follows that it is the reactive power delivered to this stiffness reactance that determines the useful output, rather than the real power, which merely supplies the incidental losses in the coupling chamber and ear canal. As a further consequence, the over-all efficiency ceases to be a useful criterion of performance; instead, it is more significant to consider the *available power response*, defined as the ratio of the mean square of the sound pressure established in the output chamber to the electric power available from a signal source of stated internal output impedance.

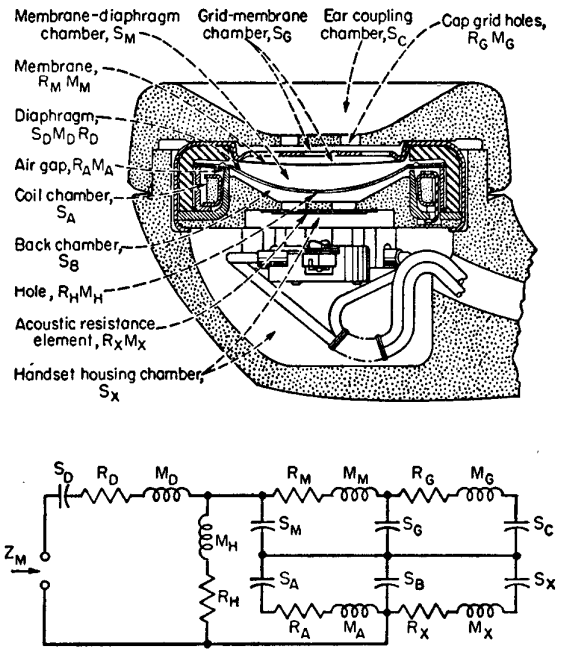

FIG. 7.12. An equivalent mechanical-impedance network representing the mechanical and acoustic elements associated with diaphragm motion in the ring-armature receiver. [After Mott and Miner, reference 3.] (*Courtesy of the Bell System Technical Journal.*)

Some of the structural design features of the ring-armature receiver can be discussed most conveniently in terms of the equivalent circuit shown in Fig. 7.12. A low-frequency cutoff in the response is introduced deliberately by providing a small hole in the center of the dome-shaped diaphragm. This has the useful effect of eliminating a good bit of interfering noise without impairing speech intelligibility. Since the hole serves to divert part of the volume current that would otherwise be delivered by the diaphragm to the chambers beyond, it must appear in the circuit diagram as the shunt-connected branch M_H,R_H. In a similar way, another portion of the volume current may be diverted by compression in the chamber S_M between the diaphragm and the flexible dust-sealing membrane. There is opportunity for still another fraction to be diverted by compression in the grid-membrane chamber S_G; and the residual volume current is finally delivered to the ear coupling chamber S_C through the impedance elements R_G,M_G that represent the holes in the grid and the receiver cap. Similar rationalization will then account for the components of volume current that return to the other side of the actuating diaphragm through the parallel paths comprising the chambers S_A,S_B,S_X.

This circuit configuration is obviously not one for which optimum values of the various circuit elements can be inferred by inspection. On the contrary, the large number of disposable parameters makes the task of finding optimum values by cut-and-try precalculation a problem of almost unmanageable complexity. It is in just such cases that it is most rewarding to adopt the expedient of modeling the mechanoacoustic structure with an all-electric network analog. In effect, this amounts to attacking the optimum-value problem by using the equivalent circuit as an analog computer. The adequacy of such a procedure was demonstrated by using it successfully to establish the structural and dimensional constants for this commercial receiver.

It has taken nearly a century of progress in all the sciences to bring within reach the goal epitomized by comparing the primitive 19th-century transducers, such as Reis's magnetostrictive knitting needle surrounded by a coil and mounted on a wooden box, with such beautifully adapted transducing mechanisms as those described above. One of the objectives of this book has been to demonstrate that much of the empiricism that characterized early assaults on the transducer problem has already disappeared. The task of removing the remaining empiricism continues to stand as a stubborn challenge to all who would seek to advance still further the frontiers of electroacoustics.

APPENDIX A

Dimensions and Units

Quantity	Symbol	Basic Dimensions QMLT	Basic Dimensions QVLT	Units in which quantity is expressed, and dimensional equivalents
Energy	U	ML^2T^{-2}	QV	joules ≡ newton meters ≡ coulomb volts
Power	W	ML^2T^{-3} ≡	QVT^{-1}	watts = joule seconds = ampere volts = coulomb volts/second
Mass	M	M	QVT^2L^{-2}	kilograms = newton seconds²/meter
Potential	V	$Q^{-1}ML^2T^{-2}$	V	volts
Current	I	QT^{-1}	QT^{-1}	amperes = coulombs/second
Transduction coefficient	T	$Q^{-1}MLT^{-1}$	VTL^{-1}	newtons/ampere = volt seconds/meter
Force factor	A	$Q^{-1}MLT^{-1}$	VTL^{-1}	newtons/ampere = volt seconds/meter
Magnetic flux	ϕ	$Q^{-1}ML^2T^{-1}$	VT	webers = volt seconds
Magnetic flux density	B	$MQ^{-1}T^{-1}$	VTL^{-2}	webers/meter²
Magnetic field vector	H	$QL^{-1}T^{-1}$	$QL^{-1}T^{-1}$	amperes/meter
Magnetization	M	$QL^{-1}T^{-1}$	$QL^{-1}T^{-1}$	amperes/meter
Magnetomotive force	$\mathfrak{F}$	QT^{-1}	QT^{-1}	ampere turns = coulombs/second
Magnetic reluctance	$\mathfrak{R}$	$Q^2M^{-1}L^{-2}$	$QV^{-1}T^{-2}$	ampere turns/weber = coulombs/volt seconds²
Inductance	L	$Q^{-2}ML^2$	$Q^{-1}VT^2$	henries = webers/ampere = volt seconds²/coulomb
Susceptibility	χ	Numeric	Numeric	
Permeability of free space	μ_o	$Q^{-2}ML$	$Q^{-1}VT^2L^{-1}$	$4\pi \times 10^{-7} = 1.257 \times 10^{-6}$ henries/meter
Relative permeability	μ	Numeric	Numeric	
Relative dielectric constant	ϵ	Numeric	Numeric	
Permittivity of free space	ϵ_o	$Q^2M^{-1}L^{-3}T^2$	$QV^{-1}L^{-1}$	$8.854 \times 10^{-12} = \frac{1}{36\pi} \times 10^{-9}$ farads/meter
Electric field	E	$Q^{-1}MLT^{-2}$	VL^{-1}	volts/meter
Electric displacement	D	QL^{-2}	QL^{-2}	coulombs/meter²
Electric polarization	P	QL^{-2}	QL^{-2}	coulombs/meter²
Capacitance	C	$Q^2M^{-1}L^{-2}T^2$	QV^{-1}	farads = coulombs/volt

Quantity	Symbol	Basic Dimensions QMLT	Basic Dimensions QVLT	Units in which quantity is expressed, and dimensional equivalents
Electric impedance, resistance, reactance	Z R X	$Q^{-2}ML^2T^{-1}$	$Q^{-1}VT$	ohms = volts/ampere = volt seconds/coulomb
Force	F	MLT^{-2}	QVL^{-1}	newtons = joules/meter = coulomb volts/meter
Pressure	P	$ML^{-1}T^{-2}$	QVL^{-3}	newtons/meter² = joules/meter³
Density	ρ	ML^{-3}	QVT^2L^{-5}	kilograms/meter³ = newton seconds²/meter⁴
Stiffness	s	MT^{-2}	QVL^{-2}	newtons/meter = coulomb volts/meter²
Compliance	c_m	$M^{-1}T^2$	$Q^{-1}V^{-1}L^2$	meters/newton = meters²/coulomb volt
Specific acoustic impedance	ρc	$ML^{-2}T^{-1}$	QVL^{-4}	kilogram/meter² second = coulomb volts/meter⁴ = newton seconds/meter³
Mechanical impedance	z_m	MT^{-1}	$QVL^{-2}T$	newton seconds/meter = kilograms/second
Acoustic impedance	Z_A	$ML^{-4}T^{-1}$	$QVL^{-6}T$	newton seconds/meter⁵ = kilograms/meter⁴ second = ohms (acoustic)

APPENDIX B

Conversion Charts*

The conversion charts presented in this Appendix were prepared to facilitate conversions between the various units most frequently encountered in electroacoustical computations. Included are charts for angular, linear, area, and volume measure; force, torque, pressure, and density; and compliance and mechanical impedance. In addition, there are charts for the inverse of several of these measures.

The charts of inverse measure are used for all conversions of the type X per unit A to X per unit B. An example of this case is volts per inch to be converted to volts per meter. It is sometimes possible to use the charts for multiple conversions when the specific units are not available on any of the charts. Thus, degrees per ounce inch torsional compliance can be expressed as radians per newton meter by first converting to radians per ounce inch and then to radians per newton meter. The desired over-all conversion factor is the product of the two factors, 1.745×10^{-2} (degrees to radians) times 1.416×10^{2} (X per ounce inch to X per newton meter) giving number of degrees per ounce inch times 2.471 equals number of radians per newton meter.

The following values for the fundamental constants were used in the preparation of the charts:

1 meter = 39.37 inches.
1 pound = 0.453592 kilograms.
Acceleration due to gravity = 980.665 cm/sec^2.
Density of H_2O at 4°C = .999973 grams/cm^3.
Density of H_g at 0°C = 13.5951 grams/cm^3.
Density of sea water at 0°C = 1.028 grams/cm^3.

* Reproduced from a manual of *Technical Data* with the kind permission of Brush Electronics Company, Cleveland, Ohio.

LENGTH

Multiply Number of → By ↓ To Obtain	Millimeters	Centimeters	Meters	Mils	Inches	Feet
Millimeters	1	10	10^{3}	$2.540 \cdot 10^{-2}$	$2.540 \cdot 10$	$3.048 \cdot 10^{2}$
Centimeters	10^{-1}	1	10^{2}	$2.540 \cdot 10^{-3}$	2.540	$3.048 \cdot 10$
Meters	10^{-3}	10^{-2}	1	$2.540 \cdot 10^{-5}$	$2.540 \cdot 10^{-2}$	$3.048 \cdot 10^{-1}$
Mils	$3.937 \cdot 10$	$3.937 \cdot 10^{2}$	$3.937 \cdot 10^{4}$	1	10^{3}	$1.200 \cdot 10^{4}$
Inches	$3.937 \cdot 10^{-2}$	$3.937 \cdot 10^{-1}$	$3.937 \cdot 10$	10^{-3}	1	$1.200 \cdot 10$
Feet	$3.281 \cdot 10^{-3}$	$3.281 \cdot 10^{-2}$	3.281	$8.333 \cdot 10^{-5}$	$8.333 \cdot 10^{-2}$	1

INVERSE LENGTH

Multiply Number of → By ↓ To Obtain	X Per Millimeter	X Per Centimeter	X Per Meter	X Per Mil	X Per Inch	X Per Foot
X Per Millimeter	1	10^{-1}	10^{-3}	$3.937 \cdot 10$	$3.937 \cdot 10^{-2}$	$3.281 \cdot 10^{-3}$
X Per Centimeter	10	1	10^{-2}	$3.937 \cdot 10^{2}$	$3.937 \cdot 10^{-1}$	$3.281 \cdot 10^{-2}$
X Per Meter	10^{3}	10^{2}	1	$3.937 \cdot 10^{4}$	$3.937 \cdot 10$	3.281
X Per Mil	$2.540 \cdot 10^{-2}$	$2.540 \cdot 10^{-3}$	$2.540 \cdot 10^{-5}$	1	10^{-3}	$8.333 \cdot 10^{-5}$
X Per Inch	$2.540 \cdot 10$	2.540	$2.540 \cdot 10^{-2}$	10^{3}	1	$8.333 \cdot 10^{-2}$
X Per Foot	$3.048 \cdot 10^{2}$	$3.048 \cdot 10$	$3.048 \cdot 10^{-1}$	$1.200 \cdot 10^{4}$	$1.200 \cdot 10$	1

AREA

Multiply Number of → BY / To Obtain ↓	Square Millimeters	Square Centimeters	Square Meters	Circular Mils	Square Inches	Square Feet
Square Millimeters	1	10^{2}	10^{6}	$5.067 \cdot 10^{-4}$	$6.452 \cdot 10^{2}$	$9.290 \cdot 10^{4}$
Square Centimeters	10^{-2}	1	10^{4}	$5.067 \cdot 10^{-6}$	6.452	$9.290 \cdot 10^{2}$
Square Meters	10^{-6}	10^{-4}	1	$5.067 \cdot 10^{-10}$	$6.452 \cdot 10^{-4}$	$9.290 \cdot 10^{-2}$
Circular Mils	$1.973 \cdot 10^{3}$	$1.973 \cdot 10^{5}$	$1.973 \cdot 10^{9}$	1	$1.273 \cdot 10^{6}$	$1.833 \cdot 10^{8}$
Square Inches	$1.550 \cdot 10^{-3}$	$1.550 \cdot 10^{-1}$	$1.550 \cdot 10^{3}$	$7.854 \cdot 10^{-7}$	1	$1.440 \cdot 10^{2}$
Square Feet	$1.076 \cdot 10^{-5}$	$1.076 \cdot 10^{-3}$	1.076·10	$5.454 \cdot 10^{-9}$	$6.944 \cdot 10^{-3}$	1

INVERSE AREA

Multiply Number of → BY / To Obtain ↓	X Per Square Millimeter	X Per Square Centimeter	X Per Square Meter	X Per Circular Mil	X Per Square Inch	X Per Square Foot
X Per Square Millimeter	1	10^{-2}	10^{-6}	$1.973 \cdot 10^{3}$	$1.550 \cdot 10^{-3}$	$1.076 \cdot 10^{-5}$
X Per Square Centimeter	10^{2}	1	10^{-4}	$1.973 \cdot 10^{5}$	$1.550 \cdot 10^{-1}$	$1.076 \cdot 10^{-3}$
X Per Square Meter	10^{6}	10^{4}	1	$1.973 \cdot 10^{9}$	$1.550 \cdot 10^{3}$	1.076·10
X Per Circular Mil	$5.067 \cdot 10^{-4}$	$5.067 \cdot 10^{-6}$	$5.067 \cdot 10^{-10}$	1	$7.854 \cdot 10^{-7}$	$5.454 \cdot 10^{-9}$
X Per Square Inch	$6.452 \cdot 10^{2}$	6.452	$6.452 \cdot 10^{-4}$	$1.273 \cdot 10^{6}$	1	$6.944 \cdot 10^{-3}$
X Per Square Foot	$9.290 \cdot 10^{4}$	$9.290 \cdot 10^{2}$	$9.290 \cdot 10^{-2}$	$1.833 \cdot 10^{8}$	$1.440 \cdot 10^{2}$	1

ANGULAR MEASURE

Multiply Number of → BY / To Obtain ↓	Seconds	Minutes	Degrees	Radians
Radians	$2.063 \cdot 10^{5}$	$3.438 \cdot 10^{3}$	5.730·10	1
Degrees	$3.600 \cdot 10^{3}$	6.000·10	1	$1.745 \cdot 10^{-2}$
Minutes	6.000·10	1	$1.667 \cdot 10^{-2}$	$2.909 \cdot 10^{-4}$
Seconds	1	$1.667 \cdot 10^{-2}$	$2.778 \cdot 10^{-4}$	$4.848 \cdot 10^{-6}$

INVERSE ANGULAR MEASURE

Multiply Number of → BY / To Obtain ↓	X Per Second	X Per Minute	X Per Degree	X Per Radian
X Per Second	1	$1.667 \cdot 10^{-2}$	$2.778 \cdot 10^{-4}$	$4.848 \cdot 10^{-6}$
X Per Minute	6.000·10	1	$1.667 \cdot 10^{-2}$	$2.909 \cdot 10^{-4}$
X Per Degree	$3.600 \cdot 10^{3}$	6.000·10	1	$1.745 \cdot 10^{-2}$
X Per Radian	$2.063 \cdot 10^{5}$	$3.438 \cdot 10^{3}$	5.730·10	1

VOLUME

Multiply Number of → BY / To Obtain ↓	Cubic Centimeters	Cubic Meters	Cubic Inches	Cubic Feet
Cubic Feet	$2.832 \cdot 10^{4}$	$2.832 \cdot 10^{-2}$	$1.728 \cdot 10^{3}$	1
Cubic Inches	1.639·10	$1.639 \cdot 10^{-5}$	1	$5.787 \cdot 10^{-4}$
Cubic Meters	10^{6}	1	$6.102 \cdot 10^{4}$	3.531·10
Cubic Centimeters	1	10^{-6}	$6.102 \cdot 10^{-2}$	$3.531 \cdot 10^{-5}$

INVERSE VOLUME

Multiply Number of → BY / To Obtain ↓	X Per Cubic Centimeter	X Per Cubic Meter	X Per Cubic Inch	X Per Cubic Foot
X Per Cubic Centimeter	1	10^{-6}	$6.102 \cdot 10^{-2}$	$3.531 \cdot 10^{-5}$
X Per Cubic Meter	10^{6}	1	$6.102 \cdot 10^{4}$	3.531·10
X Per Cubic Inch	1.639·10	$1.639 \cdot 10^{-5}$	1	$5.787 \cdot 10^{-4}$
X Per Cubic Foot	$2.832 \cdot 10^{4}$	$2.832 \cdot 10^{-2}$	$1.728 \cdot 10^{3}$	1

FORCE

Multiply Number of / To Obtain (By)	Dynes	Newtons	Grams	Kilograms	Ounces	Pounds
Dynes	1	10^{5}	$9.807 \cdot 10^{2}$	$9.807 \cdot 10^{5}$	$2.780 \cdot 10^{4}$	$4.448 \cdot 10^{5}$
Newtons	10^{-5}	1	$9.807 \cdot 10^{-3}$	9.807	$2.780 \cdot 10^{-1}$	4.448
Grams	$1.020 \cdot 10^{-3}$	$1.020 \cdot 10^{2}$	1	10^{3}	2.835·10	$4.536 \cdot 10^{2}$
Kilograms	$1.020 \cdot 10^{-6}$	$1.020 \cdot 10^{-1}$	10^{-3}	1	$2.835 \cdot 10^{-2}$	$4.536 \cdot 10^{-1}$
Ounces	$3.597 \cdot 10^{-5}$	3.597	$3.527 \cdot 10^{-2}$	3.527·10	1	1.600·10
Pounds	$2.248 \cdot 10^{-6}$	$2.248 \cdot 10^{-1}$	$2.205 \cdot 10^{-3}$	2.205	$6.250 \cdot 10^{-2}$	1

INVERSE FORCE

Multiply Number of / To Obtain (By)	X Per Dyne	X Per Newton	X Per Gram	X Per Kilogram	X Per Ounce	X Per Pound
X Per Dyne	1	10^{-5}	$1.020 \cdot 10^{-3}$	$1.020 \cdot 10^{-6}$	$3.597 \cdot 10^{-5}$	$2.248 \cdot 10^{-6}$
X Per Newton	10^{5}	1	$1.020 \cdot 10^{2}$	$1.020 \cdot 10^{-1}$	3.597	$2.248 \cdot 10^{-1}$
X Per Gram	$9.807 \cdot 10^{2}$	$9.807 \cdot 10^{-3}$	1	10^{-3}	$3.527 \cdot 10^{-2}$	$2.205 \cdot 10^{-3}$
X Per Kilogram	$9.807 \cdot 10^{5}$	9.807	10^{3}	1	3.527·10	2.205
X Per Ounce	$2.780 \cdot 10^{4}$	$2.780 \cdot 10^{-1}$	2.835·10	$2.835 \cdot 10^{-2}$	1	$6.250 \cdot 10^{-2}$
X Per Pound	$4.448 \cdot 10^{5}$	4.448	$4.536 \cdot 10^{2}$	$4.536 \cdot 10^{-1}$	1.600·10	1

TORQUE

Multiply Number of / To Obtain (By)	Dyne Centimeter	Newton Meter	Gram Centimeters	Kilogram Meters	Ounce Inches	Pound Feet
Dyne Centimeters	1	10^{7}	$9.807 \cdot 10^{2}$	$9.807 \cdot 10^{7}$	$7.062 \cdot 10^{4}$	$1.356 \cdot 10^{7}$
Newton Meters	10^{-7}	1	$9.807 \cdot 10^{-5}$	9.807	$7.062 \cdot 10^{-3}$	1.356
Gram Centimeters	$1.020 \cdot 10^{-3}$	$1.020 \cdot 10^{4}$	1	10^{5}	7.201·10	$1.383 \cdot 10^{4}$
Kilogram Meters	$1.020 \cdot 10^{-8}$	$1.020 \cdot 10^{-1}$	10^{-5}	1	$7.201 \cdot 10^{-4}$	$1.383 \cdot 10^{-1}$
Ounce Inches	$1.416 \cdot 10^{-5}$	$1.416 \cdot 10^{2}$	$1.389 \cdot 10^{-2}$	$1.389 \cdot 10^{3}$	1	$1.920 \cdot 10^{2}$
Pound Feet	$7.376 \cdot 10^{-8}$	$7.376 \cdot 10^{-1}$	$7.233 \cdot 10^{-5}$	7.233	$5.208 \cdot 10^{-3}$	1

INVERSE TORQUE

Multiply Number of / To Obtain (By)	X Per Dyne Centimeter	X Per Newton Meter	X Per Gram Centimeter	X Per Kilogram Meter	X Per Ounce Inch	X Per Pound Foot
X Per Dyne Centimeter	1	10^{-7}	$1.020 \cdot 10^{-3}$	$1.020 \cdot 10^{-8}$	$1.416 \cdot 10^{-5}$	$7.376 \cdot 10^{-8}$
X Per Newton Meter	10^{7}	1	$1.020 \cdot 10^{4}$	$1.020 \cdot 10^{-1}$	$1.416 \cdot 10^{2}$	$7.376 \cdot 10^{-1}$
X Per Gram Centimeter	$9.807 \cdot 10^{2}$	$9.807 \cdot 10^{-5}$	1	10^{5}	$1.389 \cdot 10^{-2}$	$7.233 \cdot 10^{-5}$
X Per Kilogram Meter	$9.807 \cdot 10^{7}$	9.807	10^{5}	1	$1.389 \cdot 10^{3}$	7.233
X Per Ounce Inch	$7.062 \cdot 10^{4}$	$7.062 \cdot 10^{-3}$	7.201·10	$7.201 \cdot 10^{-4}$	1	$5.208 \cdot 10^{-3}$
X Per Pound Foot	$1.356 \cdot 10^{7}$	1.356	$1.383 \cdot 10^{4}$	$1.383 \cdot 10^{-1}$	$1.920 \cdot 10^{2}$	1

PRESSURE

Multiply Number of → / To Obtain ↓ BY	Dynes Per Square Centimeter	Newtons Per Square Meter	Kilograms per Square Meter	Pounds Per Square Inch	Centimeters of Mercury at 0°C	Feet of Fresh Water at 4°C	Feet of Sea Water* at 0°C
Dynes Per Square Centimeter	1	10	9.807·10	$6.895 \cdot 10^{4}$	$1.333 \cdot 10^{4}$	$2.989 \cdot 10^{4}$	$3.073 \cdot 10^{4}$
Newtons Per Square Meter	10^{-1}	1	9.807	$6.895 \cdot 10^{3}$	$1.333 \cdot 10^{3}$	$2.989 \cdot 10^{3}$	$3.073 \cdot 10^{3}$
Kilograms Per Square Meter	$1.020 \cdot 10^{-2}$	$1.020 \cdot 10^{-1}$	1	$7.031 \cdot 10^{2}$	$1.360 \cdot 10^{2}$	$3.048 \cdot 10^{2}$	$3.133 \cdot 10^{2}$
Pounds Per Square Inch	$1.450 \cdot 10^{-5}$	$1.450 \cdot 10^{-4}$	$1.422 \cdot 10^{-3}$	1	$1.934 \cdot 10^{-1}$	$4.335 \cdot 10^{-1}$	$4.457 \cdot 10^{-1}$
Centimeters of Mercury at 0°C	$7.501 \cdot 10^{-5}$	$7.501 \cdot 10^{-4}$	$7.356 \cdot 10^{-3}$	5.171	1	2.242	2.305
Feet of Fresh Water at 4°C	$3.346 \cdot 10^{-5}$	$3.346 \cdot 10^{-4}$	$3.281 \cdot 10^{-3}$	2.307	$4.460 \cdot 10^{-1}$	1	1.028
Feet of Sea Water* at 0°C	$3.254 \cdot 10^{-5}$	$3.254 \cdot 10^{-4}$	$3.191 \cdot 10^{-3}$	2.244	$4.339 \cdot 10^{-1}$	$9.727 \cdot 10^{-1}$	1

INVERSE PRESSURE

Multiply Number of → / To Obtain ↓ BY	X Per Dyne Per Square Centimeter	X Per Newton Per Square Meter	X Per Kilogram Per Square Meter	X Per Pound Per Square Inch	X Per Centimeter of Mercury at 0°C.	X Per Foot of Fresh Water at 4°C	X Per Foot of Sea Water* at 0°C.
X Per Dyne Per Square Centimeter	1	10^{-1}	$1.020 \cdot 10^{-2}$	$1.450 \cdot 10^{-5}$	$7.501 \cdot 10^{-5}$	$3.346 \cdot 10^{-5}$	$3.254 \cdot 10^{-5}$
X Per Newton Per Square Meter	10	1	$1.020 \cdot 10^{-1}$	$1.450 \cdot 10^{-4}$	$7.501 \cdot 10^{-4}$	$3.346 \cdot 10^{-4}$	$3.254 \cdot 10^{-4}$
X Per Kilogram Per Square Meter	9.807·10	9.807	1	$1.422 \cdot 10^{-3}$	$7.356 \cdot 10^{-3}$	$3.281 \cdot 10^{-3}$	$3.191 \cdot 10^{-3}$
X Per Pound Per Square Inch	$6.895 \cdot 10^{4}$	$6.895 \cdot 10^{3}$	$7.031 \cdot 10^{2}$	1	5.171	2.307	2.244
X Per Centimeter of Mercury at 0°C.	$1.333 \cdot 10^{4}$	$1.333 \cdot 10^{3}$	$1.360 \cdot 10^{2}$	$1.934 \cdot 10^{-1}$	1	$4.460 \cdot 10^{-1}$	$4.339 \cdot 10^{-1}$
X Per Foot of Fresh Water at 4°C.	$2.989 \cdot 10^{4}$	$2.989 \cdot 10^{3}$	$3.048 \cdot 10^{2}$	$4.335 \cdot 10^{-1}$	2.242	1	$9.727 \cdot 10^{-1}$
X Per Foot of Sea Water* at 0°C.	$3.073 \cdot 10^{4}$	$3.073 \cdot 10^{3}$	$3.133 \cdot 10^{2}$	$4.457 \cdot 10^{-1}$	2.305	1.028	1

DENSITY

Multiply Number of → / To Obtain ↓ BY	Grams Per Cubic Centimeter	Kilograms Per Cubic Meter	Grams Per Cubic Inch	Ounces Per Cubic Inch	Pounds Per Cubic Inch	Pounds Per Cubic Foot
Grams Per Cubic Centimeter	1	10^{-3}	$6.102 \cdot 10^{-2}$	1.730	2.768·10	$1.602 \cdot 10^{-2}$
Kilograms Per Cubic Meter	10^{3}	1	6.102·10	$1.730 \cdot 10^{3}$	$2.768 \cdot 10^{4}$	1.602·10
Grams Per Cubic Inch	1.639·10	$1.639 \cdot 10^{-2}$	1	2.835·10	$4.536 \cdot 10^{2}$	$2.625 \cdot 10^{-1}$
Ounces Per Cubic Inch	$5.780 \cdot 10^{-1}$	$5.780 \cdot 10^{-4}$	$3.527 \cdot 10^{-2}$	1	1.600·10	$9.259 \cdot 10^{-3}$
Pounds Per Cubic Inch	$3.613 \cdot 10^{-2}$	$3.613 \cdot 10^{-5}$	$2.205 \cdot 10^{-3}$	$6.250 \cdot 10^{-2}$	1	$5.787 \cdot 10^{-4}$
Pounds Per Cubic Foot	6.243·10	$6.243 \cdot 10^{-2}$	3.810	$1.080 \cdot 10^{2}$	$1.728 \cdot 10^{3}$	1

COMPLIANCE

Multiply Number of → / To Obtain ↓ BY	Centimeter Per Dyne	Meton (Meters Per Newton)	Inches Per Ounce
Inches Per Ounce	9.136×10^{-5}	9.136×10^{-2}	1
Meton (Meters Per Newton)	10^{-3}	1	1.095×10
Centimeters Per Dyne	1	10^{3}	1.095×10^{4}

LINEAR MECHANICAL IMPEDANCE

Multiply Number of → / To Obtain ↓ BY	Dynes Per Centimeter Per Second	Newtons Per Meter Per Second	Ounces Per Inch Per Second
Ounces Per Inch Per Second	1.095×10^{4}	1.095×10	1
Newtons Per Meter Per Second	10^{3}	1	9.136×10^{-2}
Dynes Per Centimeter Per Second	1	10^{-3}	9.136×10^{-5}

INDEX OF NAMES

[An attempt has been made to give the full name and terminal date or dates for each person listed, but in several instances part of this information is still wanting. I shall be grateful to any reader who can supply any of the missing names or dates, so that more complete data can be included in any revision of this tabulation. F.V.H.]

ABRAHAM, Henri (1868–1943), 51
ADDISON, Joseph (1672–1719), 10
ADER, Clément (1841–1925), 60
AIGNER, Franz (1882–1945), 66
ALDINI, Giovanni (1762–1834), 13
ALEXANDERSON, Ernst Frederick Werner (1878–), 66
AMPÈRE, André Marie (1775–1836), 14, 15, 112
ARAGO, Dominique François Jean (1786–1853), 14
ARKELL, Frederick Granville (1882–), 76
ARNOLD, Harold DeForest (1883–1933), 41, 64*n*

BAILEY, Austin (1893–), 55*n*
BALDWIN, Nathaniel (1878–), 73, 74
BALLANTINE, Stuart (1897–1944), 41*n*, 103, 173*n*
BANKS, Sir Joseph (1743–1820), 12*n*
BARKER, Alfred Cecil (1899–), 76
BARLOW, Peter (1776–1862), 14, 15
BARRETT, Sir William Fletscher (1844–1925), 21
BAUER, Benjamin Baumzweiger (1913–), 215*n*
BEATSON, W. (–), 19, 20
BECQUEREL, Antoine César (1788–1878), 42
BECQUEREL, Antoine Henri (1852–1908), 42
BEDFORD, Alda Vernon (1904–), 84*n*
BELL, Alexander Graham (1847–1922), 3, 22–24, 26–34, 41, 58, 60
BELL, Chichester Alexander (–1924), 39
BERANEK, Leo Leroy (1914–), 5, 173*n*
BERGER, Christian (–), 60
BERLINER, Emile (1851–1929), 34, 35
BERNARD, Marcel (–), 84
BIGGAR, John Stuart (–), 63
BIOT, Jean Baptiste (1774–1862), 14
BLAKE, Francis (1850–1913), 32, 34, 35
BLOCH, Alfred (1904–), 110, 111
BOCCIARELLI, Carlo Vittorio (1902–), 187*n*
BÔCHER, Maxime (1867–1918), 93*n*
BODE, Hendrik Wade (1905–), 93*n*, 94*n*
BONAPARTE, Napoléon (1769–1821), 13
BONN, Theodore Hertz (1923–), 170*n*
BOSTWICK, Lee Gordon (1900–), 70, 85
BOUDETTE, Clayton Merchant (1896–), 72*n*
BOUDETTE, Reuben Timothy (1868–1933), 72*n*
BOURSEUL, Charles (1829–1912), 24–27
BOYLE, Robert William (1883–), viii, 49–52
BRANLY, Désiré Eugène Édouard (1844–1940), 65
BRAUN, Karl Ferdinand (1850–1918), 40
BREWSTER, Sir David (1781–1868), 14*n*
BROGLIE, Louis-César-Victor-Maurice, Duc de (1875–), 48
BROGLIE, Louis Victor, Prince de (1892–), 48
BROOKS, Harvey (1915–), vi
BROWN, Sidney George (1873–1948), 49, 59, 74, 75, 83*n*
BUCHER, Elmer Eustice (1885–), 73*n*
BUEHLER, Ernest (1913–), 57*n*
BUMSTEAD, Henry Andrews (1870–1920), 46
BUNDY, Francis Pettit (1910–), vi
BURSTYN, Walther (1877–), 42
BUTTON, Leroy Ralph (1883–), 86

CADY, Walter Guyton (1874–), viii, 51, 53–56

CAMPBELL, George Ashley (1870–), 66
CAPPS, Frank Lushbaugh (1869–1943), 60, 73
CAVALLO, Tiberius (1749–1809), 11
CHAFFEE, Emory Leon (1885–), vii
CHAMBERS, Frederick John (–), 38
CHILOWSKY, Constantin (1880–), 46, 48
CHRISTIE, Samuel Hunter (1784–1865), 22
CLARK, Latimer (1822–1898), 9*n*
CLAUSIUS, Rudolf Julius Emmanuel (1822–1888), 22
COHEN, I Bernard (1914–), viii, 8*n*, 9*n*
COLBY, John Warren (–), 87
COLIN, Victor-Hubert, Cap. de Frégate (Rés., retr.) (1868–1941), 47, 48
COLLAR, Arthur Roderick (1908–), 93*n*
COLVIN, William, Jr. (–), 173*n*
COMPTON, Karl Taylor (1887–1954), 46
COOKE, Sir William Fothergill (1806–1879), 27
COULOMB, Charles Augustin de (1736–1806), 42, 116
COULSON, Thomas (1886–), 3*n*, 16*n*
CRANDALL, Irving Bardshar (1890–1927), 41, 172*n*
CROZIER, William Dwight (1900–), 169*n*
CURIE, Paul Jacques (1855–1941), 22, 42–44
CURIE, Pierre (1859–1906), 22, 42, 43
CURTIS, Alfred Stanley (1890–1938), 76
CUTTRISS, Charles (1849–1905), 58, 59

D'AMOUR, Paul-Georges Huguet (–), 72
DAVY, Sir Humphry (1778–1829), 14
DE BROGLIE. *See* BROGLIE
DE FOREST, Lee (1873–), (64)
DELEZENNE, Charles Édouard Joseph (1776–1866), 19
DICKSON, Leonard Eugene (1874–1954), 95*n*
DIMATTIA, Alfred Louis (1910–), 173*n*
DOLBEAR, Amos Emerson (1837–1910), 31–33, 41
DOPPLER, Christian Johann (1803–1853), 45, 85
DORSEY, Herbert Grove (1876–), 76
DOWD, Peter A. (–), 32, 33
DRAWBAUGH, Daniel (1827–1911), 32
DUDDELL, William du Bois (1872–1917), 49
DUHEM, Pierre Maurice Marie (1861–1916), 44
DUNCAN, Harry L. (–), 71
DUNCAN, William Jolly (1894–), 93*n*
DYAR, Harrison Gray (1805–1875), 11

EDELMAN, Philip E. (1894–), 169*n*
EDISON, Thomas Alva (1847–1931), 31, 32, 34, 35, 37, 38, 41, 61, 62
EGERTON, Henry Clifford (1883–), 73
EHRET, Cornelius Dalzell (1874–), 63
ESPENSCHIED, Lloyd (1889–), 39*n*, 67*n*
EVERSHED, Sydney (1857–1939), 74–76

FABRY, Charles (1867–1945), 51
FAHIE, John Joseph (1846–1934), 9, 11*n*, 12*n*, 13
FANGER, Herman Joseph (1895–), 85
FARADAY, Michael (1791–1867), 8, 112
FARRAND, Clair Loring (1895–), 71, 72, 75
FAY, Richard Dudley (1891–), 76
FESSENDEN, Reginald Aubrey (1866–1932), 39, 40, 42, 45, 61, 76, 85
FERRIÉ, Gustave Auguste (1868–1932), 49
FIELD, Stephen Dudley (1846–1913), 75, 76
FINCH, Edwin David (1838–1879), 87
FIRESTONE, Floyd Alburn (1898–), 110
FLANNAGAN, Coke (1892–), 90*n*
FLEMING, Sir John Ambrose (1849–1945), 112, 113
FLORISSON, Charles Louis (1897–), 50*n*
FORBES, George (1849–1936), 40
FORD, Francis J. W., *D.J.* (1882–), 54*n*, 56
FOURIER, Jean Baptiste Joseph, Baron (1768–1830), 177, 178, 189, 222
FRANKLIN, Benjamin (1706–1790), 8, 9
FRAZER, Robert Alexander (1891–), 93*n*

FREDERICK, Halsey Augustus (1887–), 37*n*, 87
FRIEDEL, Charles (1832–1898), 44

GARRETT, Thomas Alexander (1862–1929), 61
GAUSS, Karl Friedrich (1777–1855), 15–17
GERLACH, Erwin (1890–), 78
GILLILAND, Ezra T. (1846–1903), 62
GOLDMAN, Robert Barnett (1927–), 209*n*
GOVI, Gilberto (1826–1889), 12*n*
GRANT, John (–1923), 39
GRAY, Elisha (1835–1901), 5, 30–32, 38, 58, 86*n*
GRAY, Stephen (?–1736), 1, 10
GREAVES, Valentine Ford (1884–), 169*n*
GREEN, G. (–), 169*n*
GUÉRITOT, Maurice (–), 78
GUILLEMIN, Amédée Victor (1826–1893), 20
GUILLEMIN, Ernst Adolph (1898–), 93*n*
GUYE, Charles-Eugène (1866–1942), 46

HACKLEY, Reginald Armstrong (1907–), 89*n*
HAHNEMANN, Walter Max (1879–1944), 66
HÄHNLE, Walter (1886–), 110*n*
HALSEY, Edward S. (1869–), 73
HALSKE, Johann Georg (1814–1890), 58
HAMEL, Joseph J. von (1788–1862), 15*n*
HAMILTON, Sir William Rowan (1805–1865), 114
HAMMOND, John Hays, Jr. (1888–), 67*n*
HANNA, Clinton Richards (1899–), 59, 67, 74*n*, 169*n*
HARBAUGH, Fred Joseph (1898–), viii
HARRISON, Henry Charles (1887–), 66–68
HAÜY, Abbé René Just (1743–1822), 42
HAYES, Harvey Cornelius (1878–), 51*n*
HAYS, Jenny Ward (–), 87
HEBB, Malcolm Hayden (1910–), vi, 111
HECHT, Karl Heinrich (1880–), 66
HELMHOLTZ, Hermann Ludwig Ferdinand von (1821–1894), 22, 40, 103
HENRY, Joseph (1797–1878), 3, 16–18
HERSH, John Franklin (1920–), 159*n*, 183*n*, 205*n*
HEWLETT, Clarence Wilson (1886–), 77
HIGH, Jurjen S. (–), 88
HILLIARD, John Kenneth (1901–), 90, 171*n*
HONDA, Kotaro (1870–1954), 21
HOPKINS, Marcus Clarence (1877–1937), 71
HOUSTON, Edwin James (1847–1914), 62*n*
HUGHES, David Edward (1831–1900), 35, 36, 62*n*
HULL, Albert Wallace (1880–), 51
HUNNINGS, Henry (1842?–), 35, 37
HUNT, Frederick Vinton (1905–), 106*n*, 175*n*
HUNTER, Philip Vassar (1883–), 49

IZARN, Joseph (1766–1834), 13

JACOBI, Moritz Hermann von (1801–1874), 22
JANSZEN, Arthur August (1907–), 175*n*, 183*n*
JEFFERSON, H. (–), 110, 111
JENSEN, Peter Lauritz (1886–), 59
JERVIS-SMITH, Frederick John (1848–1911), 38
JEWETT, Frank Baldwin (1879–1949), 64*n*
JOHNSEN, Frederik Alfred (1887–1930), 38
JOHNSON, John Henry (–), 5*n*
JONES, Warren Clark (1891–), 90*n*
JOULE, James Prescott (1818–1889), 20–22

KELLER, Arthur Charles (1901–), 86
KELLOGG, Edward Washburn (1883–), viii, 59, 65, 79–83, 91, 143, 153, 173*n*
KELVIN, (Sir William Thomson) 1st Baron [Lord] (1824–1907), 7, 22, 43, 44, 78
KENNELLY, Arthur Edwin (1861–1939), 66, 96, 99, 101, 102, 229
KILROY, Willie Dickson (1875?–), 74–76

KIRCHER, Raymond John (1907–), 111*n*
KIRCHHOFF, Gustav Robert (1824–1887), 22, 106
KLAR, Ernst (–), 173*n*
KLIPSCH, Paul Wilbur (1904–), 91
KLUPATHY, Eugen von (1861–1931), 60
KNOWLES, Hugh Shaler (1904–), viii
KNUDSEN, Vern Oliver (1893–), 65
KRANZ, Frederick William (1887–), 169*n*
KYLE, Colin (1894–), 173*n*

LABORDE, Jean Baptiste de (1730–1777), 8
LAKATOS, Emory (1905–), 67*n*
LANE, Clarence Edwin (1892–1951), 72
LANGEVIN, Paul (1872–1946), 44, 46–52, 55, 56
LANGMUIR, Irving (1881–), 85, 86
LAPLACE, Marquis Pierre Simon de (1749–1827), 14
LA RIVE, Auguste Arthur de (1801–1873), 19, 20, 57
LAWTHER, Harry Preston (1891–), 67, 77
LE CORBEILLER, Philippe Emmanuel (1891–), viii, 110
LEGAT, Wilhelm von (–), 27, 30
LEGG, Victor Eldred (1897–), 214*n*
LEIBNIZ, Baron Gottfried Wilhelm von (1646–1716), 23
LENZ, Heinrich Friedrich Emil (1804–1865), 113, 146
LESAGE, Georges-Louis (1724–1803), 11
LICKLIDER, Joseph Carl Robnett (1915–), 29
LINDSAY, Robert Bruce (1900–), 86*n*
LINDSEY, Lucius Arthur (1875–1941), 63
LIPPMANN, Gabriel (1845–1921), 43
LISSAJOUS, Jules Antoine (1822–1880), 220
LODGE, Sir Oliver Joseph (1851–1940), 59–61, 63, 65
LOSURDO, Antonino (1880–), 52
LUCAS, William (1863–1945), 61
LUMIÈRE, Louis Jean (1864–1948), 70, 71

MCLACHLAN, Norman William (1888–), 169*n*
MCMILLAN, Edwin Mattison (1907–), 114
MAJORANA, Quirino (1871–), 39
MARRIAN, J. P. (–), 19, 20
MARTIN, William Hennick (1889–), 83, 84
MASON, Warren Perry (1900–), 67*n* 109
MASSA, Frank (1906–), 79*n*, 89
MATTEUCCI, Carlo (1811–1868), 19, 21
MAWARDI, Osman Kamel (1917–), 166
MAXFIELD, Joseph Pease (1887–), 67–69
MAXWELL, James Clerk (1831–1879), 22, 216
MAXWELL, Joseph W. (1833–1906), 60
MAYER, Julius Robert von (1814–1878), 22
MERRILL, Albion Parvis (1882–), 87
MEYER, Erwin Walter (1899–), 172*n*
MILHAUD, Edgard (1873–), 46
MILLER, John Milton (1882–), 56
MILLS, John (1880–1948), 64*n*
MINER, Russell Cavine (1908–), 215, 216, 231–234
MINTON, John Preston (1889–), 76*n*, 87, 89
MOIGNO, Abbé François Napoléon Marie (1804–1884), 11*n*
DU MONCEL, Vicomte Théodose Achille Louis (1821–1884), 25, 26
MORECROFT, John Harold (1881–1934), 46, 51
MORSE, Samuel Finley Breese (1791–1872), 17, 18, 31
MORTIMER, Cromwell (?–1752), 1*n*
MOTT, Edward Elmer (1904–), 215, 216, 231–234

NAGAOKA, Hantarō (1865–1950), 21
NEUMANN, Carl Gottfried (1832–1925), 189
NEWTON, Sir Isaac (1642–1727), 23
NICOLSON, Alexander McLean (1880–1950), 52, 54–56, 83*n*
NORDENSWAN, Robert (1885–), 76
NORTON, Edward Lawry (1898–), 66–68, 109

OERSTED, Hans Christian (1777–1851), 13, 14
OHM, Georg Simon (1787–1854), 15, 217
OLIVER, Bernard More (1914–), 159*n

OLNEY, Benjamin (1887–), 88
OLSON, Harry Ferdinand (1902–), viii, 5, 79, 84*n*, 89, 165

PAINLEVÉ, Paul (1863–1933), 46
PAGE, Charles Grafton (1812–1868), 18–20, 22, 30, 42
PARIS, Edward Talbot (1889–), 40*n*
PARRY, Robert Davies (–), 84, 165
PETERSON, Charles Wallace (1893–), 75
PICKARD, Greenleaf Whittier (1877–), 39
PIERCE, George Washington (1872–), vii, 55, 56, 61, 86*n*, 96, 101, 229
PIPES, Louis Albert (1910–), 95*n*
POCKELS, Friedrich Carl Alwin (1865–1913), 44
POGGENDORFF, Johann Christian (1796–1877), 14–16
POINCARÉ, Jules Henri (1854–1912), 93*n*
POISSON, Siméon Denis (1781–1840), 185
POLLACK, Irwin (1925–), 29
POLLÁK, Anton (–), 59
PORTA, Giambattista della (1538?–1615), 9
PREECE, Sir William Henry (1834–1913), 40
PRESCOTT, George Bartlett (1831–1894), 11*n*, 23*n*, 31*n*
PRESTON, John (1900–), 84*n*
PRIDHAM, Edwin Stewart (1881–), 59
PRITCHARD, Robert Leslie (1924–), 161*n*, 175*n*, 193*n*
PUPIN, Michael Idvorsky (1858–1935), 51

QUIMBY, Shirley Leon (1893–), 51
QUINAN, Lt. Cdr. Johnstone Hamilton, U.S.C.G. (ret.) (1861–1940), 45*n*

RAGUET, Capt. Edward Cook, U.S.N. (ret.) (1886–), 46
RAHBECK, Knud (1891–), 38
RAINEY, Paul Miller (1880–1946), 63
RAISBECK, Gordon (1924–), 111*n*
RANKINE, Alexander Oliver (1881–), 80*n*
RAWLINSON, William Ferdinando (1893–), 49
RAYLEIGH, (John William Strutt) 3d Baron [Lord] (1842–1919), 37, 86, 103
REDDING, Jerome (1841–1939), 58
REIS, Johann Philipp (1834–1874), 26–30, 33, 235
RICE, Chester Williams (1888–1951), 59, 65, 79–83, 87, 143, 153
RICHARDSON, Lewis Fry (1881–1953), 45, 46, 85
RICKER, Norman Hurd (1896–), 72
RIEGGER, Hans (1883–1926), 82, 143, 187*n*
RINES, David (1884–), viii
RINGEL, Abraham Sumer (1897–), 76, 84*n*, 89, 165
RITCHIE, William (1790–1837), 15
RITTER, Johann Wilhelm (1776–1810), 12*n*
ROMAGNOSI, Giovanni Domenico (1761–1835), 12, 13
RONALDS, Sir Francis (1788–1873), 11
RÖNTGEN, Wilhelm Konrad (1845–1923), 43
RUHMKORFF, Heinrich Daniel (1803–1877), 5
RUTHERFORD, (Sir Ernest Rutherford) 1st Baron [Lord] (1871–1937), 48, 49, 51
RYDER, Robert Morgan (1915–), 111*n*

SABINE, Paul Earls (1879–), vi
ST. CLAIR, Hillary W (1909–), 77
SANDEMAN, Edward Kenneth (1897–), 91
SAVART, Félix (1791–1841), 14
SAWYER, Charles Baldwin (1894–), 52, 53*n*
SCHILLING, Baron Paul Ludovitsch (1786–1837), 15, 16, 18
SCHOTTKY, Walter Hans (1886–), 78, 103*n*
SCHULTZ, Theodore John (1922–), 172*n*
SCHUMACHER, Heinrich Christian (1780–1850), 15*n*
SCHWEIGGER, Johann Salomo Christoph (1779–1857), 12*n*, 14–16
SEIGNETTE, Pierre (1660?–1719), 52
SHAW, Thomas (1883–), 64*n*
SHEA, Timothy Edward (1898–), 107*n*
SHELDON, Samuel (1862–1920), 62
SHORTER, Donovan Ernest Lea (1910–), 173*n*

SHREEVE, Herbert Edward (1873–1942), 63, 64
SIEMENS, Carl Heinrich von (1829–1906), 58*n*
SIEMENS, Ernst Werner von (1816–1892), 22, 58, 59, 60
SILLIMAN, Benjamin (1779–1864), 16*n*
SMITH, Benjamin Spalding (1887–), 49
SMITH, Preston Wood, Jr. (1923–), 112*n*
SMYTH, Albert Henry (1863–1907), 9*n*
SOEMMERRING, Samuel Thomas (1755–1830), 12, 15*n*
SOKOLNIKOFF, Elizabeth Stafford (Mrs. I.S.) (1902–), 95*n*
SOKOLNIKOFF, Ivan Stephan (1901–), 95*n*
SPENCER, Albert L. (–), 29, 32
STARR, Arthur Tisso (1905–), 107*n*
STEINBERGER, Louis (–), 88
STEINBERGER, Raymond Leonard (1898–), 86
STEINHEIL, Karl August von (1801–1870), 18
STOKES, Sir George Gabriel (1819–1903), 86, 155
STONE, John Stone (1869–1943), 65
STRADA, Famianus (1572–1649), 9, 10
STROH, John Matthias Augustus (1828–1914), 70
STURGEON, William (1783–1850), 16
SYKES, Adrian Francis (1889–), 82

TAINTER, Charles Sumner (1854–1940), 39
TAIT, Peter Guthrie (1831–1901), 7*n*
TAYLOR, Theodore F. (–), 78
TAYLOR, William Bower (1821–1895), 12*n*, 13, 16*n*
TELLEGEN, B(ernardus) D(ominicus) H(ubertus) (1900–), 111
THÉVENIN, Léon-Charles (1857-1926), 116
THOMPSON, Roy Edwin (1887–1950), 86
THOMPSON, Sylvanus Phillips (1851–1916), 27
THOMSON, Sir Joseph John (1856–1940), 21
THOMSON, Elihu (1853–1937), 62*n*
THURAS, Albert Lauris (1888–1945), 88, 90
TONKS, Lewi (1897–), 51
TOURNIER, Marcel Charles (1888–), 48
TOWER, Charles Homer (1881–1949), 52, 53*n*
TOWER, Frank Stanley (1891–1946), 74
TROWBRIDGE, John (1843–1923), 62, 63
TUCKER, William Sansome (1877–), 40
TURNBULL, Laurence (1821–1900), 11*n*

VAN DYKE, Karl Skillman (1892–), 55
VANNI, Giuseppe (1862–1934), 38
VILLARI, Emilio (1836–1904), 21
VOGT, Hans (1890–), 169*n*, 173*n*
VOIGT, Woldemar (1850–1919), 44
VOLTA, Count Alessandro (1745–1827), 12
VERNE, Jules (1828–1905), 24
VREELAND, Frederick King (1874–), 96

WALLACE, Robert Lee, Jr. (1916–), 111*n*
WARTH, Nathaniel G. (–), 63
WARTMANN, Élie-François (1817–1886), 19, 20
WATSON, Thomas Augustus (1854–1934), 31, 60, 73
WEAVER, William Dixon (1857–1919), 9*n*
WEBER, Wilhelm Eduard (1804–1891), 15, 22
WEBSTER, Arthur Gordon (1863–1923), 66, 93*n*
WEGEL, Raymond Lester (1888–), viii, 66, 74, 83, 93*n*, 165–167*n*, 233
WEIL, Maximilian (1891–), 90
WEINBERGER, Julius (1893–), 79*n*, 88
WENTE, Edward Christopher (1889–), viii, 42*n*, 82, 88*n*, 89, 90, 143, 169
WERLEIN, (–), 49, 50, 52
WERTHEIM, Wilhelm (1815–1861), 19, 20
WHEATLAND, David Pingree (1898–), vii
WHEATSTONE, Sir Charles (1802–1875), 22, 27, 36
WHITNEY, Willis Rodney (1868–), 79
WHITTAKER, Edmund Taylor (1873–), 93*n*
WIEDEMANN, Gustav Heinrich (1826–1899), 20

WIENER, Francis Michael (1911–), 173*n*
WILE, Frederic William (1873–1941), 34
WILLIAMS, Selden Thornton (1892–), 89
WILLS, Albert Potter (1873–1937), 51
WOLFF, Irving Gutman (1894–), 88
WOLF, Robert (1881–), 90*n*

YEUNG, Ying-Wa (Mrs. Chaang Wuang) (1926–), 110*n*
YOUNG, Thomas (1773–1829), 185

ADDENDA TO INDEX OF NAMES

BAUER, Benjamin Baumzweiger (1913–1979)
CADY, Walter Guyton (1874–1974)
CAMPBELL, George Ashley (1870–1954)
CHAFFEE, Emory Leon (1885–1975)
COLBY, John Warren (1857–1928)
COLVIN, William, Jr. (1871–1937)
DE FOREST, Lee (1873–1961)
DI MATTIA, Alfred Louis (1910–1978)
DORSEY, Herbert Grove (1876–1967)
DOWD, Peter Ambrose (1836–1922)
EDELMAN, Philip Ephraim (1894–)
EHRET, Cornelius Dalzell (1874–1956)
FARRAND, Clair Loring (1895–1981)
FAY, Richard Dudley (1891–1964)
FORD, Francis J. W., D. J. (1882–1975)
GREEN, George (1881–)
HAMMOND, John Hays, Jr. (1888–1965)
HAYES, Harvey Cornelius (1878–1968)
HEWLETT, Clarence Wilson (1886–1976)
HULL, Albert Wallace (1880–1966)
HUNT, Frederick Vinton (1905–1972)
JEFFERSON, Harold (1914–)
JENSEN, Peter Lauritz (1886–1961)
KELLOGG, Edward Washburn (1883–1960)
KILROY, Willie Dickson (1876–)
KNUDSEN, Vern Oliver (1893–1974)
KRANZ, Frederick William (1887–1979)
LE CORBEILLER, Philippe Emmanuel (1891–1980)
MARTIN, William Hennick (1889–1974)
MERRILL, Albion Parvis (1840–1920)
MEYER, Erwin Walter (1899–1972)
OLSON, Harry Ferdinand (1902–1982)
PARRY, Robert Davies (1883–1944)
PICKARD, Greenleaf Whittier (1877–1956)
PIERCE, George Washington (1872–1956)
PIPES, Louis Albert (1910–1971)
RICKER, Norman Hurd (1896–1980)
SABINE, Paul Earls (1879–1958)
SAWYER, Charles Baldwin (1894–1964)
SOKOLNIKOFF, Ivan Stephan (1901–1976)
VAN DYKE, Karl Skillman (1892–1966)
WARTH, Nathaniel Gates (1864–1939)
WEINBERGER, Julius (1893–1978)
WENTE, Edward Christopher (1889–1972)
WHITNEY, Willis Rodney (1868–1958)
WIENER, Francis Michael (1911–1966)

INDEX OF SUBJECTS

Accession to inertia, 145, 151, 156–157, 203
Acoustic impedance of piston radiator, effect of baffle on, 157
  in bass-reflex enclosure, 160
  simulative networks for, 158
Added-mass method, 119, 156
Admittance, motional, 136
Admittance and impedance diagrams, 135
Amplifier, Ehret's basic claim on, 63
Analog computer, equivalent circuit used as, 151–153, 235
Analogies, electromechanical, 66; *see also* Equivalent circuits
Analogous circuits, realizability of, 108
"Ancients have stolen our invention," 59
Animal-tissue transducer, 5, 30
Antireciprocal coupling, 105
Antisymmetry, burdens of, 109
Applied acoustics frontiers, 3
Arc transmitter, 47, 48

Baffles, acoustic, 86, 87
Balanced-armature transducer, analysis of, 228–231
  configurations, 60, 73
  as loudspeaker motor, 73–74
  prototype structures for, 213–215
Balanced-diaphragm transducer, 59
Bass-reflex enclosure, 87–88, 160–164
  disclosure of, 88
  equivalent circuits for, 160
  proper "tuning" of, 163–164
Battery, primary, discovery of, 12
"Bellowing telephone," Lodge's, 60
Bells, electrostatic ringing of, 8, 9
Blocked impedance, vector locus of, 100–101, 232
  interpolation for, 118

Canonical equations, 93
  transposition of F and v in, 109–110
Carbon microphone, 4, 34–37
  as hydrophone, 48
Chilowsky's trial by invention, 46*n*
Clicks from condenser discharge, 7
Condenser microphone, 169–173
  Altec-Lansing *Model 21B*, 171
  calibration of, 173
  operating features of, 169–170
  resonance frequency of, 170–172
Conductors and insulators, 1, 2
Conical diaphragm. *See* Diaphragm
Core impedance, 227
Coupling, antireciprocal, 105
  coefficient of. *See* Electromechanical coupling *and under transducer types*
Coupling equations, canonical, 93
  electrostatic, 179–180, 192, 194
  moving-armature, 226–227
  moving-conductor, 146
Crystal control of frequency, 53–57
  Judge Ford on the invention of, 56
  patent status of, 56
  with 4-terminal crystal, 53
  with 2-terminal crystal, 55

Degrees of freedom, multiple, 101
  introduced by bass-reflex enclosure, 88, 159–164
  introduced by receiver housing, 234–235
Determinant of impedance coefficients, 94
Diametral frequencies, 99–100
  for electrostatic loudspeakers, 205–207
Diaphragm, compliant suspension for, 59
  conical, proposed, 58
    influence of, on loudspeaker response, 154
    modifications claimed, 70–72
  deflection of due to bias, 183–186
    for compliance measurement, 184–185
    as index of coupling coefficient, 186
    measured by capacitance change, 183
    nonuniform, 185, 205
      influence of, on "fall in," 185, 197
      related to "stray" capacitance, 205–206
  flat, with pleats, 70
  proposals to use large, 60–61

Diaphragm, segmentation of, 84–86
with variable mass and stiffness, 83–84, 165–166
Diffraction, effect of, on microphone calibration, 173
Diffraction "bright spot," 40
Dip angle, 100–101
Directional transducer, for echo ranging, 45
in theater systems, 90
Directivity, control of, by segmentation, 85, 173*n*, 175
excess, in electrostatic loudspeakers, 174
of horn loudspeakers, 90
Direct-radiator loudspeaker, prototype, 81–82, 153–154; *see also* Dynamic loudspeaker
Distortion, harmonic, abatement with time constant, 212
rationale of, 210–211
analysis of, for single-sided electrostatic units, 192–194
for push-pull electrostatic units, 209–212
relation of, to linearity, 4
in telephone receivers, 226
third-harmonic, in push-pull electrostatic units, 209–210
Doppler-shift compensation in echo ranging, 45
Double-cone diaphragm, 72
Duality, between electromagnetic and electrostatic systems, 205
mixed, 110
in network analogs, 110–111, 150–151
Dynamic loudspeaker, equivalent circuits for, 147–150
impedance analysis of, 166–167
performance, of illustrative example, 156–167
influence of baffle on, 157–159
influence of housing on, 159–165
of prototype, 150–155
effect of diaphragm parameters on, 154
medium on, 155
typical structure of, 143–144
see also Moving-coil transducer

Earphone, defined, 4; *see also* Receiver *and* Moving-armature transducer
Echo ranging, 45–50
bottom echoes by ultrasonic, 48
first echoes from submarine by, 50
iceberg detected by, 45
proposals for ultrasonic, 45–46
Eddy currents, magnetic shielding due to, 221, 229
effect of, on force factor, 233
on impedance, 232
Eddy-current factor, complex, 232
Eddy-current loudspeaker, Hewlett's, 77
Efficiency, 122–123
alternative expressions for, 124–128
maximum, locus of, 127
reactance conditions for, 140–141
potential, 129–133
interpretation of, 132–133
usefulness of, 131
Electric-circuit modeling, 108, 151–153 181, 235
of dynamic loudspeaker, 151–152
of ring-armature receiver, 235
Electric-impedance analysis. *See* Impedance
Electric-network analogs, 66–67
equivalence criteria for, 106–109
of magnetic circuits, 228–231
to simulate acoustic impedances, 158–162
to simulate magnetic losses, 232–233
see also Equivalent circuits
Electric-network theorems, relevance of, 116
Electric recording, 67–69
Electric transmission circuits, theory of, developed, 66
Electrical chimes, 8
Electrical "jack" (electrostatic motor), 8
Electrical piano, 8
Electroacoustic transducer, defined, 2
first electromagnetic, 17
first electrostatic, 8
see also under transducer types
Electroacoustics, underwater, 44–52
Electrochemical transducers, 11, 12
Electrodynamic transducer, basic equations for, 114–115, 146; *see also* Dynamic loudspeaker
Electromagnet, multiturn winding for, 16
Electromagnetic induction, Henry and, 16*n*

Electromagnetic terminology, Ampère's, 14
Electromagnetic transducer. *See* Moving-armature transducer
Electromagnetism, discovery of, 12–13
Electromechanical contribution, to electric impedance, 134
to mechanical impedance, 134
of negative stiffness, 181ff, 225ff
Electromechanical coupling, types of, 6
canonical equations for, 93
coefficient of, defined by critical frequencies, 140
and filter band width, 141–142
see also under transducer types
used in electric-wave filters, 67
Electromechanical systems, designed as electric filter analogs, 67
Electromechanical telephone repeater, 63–64
Electromechanical transformers, nature of, 109
inverting properties of, 150–151
Electrometer, capillary, 41
pith-ball, 10
Electrostatic and electromagnetic systems contrasted, 139
Electrostatic forces, bells rung by, 8–9
fitness for generating sounds in air, 168
Electrostatic loudspeaker, design features of, 173–175
literature on, *ca.* 1930, 169*n*
patents on, *ca.* 1930, 173*n*
push-pull type, analysis of, 187–191, 194–202
constant-charge operation of, 188–189, 199, 210–212
equilibrium and stability of, 195–202
equivalent circuits for, 199–205
harmonic distortion in, 208–212
impedance analysis of, 202–208
potential efficiency of, 207
single-sided type, analysis of, 176–187, 192–193
capacitance change under bias, 183
coefficient of coupling for, 181
related to capacitance change, 186
equilibrium and stability of, 181–186, 197
equivalent circuits for, 180
harmonic distortion in, 192–193
Electrostatic projector, sound power of, 47
Electrostatic telegraph, 10–12
Electrostatic transducers, primitive, 7
for underwater sound, 47
see also Condenser microphone *and* Electrostatic loudspeaker
Equivalent circuits, use of, as analog computer, 151–153, 235
contrasted with circuit analogs, 108
for dynamic loudspeaker, 147–150
for electrostatic loudspeaker, 180, 199–206
for moving-armature transducer, 228
rationale for, 107, 159–162, 234–235
transformations of, 108
see also Electric-circuit modeling, Electric network analogs

Feedback, electromechanical, 67
Fessenden oscillator, 45*n*
Filters, electromechanical coupling in, 67
Fixed winding linking variable magnetic field, 115
Force factor, definition of, 121–122
for dynamic loudspeaker, 149
for electrostatic loudspeaker, 180
for telephone receiver, 225, 230, 233
Franco-British Commission, visit of, 51
Frictional transducers, 38

Galvanic music, 18–19
Generalized equivalent circuit, 133ff; *see also* Equivalent circuits
Gyrator, proposed, 111
similarity of electromechanical transformer to, 150–151

Harmonic distortion, analysis of, 192–194, 209–212, 226; *see also* Distortion
Hebb's quadrature transformation, 111–112
Hewlett's "tone generator," 77
"High fidelity," early claim for, 59
Horns, acoustical, 89–91
Housing, closed, with damping material, 60
Howling telephone, Hughes's, 36
Hydrophone, defined, 4
mica-dielectric transducer used as, 47
sensitivity of, enhanced by focusing, 48

Hysteresis factor, complex, 221ff
Hysteresis loop, 218
  minor, typical, 219
    approximated by ellipse, 220
  terminology associated with, 219–220

Induced-current drive, 45*n*, 75–77
Inductive coupling to voice coil, 76–77
Inductor-type (pseudo) loudspeaker motor, 75
Impedance, driving-point, of transducer, 95
  electromechanical transfer, 105
    reversibility criterion for, 105
  see also Motional impedance
Impedance and admittance frequencies, 139, 205–207
Impedance analysis, general, 117–142
  of dynamic loudspeaker, 155–165
  of electrostatic loudspeaker, 202–208
  of moving-armature earphone, 228–229, 232
Impedance concept, extended to mechanics and acoustics, 66
Intensity magnet, 16
Interallied Conference on Submarine Detection (1918), 46*n*
Interference between front and back radiation, 86
  elimination of, with baffle, 86–87
Invention, and the telephone, 23–29
  criteria of, 23–24
Inverting transformer, 111

Jets, liquid, modification of by sound, 39
  use of as transducers, 38

Labyrinth, acoustical, 88
Leakage flux, 125, 217
Lecture-table diaphragm, Pierce's, 61
Linearity, defined, 4
Living-tissue transducer, 5, 30
Loudspeaker, definitions of, 4
  the first, 29

Magnetic circuit, 216–221
Magnetic flux, dependence of on current and gap length, 223
Magnetomechanical effects, various, 20–21
Magnetoresistance effect, use of, for telephone repeater, 63
Magnetostriction, converse effect, 19–21
  "discovered," 20
  first observed, 18
Market statistics, transducer, 2*n*
Mass-control, of direct-radiator diaphragm, 81–82, 153–154
  phase relations for, 97
Maxwell stress, in magnetic field, 216
Mechanical constants, effective, 145
  electromechanical modification of, 47
  evaluation of, 119, 157, 184, 207
  terminology defined, 121
Mechanical power-utilization factor, 123
Mechanisms of transduction, classification of, 6
Mercury-arc tube, as amplifier, 64
  in Vreeland oscillator, 96
Microphone, carbon, 4, 34
  hot-wire, 40
  ionization, 5
  origin of word, 36
  see also Condenser microphone
Microphonic amplifier, Edison's, 62
  obsolescence of, 65
  various proposals for, 61–63
Mid-century prospect, 21–22
Mobility pairing (*E–v*, *I–F*), 110
Motional impedance, alternative expressions for, 124
  circular locus of, 99
  discovery of, 95–96
  network representation of, 148
Motional-impedance circle, point-by-point construction of, 118
Movie screen as diaphragm, 61, 169*n*
Moving-armature transducer, 6–7, 24–25, 33, 213–235
  with adjustable air gap, 74
  design features of, 214–216
    influence of magnetic materials on, 214
  typical configurations of, 213
  for ultrasonic signaling, 46
  variable-area gap type of, 75
  vector-impedance locus for, 229
Moving-coil electroacoustical transducer, the first, 58–59
Moving-coil transducer, with distributed windings, 78
  inductively coupled, 75–77
  ribbon-diaphragm type, 78
  see also Dynamic loudspeaker

Moving conductor, in fixed magnetic field, relations for, 114
Multiple-unit construction, of cone and voice coil, 84
  for control of directivity, 85
Multiplier, Poggendorff-Schweigger's electromagnetic, 14

Ohm's law, 15
  of magnetic circuit, 216
Oscillator, positive-feedback electromechanical, 36, 67
  Pierce, crystal; *see* Crystal control
Orthophonic Victrola, 68
  management's dubiety concerning, 69

Passive transducer, defined, 4
Permeability, incremental, 220
  complexness of, 221
Phase relation, between *B* and *H*, 220
  representation of by elliptic path of operation, 220–221
Phase-inverter housing, 87; *see also* Bass-reflex enclosure
Phonetron, 72
Phonograph, Edison's, 37
  first all-electric, 69
Phonograph records, 39, 68–69
Physical realizability, 93–94, 109, 130, 132
Pierce oscillator, 55
Piezoelectric effect, converse, 43–44
  discovery of, 42
  first application of, 43
  first use as hydrophone, 49
  prediction of, 43
  in Rochelle salt, 52
Piezoelectric oscillator. *See* Crystal control
Piezoelectric relations formulated, 44
Piezoelectric resonator, 53
Potential efficiency, 129–133
Projector, definition of, 4
  and hydrophone, use of same transducer for, 50
Push-pull electrostatic loudspeaker. *See* Electrostatic loudspeaker
Pyroelectricity, 42–43

Q, defined, in terms of energy, 99
  as rate of phase change, 98
Quadrantal frequencies, 99
  Q in terms of, 100
Quartz, Boyle's search for, 50–51
  substitutes for, 57
  Werlein's "mother" crystal of, 49
"Quartz piézo-électrique", the Curies', 43
Quartz crystals grown, 57
Quartz mosaic transducer, 50
Quartz receiver, for underwater sound, 49
Quartz transducer, high output of, 49–50
Quaternions, 114

Radio broadcast, Fessenden's first, 40
Radio receiver, all-a.c., 81
Radiola Loudspeaker *Model 104*, 80–81
Radiotelephony, beginnings of, 39
  continuous carrier, need for in, 40
  liquid jets as modulators for, 38–39
Reactance, typical behavior of, 138–139
Reactance conditions for diametral frequencies, 137–138
Realizability criteria, physical, 93–94, 130, 132
  practical, for analogous circuits, 108
Receiver, telephone, definition of, 4
  Bell's, with permanent magnet, 33
  Gray's moving-armature, 30
  Reis's magnetostriction, 29
  see also Moving-armature transducer
Reciprocating electromagnetic transducer, Henry's, 16*n*
Reciprocity, in coupled systems, 103–104
  and symmetry, 103–106
  theorems, 103–104
  violation of, 114
Reflections, sound, influence of on vector-impedance locus, 102
Relaxation oscillator, electrostatic, 8
Relay, Hughes's voice, 36
  telegraph, Henry's first, 17
Reversibility, definition of, 4
  examples of limited, 5
  of transduction coefficient, 104–105
    relation of, to reciprocity, 104
Ribbon loudspeaker, 78
Ribbon microphone, 79
Ring-armature receiver, blocked impedance of, 232
  evolution of, 215–216
  force factor of, 233
  magnetic circuit of, 231
  mechanacoustic loading of, 234–235
  equivalent circuit for, 234

Segmentation, of cone, 83–84
for phase control, 85–86
Self-excited electromechanical system, 36, 67
Ship's side as diaphragm, 60–61
Sign conventions, electromagnetic, 112–116
embodied in space operator, 112–113, 115–116
and symmetry, 112
Single-sided electrostatic loudspeaker. *See* Electrostatic loudspeaker
Space operator, properties of, 114
first use of, v
Space *or* time imaginary, universal appearance of, 116
Spark discharge, sounds made by, 1, 7
Stability in electrostatic units, dynamic, 198–202
static, 183, 195–197
see also Electrostatic loudspeaker
"Stiffness" control, for condenser microphone, 170
phase relations for, 97, 170
Stray capacitance, in electrostatic loudspeakers, 205–207
Summary Technical Report, Div. 6, vol. 13, availability of, 117*n*
Symmetry, and equivalent circuits, 105
of impedance determinant, 106
Sympathetic loadstones, 10
Sympathetic telegraph, 9

Telegraph, 11–18
electrochemical, 11
electrostatic, 10, 11
Henry's demonstration, 16*n*, 17
magnetic-needle, 14–16
Morse's printing, 17–18
pulse-time modulation used with, 11
single-channel, 11
sympathetic, 9
synchronous dial, 11
Telegraphic codes, 15–16
Telephone, 23–41
Bell judged inventor of, 23–24
origin of word, 26, 27*n*
patent litigation about, 30–32
precursors of, 24–30
Telephone systems, electrostatic, 41
Terminology, electroacoustical, 3–7
American Standard Acoustical, 4*n*
Thermophone, as calculable source, 41
as telephone receiver, 40
Thunder and lightning, 1, 5
Transducers, balanced-diaphragm, 59
classification of, 6–7
defined, 2
designed as band-pass filters, 67
electrochemical, 11, 12
statistics of literature on, 91
see also under transducer types
Transduction coefficient, defined, 92–93
for dynamic loudspeaker, 146
for electrostatic loudspeaker, single-sided, 180–181
push-pull, 199–202
for moving-armature earphone, balanced-armature, 230
bipolar, 228
monopolar, 222
relation of, to force factor, 121–122
Transmitter, telephone, defined, 4
carbon, invented by Edison, *et al.*, 34–37
liquid types of, 30–31
multiple loose contact, 36–37
variable-contact-pressure type of, 34
Two-way loudspeaker systems, 89–90

Ultrasonics, applications of, 3
echo ranging with, proposals for, 45–46
first success with, 48
French-British liaison (1916–1918), 49
research programs launched (1918), 51–52
underwater transmission across Seine with, 48
Undulation, doctrine of, 27–29

Vacuum, operation in, to unload diaphragm, 123
Vacuum-tube amplifier, introduced, 64
built in with loudspeaker, 80
Variable-area diaphragm, need for, 83
nature's provision of, 83, 165
helping nature, 83–85, 173*n*, 175
Variable-mass voice coil, 84
Vector-admittance locus, 135–142
for electrostatic loudspeaker, 204
Vector-impedance locus, 97–101
modified by reflections, 102
for multiresonant transducers, 101, 163–167
Versor, 114